8-2017

Application of Glycoconjugate-Functionalized Magnetic Nanoparticles as Potent Anti-Adhesion and Anti-Bacterial Agents

Yash S. Raval
Clemson University, yraval@g.clemson.edu

APPLICATION OF GLYCOCONJUGATE-FUNCTIONALIZED MAGNETIC NANOPARTICLES AS ANTI-ADHESION AND ANTI-BACTERIAL AGENTS

A Dissertation
Presented to
the Graduate School of
Clemson University

In Partial Fulfillment
of the Requirements for the Degree
Doctor of Philosophy
Microbiology

by
Yash S. Raval
August 2017

Accepted by:
Dr. Tzuen-Rong J. Tzeng, Committee Chair
Dr. Olin Thompson Mefford
Dr. Yanzhang Wei
Dr. Xiuping Jiang

ABSTRACT

Magnetic nanoparticles (MNPs) are currently being extensively studied in multitude of biomedical applications because of their exceptional biocompatibility. By attaching different targeting ligands/molecules, MNPs have been broadly used in magnetic hyperthermia, cancer therapy, targeted drug delivery, MRI imaging, pathogen detection, and biological cell-separation. In this dissertation, MNPs coated with polyethylene oxide (PEO) based polymer (PEO-MNPs) and functionalized with bacterial adhesin-specific glycoconjugate molecule Neu5Ac(α2-3)Gal(β1-4)-Glcβ-sp (GM3-MNPs), are investigated for their interactions with enterotoxigenic *Escherichia coli* (*E. coli*). It also describes the feasibility of using alternating magnetic fields (AMF) for targeted killing of *E. coli* K99 (*EC* K99) strain using MNPs. Lastly, the interactions of MNPs with normal human colon cells CCD-18Co are explored to assess their *in vitro* biocompatibility.

First, GM3-MNPs were synthesized via 'click chemistry' platform. Specific aggregation of *EC* K99 was seen due to interactions occurring between GM3-MNPs and adhesin molecules of *EC* K99. These interactions were observed by means of fluorescence microscopy, transmission electron microscopy (TEM), and colony forming units (CFU) assays. The preliminary cytotoxicity assay performed on normal colon cells CCD-18Co indicated excellent biocompatibility of GM3-MNPs. Thus, such glycoconjugate-functionalized MNPs can be effectively utilized as anti-adhesion and anti-bacterial agents for reducing gastro-intestinal (GI) tract infections.

Next, GM3-MNPs were used along with AMF for targeted killing of *EC* K99 cells. CFU/ml assays indicated that killing rate of EC K99 was mainly dependent on concentration of GM3-MNPs and AMF exposure time. Clinically relevant reduction in CFU/ml of *EC* K99 was achieved after 120 minutes of AMF exposure in presence of GM3-MNPs in both pure and mixed bacterial culture environment. Extensive cell-membrane damage was observed via fluorescence microscopy and TEM imaging of *EC* K99 cells after AMF exposure in presence of GM3-MNPs. AMF exposure in presence of GM3-MNPs also caused significant decrease in intracellular ATP levels of *EC* K99. These results suggest that bacterial specific glycoconjugate MNPs along with AMF can be efficiently employed as novel non-antibiotic platform to inactivate targeted bacterial pathogens.

Finally, the overall biocompatibility of GM3-MNPs was examined in CCD-18Co cells and compared to that of PEO-MNPs. GM3-MNPs were found to have relatively stable hydrodynamic diameter in cell-culture media DMEM whereas PEO-MNPs drastically increased their size on account of protein-corona formation. Both cytotoxicity and ATP assays revealed that GM3-MNPs exhibited great biocompatibility in the cells. CCD-18Co cells also maintained their overall cell-membrane integrity in the presence of GM3-MNPs. Interestingly, GM3-MNPs were able to substantially decrease the glutathione (GSH) levels in the cells leading to increased oxidative stress. Thus, by properly controlling surface properties of glycoconjugate functionalized MNPs and attaching different drugs, they can be potentially used as colon specific drug-delivery carriers for therapeutic applications.

DEDICATION

I would like to dedicate this work to my Lord and spiritual Guru, *Sri Sathya Sai Baba*, for His constant blessings and divine guidance and to my parents, grandparents and all my family members for their good wishes and support throughout this endeavor.

ACKNOWLEDGMENTS

TABLE OF CONTENTS

LIST OF TABLES

LIST OF FIGURES

List of Figures (Continued)

Figure   Page

List of Figures (Continued)

Chapter 1

Literature Review

Antibiotic Resistance in Bacteria

Currently, there are more than 160 different kinds on antibiotics available for therapeutic purposes [1]. However, unrestricted and prolonged usage of antibiotics has resulted in rapid emergence of new strains of microorganisms that have developed resistance to these drugs and over a period of time they have evolved as multi-drug resistant microorganisms. For example, the first penicillin-resistant strain of *Streptococcus pneumoniae* was observed in USA in 1974 in a patient suffering from pneumococcal meningitis [2]. Methicillin resistant *Staphylococcus aureus* (MRSA) and vancomycin resistant *Enterococci* (VRE) were first identified in the 1960s [3] and in the mid-1980s [4] respectively. Some of the mechanisms commonly found in these antibiotic-resistant pathogens are alteration of drug target, degradation of drugs by producing enzymes, changes in target accessibility and increased drug efflux [5] (Figure 1.1). According to a recent report by CDC, approximately 2 million people in the US have illnesses related to antibiotic resistant infections and each year at least 23,000 deaths occur as a result of such infections [6]. Given the fact that developing new antibiotics is a slow and costly affair, there is an urgent need to treat such infections by employing therapies that do not require the traditional usage of antibiotics [7-9].
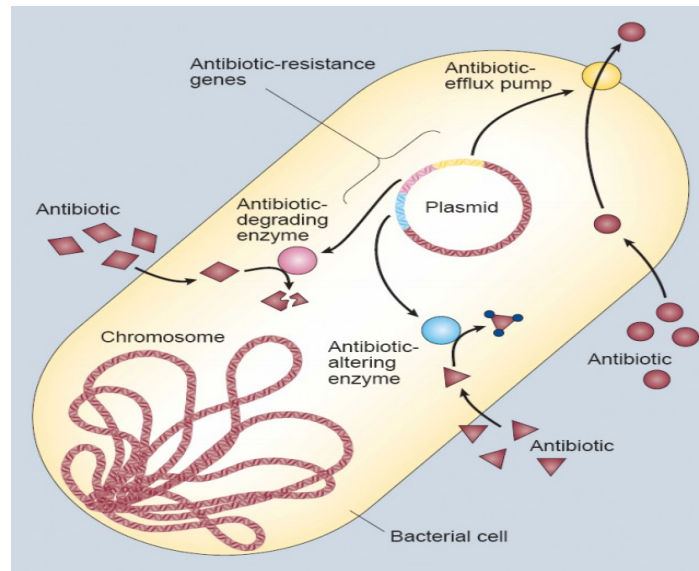
Figure 1.1 Different mechanisms employed by bacteria to render antibiotic useless. Reprinted from [5] - Reproduced with permission from Nature Publishing Group.

Role of Adhesin in Bacterial Attachment and Pathogenesis

Pathogen attachment is a very complex phenomenon and a vital process to initiate infection in the host-cell. The microorganisms have to initially colonize themselves onto the host-cell surfaces and grow in sufficient numbers in short span of time to produce clinical symptoms [10, 11]. Bacterial pathogens typically target animal or human host by attaching onto epithelial and mucosal surfaces of respiratory tract, gastrointestinal tract and genitourinary tract [12]. Bacterial adhesion is essential since pathogens have to overcome different nonspecific defense mechanisms like sneezing and fluid flow occurring in the host. Adhesion also enables the pathogen to utilize host-cell nutrients in order to multiply rapidly along with enabling the pathogen to deliver toxin in the host-cell and ultimately penetrating into the host tissue [13].

Bacterial pathogens utilize two primary mechanisms to adhere onto host cells, namely carbohydrate-protein recognition and protein-protein interaction [14]. Most of the studies to understand adhesion mechanisms are done by linking carbohydrate-protein recognition process since it is very difficult to elucidate the protein-protein interaction on account of protein instability and its changing conformations [15]. The carbohydrate-protein interaction that binds bacterial pathogens onto the host-cell tissue are mediated by specialized structures called adhesin/fimbriae, which have lectin proteins and are located on the microbial surface. Fimbriae are typically expressed by almost every gram-negative bacterial species that has been studied [16]. It should be however noted that bacterial adhesion mediated by fimbriae is a highly specific phenomenon. The adhesion structures have a high degree of preference for a particular host-cell tissue. For example, *E. coli* usually colonizes GI tract whereas *Streptococci* colonize the skin and esophagus in humans [17]. Several comparative studies have been done to address the species specificity of bacterial adhesins for a particular type of host-cell receptor [14].

Biological Importance of Carbohydrates in Pathogenesis

It was only in the early 1990s that carbohydrates were recognized as important biomolecules, which had great diversity, and thereby carbohydrate molecules were explored for finding their applications in medical and pharmaceutical industries [18]. Apart from their roles in cell metabolism, carbohydrates play an important role in various biological processes like inflammation [19], cancer metastasis [20] and cell-signaling to

name a few. They also play modulatory role in hormone signaling and typically act as receptor molecules for attachment of antibodies, proteins and other biomolecules [19]. Adherence of pathogens onto host-cell is one of earlier events that can trigger the onset of infection. The binding affinity of a single carbohydrate-protein interaction is generally weak on account of monovalency. However, multiple interactions between the carbohydrate molecule and its respective protein result in polyvalency, which greatly enhances the binding capacity and thereby aids in the adherence process [21, 22]. By taking advantage of these multiple adherence factors, a large number of bacteria, their toxins, and viruses are able to gain entry into the host-cell and exert their harmful effects on the host-cell.

The adhesion process of bacteria attaching onto the host-cell is complex in nature. This attachment is mediated by bacterial lectins that are present on their surface. These lectins, generally in the form of fimbriae, recognize specific glycolipid or glycoprotein receptors present on the host-cell surface [23]. *E. coli* is one such enteropathogen that expresses different types of pili e.g., Type-1 pili, P-type fimbriae, S-type fimbriae, etc. Table 1.1 gives us more information regarding the receptor specificity of these bacterial fimbriae.

Organism	Target tissue	Carbohydrate	Structure
E. coli Type 1	Urinary	Manα3Manα6Man	GP
E. coli P	Urinary	Galα4Gal	GL
E. coli S	Neural	NeuAc (α2-3)Galβ3GalNAc	GL
E. coli CFA/1	Intestinal	NeuAc (α2-8)	GP
E. coli F1C	Urinary	GalNAcβ4Galβ	GL
E. coli F17	Urinary	GlcNAc	GP
E. coli K1	Endothelial	GlcNAcβ4GlcNAc	GP
E. coli K99	Intestinal	NeuAc(α2-3)Galβ4Glc	GL
C. jejuni	Intestinal	Fucα2GalβGlcNAc	GP
H. pylori	Stomach	NeuAc(α2-3)Galβ4GlcNAc	GP
		Fucα2Galβ3(Fucα4)Gal	GP
K. pneumoniae	Respiratory	Man	GP
N. gonorrhoea	Genital	Galβ4Glc(NAc)	GL
N. meningitidis	Respiratory	[NeuAc(α2–3)] Galβ4GlcNAcβ3Galβ4GlcNAc	GL
P. aeruginosa	Respiratory	L-Fuc	GP
	Respiratory	Galβ3Glc(NAc)β3Galβ4Glc	GL
S. typhimurium	Intestinal	Man	GP
S. pneumoniae	Respiratory	NeuAcα2-3Galβ1-4GlcNAcβ1-3Galβ1-4Glc	GL
S. suis	Respiratory	Galα4Galβ4Glc	GL
GP = glycoprotein, GL = glycolipids			

Table 1.1: Receptor specificity of bacterial fimbriae. Modified from [24]. Reproduced with permission from Elsevier Ltd.

Apart from bacterial pathogens, their toxins and even viruses have been shown to bind to specific carbohydrate molecules. The viral protein hemagglutinin has been shown to bind to host-cell N-Acetylneuraminic acid and this interaction has been found to be polyvalent in nature [22]. Similarly, other viruses like rotavirus and Sendai virus have been found to attach to specific carbohydrate ligands [22]. Clinically important bacterial pathogens like enterotoxigenic *E. coli*, *Vibrio cholera*, *Shigella dysenteriae* all produces lethal toxins which are responsible for causing diseases ranging from mild diarrhea to lethal toxic shock induced death in humans. These toxins are able to exert their toxic effects by entering the host-cell after binding to their carbohydrate receptors. It has been found that cholera toxin and heat-labile enterotoxin attach themselves onto the luminal side of the intestinal epithelium by binding to GM1 gangliosides [25]. The Shiga-like toxins have been found to bind onto the host-cell receptors through Gb_3 ceramide glycolipids [26, 27].

Enterotoxigenic *Escherichia coli*

E. coli is one of the most common types of bacteria naturally occurring in the digestive tract of humans and animals. While most of the *E. coli* strains are harmless to humans and animals, there are few *E. coli* serogroups that are mainly responsible in causing bacterial infection. These strains typically tend to be host-specific. The prevalence of the serogroups and presence of adhesins are considered to be the primary factors that facilitate intestinal colonization of *E. coli*. Based on different serological features, enteric *E. coli* have been classified into 5 different groups: 1) Enterotoxigenic *E. coli* (ETEC), 2) Enteropathogenic *E. coli* (EPEC), 3) Enteroinvasive *E. coli* (EIEC), 4) Enterohemorrhagic *E. coli* (EHEC), and 5) Enteroaggregative *E. coli* (EAEC) [28]. The production of different types of toxins by these serovar groups is considered to play very crucial role in producing clinical signs of infection. *E. coli* belonging to the ETEC group is responsible for causing traveler's diarrhea in humans and bloody diarrhea in neonatal calves, pigs and lambs [29]. Though enough reports have cemented the importance of adhesins in the overall process of infection caused by *E. coli* in humans, few studies have been conducted to understand the pathogenesis of ETEC strains in farm animals. ETEC adhere to small intestinal microvilli membranes *in vivo* via adhesins and produce enterotoxins that act on enterocytes and thereby causing diarrhea [30]. Recently, numerous studies have reported an increase in multi-drug resistance of this strain associated with antibiotic treated animal feed [31-34]. *E. coli* K99 is the main causative agent of bloody diarrhea in young calves, lambs and pigs, a condition also known as colibacillosis [35]. The disease typically affects newborn animals within 2-3 weeks of

birth. This strain bears K99 antigen which also acts as fimbriae and adheres the bacterium onto the ileal villus epithelium of calf and pigs [36-39]. *E. coli* K99 strain specifically attaches to small intestinal mucus and recognizes sialic acid derivatives present on glycolipid receptors [40]. Experimental studies have shown that glycoprotein glycans isolated from bovine plasma inhibited the fimbriae specific adherence of *E. coli* K99 to mucus glycoproteins [41]. Oral administration of these glycans protected young calves from the infection and reduced the number of bacteria present in small intestine mucus by 100 folds. This showed that such glycans could effectively act as anti-adhesive molecules, which can prevent colibacillosis in young farm animals.

Role of Carbohydrates in Anti-adhesion Therapy

It was not until 1990s that the concept of using carbohydrates as natural anti-adhesive agents came into limelight. The need for finding new strategies in order to combat the growing concern of antibiotic-resistant strains of microorganisms, aided the research in glycol-biology field with special focus in microbiological context. Several studies were carried out in this aspect and showed the feasibility of carbohydrates as an alternative to conventional antibiotic treatment [42-44]. The concept of using carbohydrates as new anti-adhesion agents is mainly based upon the following hypotheses: 1) Microbial infection is initiated due to binding of the pathogen onto the host-cell and 2) Anti-adhesive agents must either interfere with the binding of pathogen to the host or help in detachment of microbes from the host tissues during early stages of infection [13, 45]. Since these anti-adhesive agents interfere with adhesin-host-cell

receptor (proteins) interactions, it would be much easier to develop analogues that interact with carbohydrate receptors as it is difficult to elucidate the exact protein structure [44].

Numerous natural carbohydrates and synthetic glycoconjugates have been used to understand this mechanism of anti-adhesion in bacteria and viruses [43, 46, 47]. Since synthetic glycoconjugates typically have low binding affinity, they can be used as polymers, dendrimers and liposomes in order to attain multivalency and achieve effective high affinity and inhibitory effect against various carbohydrate receptors and this has been shown in both *in vitro* and *in vivo* studies [48, 49].

Role of Carbohydrate Functionalized Nanomaterials in Pathogen Detection

Rapid, sensitive and reliable methods for detection of microorganisms hold the key for accurate diagnosis of infectious diseases. Conventional techniques commonly used for this purpose include culture and colony counting, polymerase chain reaction and immunological assays [50-53]. However, these approaches are laborious, time-consuming and having low sensitivity thresh-hold levels. Moreover, you encounter numerous false-negative results by using the above-mentioned conventional methods. It is in this context that the use of nanomaterials has provided a great impetus for rapid and accurate detection of microbial pathogens in food and clinical samples. These nanomaterials can act as unique nano-biosensor for specific detection of complex biologically relevant molecules like proteins, nucleic acids and enzymes [54]. It is now

possible to specifically detect microorganisms by functionalizing nanoparticles with specific antibodies and ligands. Since carbohydrate molecules are actively involved in host-cell recognition process leading to pathogenicity, coating the nanomaterials with such glycan molecules can provide a unique platform in rapid detection of pathogens including bacteria, virus and parasites. The underlying principle in this approach depends on the fact that providing multiple copies of different glycan molecules on the surface of nanomaterials would mimic the glycan present on the outer envelope of pathogen or the cell glycocalyx itself. Several studies have been carried out in this regard by exploiting the unique optical and magnetic properties of gold nanomaterials and magnetic nanomaterials respectively for rapid and specific detection of pathogens [55-65]. The adhesin-specific functionalized magnetic nanoparticles that we will be using in this research, can potentially find their application as unique nano-biosensor for rapid pathogen detection.

Lin *et al.* were one of the first few groups who used mannose functionalized thiol-coated gold nanoparticles as novel and sensitive agents for detecting *E. coli* cells in biological fluids proving the usefulness of carbohydrate functionalized nanoparticles in studying carbohydrate-protein adhesion [66]. They observed bacterial strain-specific aggregation of mannose functionalized gold nanoparticles via TEM imaging and UV-Vis spectroscopy. *E. coli* ORN 178 strain, which has FimH gene and type 1 pili showed specificity towards mannose functionalized gold nanoparticles whereas *E. coli* ORN 208 strain, which lacked FimH gene and type 1 pili did not bind to nanoparticles.

Carbohydrate functionalized nanoparticles were also employed to rapidly detect bacterial toxins in biological solutions. Schofield and co-workers synthesized gold glyconanoparticles coated with lactose for colorimetric detection of cholera toxin (B subunit) [63]. They noticed a rapid change in the color of the gold nanoparticle solution when cholera toxin B was added to it and this was attributed to the shift in surface plasmon band of the nanoparticle solution, which takes place due to aggregation of these nanoparticles in presence of the toxin. Similarly, another study was undertaken by Kulkarni *et al.* in which they synthesized biocompatible glycan conjugated gold nanoparticles for selective inhibition of shiga toxin 1 and 2 in Vero monkey kidney cell-line [64]. Their nanoparticles were functionalized with analogues of Pk trisaccharide molecules, which can mimic the glycolipid glycans present on the cell-surface receptors to which the toxin can attach. The results obtained by this work suggested a dose-dependent inhibition of Stx toxin in Vero cells.

Role of Carbohydrate Functionalized Nanomaterials in Anti-Adhesion Antimicrobial Therapy

Advances in the fields of nanomaterials synthesis and synthetic glycoconjugate production have seen a rapid increase since early 2000. As new technologies are being developed, it has become relatively easy to custom synthesize different carbohydrate molecules/glycan conjugates and use them to bio-functionalize nanoparticles that can be then utilized in anti-adhesion therapies. Some of the most commonly employed nanomaterials in anti-adhesion therapies are gold nanoparticles, carbon nanotubes and

magnetic nanoparticles [67, 68]. To be effectively used as anti-adhesion agents, the carbohydrate molecules needs to have multivalent interactions with the host-cell surface receptors. For bacterial pathogens to initiate infection, they must be able to bind to host cell-surface receptors. These binding interactions are either carbohydrate-protein or carbohydrate-carbohydrate interactions in nature. Thus, in order to interrupt/inhibit these interactions, carbohydrate analog molecules that mimic the cell-surface receptors are frequently coated on the surface of nanoparticles thereby acting as novel anti-adhesion antimicrobial agents. Some of the early research studies carried out in these fields included gold and magnetic nanoparticles functionalized with mannose or galactose derivatives.

For example, Huang *et al.* used silica-coated magnetic nanoparticles functionalized with mannose for rapid detection and separation of *E. coli* from medium [69]. After incubating mannose coated magnetic nanoparticles with bacterial cells, they applied external magnetic field to rapidly isolate the bacterial cells and their capture efficiency was ~88%. When these captured *E. coli* cells were observed under fluorescence microscopy and TEM imaging, they found large aggregates of nanoparticles-bacterial cells complex. These complex structures were attributed to lectin-carbohydrate interactions taking place between adhesin molecules of *E. coli* and mannose molecules present on the surface of magnetic nanoparticles. Similar studies were carried out by Qu *et al.* wherein they functionalized the surface of polymeric nanoparticles with multiple copies of mannose/galactose and found out that *E. coli* 178 cells would agglutinate only in presence of mannose functionalized nanoparticles whereas *E. coli*

O157:H7 cells would aggregate only in the presence of galactose functionalized polymeric nanoparticles [60, 70]. Few other studies also showed anti-adhesion properties of carbohydrate-functionalized nanoparticles in mammalian cells as well as in turkey poults infected with *Helicobacter pylor*i and *Campylobacter jejuni* respectively [68, 71].

Magnetic Nanoparticles

Synthesis of magnetic nanoparticles: The synthetic approach to manufacture magnetic nanoparticles plays a very important role in determining the size, shape and its magnetic properties. Some of the main advantages of using superparamagnetic nanoparticles in the biological environment are increased surface area, improved diffusion rates in body fluids and tissues and high colloidal stability [72]. Commonly used approaches for synthesizing magnetic nanoparticles are co-precipitation, thermal decomposition, sol-gel synthesis, micro-emulsion, ligand-exchange reaction, hydrothermal and high-temperature reactions, polyol methods, spray pyrolysis, and aerosol/vapor methods [73]. Nonetheless, the common aim of all the above-mentioned synthesis methods is to achieve a highly stable and monodisperse nanoparticle suspension with suitable size requirements. Moreover, it has been noticed that the size and shape of the nanoparticle is also dependent on the temperature, reaction time-period and concentration of the reagents. Keeping in view that these nanoparticles would interact with different biomolecules once they enter biological environment, it is imperative to make sure that the synthesized nanoparticles are highly nontoxic and in most of the cases, this depends on the method of nanoparticle synthesis [74]. Recently, nanoparticle

synthesis through high-temperature thermal decomposition technique has been efficaciously used in producing iron-oxide nanocrystals with enhanced controls in size distribution, shape and monodispersity with high degree of biocompatibility [75].

Stabilization of magnetic nanoparticles with polymers: Uncoated magnetic nanoparticles tend to aggregate rapidly at neutral pH and in various biological environments. This aggregation takes place because of the strong dipole attractions in form of Van der Waals forces, occurring between the particles. To overcome this problem, stearic or electrostatic repulsion must be achieved which would then stabilize the nanoscale colloidal suspension. Addition of different polymers onto the core of magnetic nanoparticles would render high stability in biologically aqueous environments. The stabilizing agents can be briefly categorized into 3 classes' namely 1) monomeric stabilizers which includes various functional groups like carboxylates, phosphates, and sulfates, 2) inorganic stabilizers which includes gold, silver, and silica, and 3) polymer stabilizers which are the most commonly used materials for stabilizing core magnetic nanoparticles [74].

Some of the most commonly used polymer coatings for stabilizing core magnetic nanoparticle are dextran, starch, alginate, chitosan, polyethylene glycol (PEG) or polyethylene oxide (PEO), polyvinyl alcohol (PVA), polyethylene oxide (PEO), polyacrylic acid (PAA), and polyethylene amine (PEI) to name a few. Most of these polymers are reported to have good biocompatibility properties and thereby are extensively used in biomedical applications [76]. It has been also noticed that the

molecular weight and surface charge of these polymers play crucial role in determining the stability of nanoparticle suspension in biological environments [72, 74, 77, 78].

PEG can be broadly classified into 2 categories depending on the type of terminal end group: 1) Monofunctional PEG - which has same functional group on both its ends and 2) Heterobifunctional PEG - which has 2 different reactive groups on each ends. Some of the most commonly used end terminal groups for PEGylation are acid chlorides, carbonates, aldehydes, amides, amine, carboxylic acids, NHS esters, etc. [78-81].

Some of the early studies involving usage of PEO for biomedical applications were carried out in 1970s. Abuchowski *et al*., for the first time, showed covalent attachment of PEG molecule (PEGylation) to bovine live enzyme, catalase [82]. They observed that attachment of PEG significantly increased the blood circulation time of these enzymes without triggering any immune response in mice. Since PEG is a known biocompatible polymer having no known cross-reaction with water molecules, it has been used extensively for drug delivery applications. Covalently attaching drug/protein molecules to PEG can increase its water solubility and overall hydrodynamic size. This actually helps in prolonged circulatory time as the increase in size diameter reduces its renal clearance rate. Some of advantages of attaching PEOs onto nanoparticles are that they are highly stable, biocompatible and approved by FDA, amphiphilic in nature, soluble in water as well as in many other solvents, can act as carrier molecule in different pharmaceutical products and the ease of manipulating its surface chemistry for wide-spread use in different biomedical applications [72, 83-87].

14

Magnetic Properties

Generally, almost all materials are magnetic in nature to a certain level. When exposed to external magnetic field (H), they display varying amount of small magnetism. Accordingly, they can be classified as either 1) paramagnetic or 2) diamagnetic materials. Also, there are few materials that exhibit higher ordered magnetic states even in the absence of externally applied magnetic field. Such materials have been distinctly classified into 3 categories namely ferromagnetic, ferrimagnetic and antiferromagnetic materials. This classification has been based on the magnetic susceptibility of the magnetic materials.

In paramagnetic materials, the magnetic moments are aligned parallel to H and they tend to retain their magnetic properties even when the external magnetic field is removed. In the case of diamagnetic materials, their magnetic properties are lost as soon as external field is removed. It should be noted that both para- and dia-magnetic materials have no collective magnetic interactions and their magnetic domains are not ordered. In ferri- and ferro-magnetic materials, the magnetic moments are also aligned parallel to H, however, there is a subtle difference in the coupling interactions that take place between the electrons of the magnetic material. The antiferromagnetic materials have the magnetic moments that are aligned anti-parallel to H. One of the unique features of all of the above 3 materials is that they exhibit highly ordered state magnetic domains and large spontaneous magnetization [88].

When the size of the nanoparticle goes below a certain value (~20 nm), then each individual nanoparticle can behave as a single magnetic domain that exhibits

superparamagnetic properties. When external magnetic field is applied, the magnetic dipoles to such nanoparticles will reorient and in the absence of magnetic field, the net magnetic moment will be zero. In contrast to paramagnetic materials, in superparamagnetic materials, the electrons spin alignment occurs in a single domain nanoparticle and not in a single atom. This is the reason as to why superparamagnetic nanoparticles respond very quickly in presence of external magnetic field [88]. When such nanoparticles are effectively stabilized with polymer coatings, they find myriad applications in the medical field.

Use of Magnetic Nanoparticles in Magnetic Hyperthermia for Therapeutic Applications

Hyperthermia is a type of treatment therapy wherein there is a drastic temperature increase in the body tissues. Hyperthermia therapy has been used for treating cancer since 1957 [89]. Typically, heat treatment by means of hyperthermia can be classified into 3 categories: mild temperature hyperthermia (37^0C to 42^0C), moderate hyperthermia (43^0C to 46^0C) and thermal ablation ($>46^0C$). Moderate hyperthermia is clinically approved treatment option for cancer therapy. Some of the cellular processes, which are directly affected by hyperthermia, are protein degradation, heat stress, and induction of apoptosis in cancer cells [90]. In the last decade, several studies have established the potential of using nanomaterials in cancer therapy and disease management. Various biomolecules like DNA, RNA, peptides, mRNA, and antibodies have been used as targeting ligands to specifically deliver the nanomaterials to cancer cell/tissue. Among the different kinds of

nanomaterials used in cancer treatment, magnetic nanoparticles have been extensively studied because of their biocompatibility and multi-functionality. When magnetic nanoparticles are exposed to alternate magnetic fields, they generate heat and increase the temperature of the surrounding environment (conversion of magnetic energy into heat energy). This application is known as magnetic hyperthermia and it has been successfully employed in treating different kinds of cancers *in vitro* and *in vivo* [91]. This heat generation occurs because of Neel and Brown relaxation and hysteresis losses [92, 93] (Figure 1.2). The heat generation efficiency of MNPs in presence of AMF is measured in terms of specific absorption rate (SAR). The higher the SAR value, the better is the heat producing capacity of MNPs. It has been reported that SAR value is influenced by number of factors like nanoparticle size and its surface chemistry, its shape and applied frequency and field intensity of AMF [72]. Also, SAR value is dependent upon the exposure time of AMF and the solvent in which MNPs are suspended.
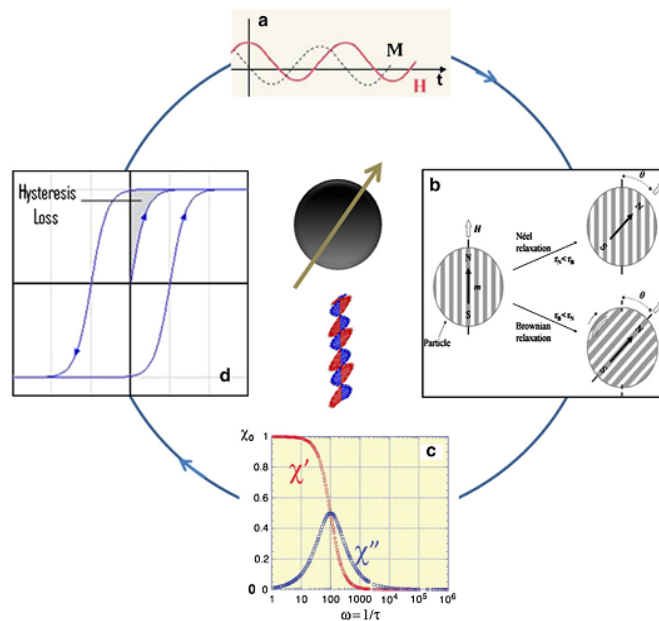
Figure 1.2 Schematic representation showing possible mechanisms of conversion of magnetic energy into heat energy. Reprinted from [89] - Reproduced with permission from Elsevier Ltd. and IEEE.

Magnetic hyperthermia therapy using magnetic nanoparticles has been clinically used for treating tumors along with traditional chemotherapy and radiation therapy [94-96]. Moreover, several studies have also attached a targeting molecule (e.g., antibody, protein molecule, anti-cancer drug) for cancer cells specific therapy using MNPs. In majority of these studies, due to presence of targeting molecule on the surface, the nanoparticles are able to attach and enter only in cancer specific cells. This has been found to be extremely advantageous as once the nanoparticles are attached to the cancer cells, applying alternate magnetic fields will heat up only the cancer specific cells/tissue leaving the non-cancer cells/tissue harmless [72, 90, 97-102] (Figure 1.3).
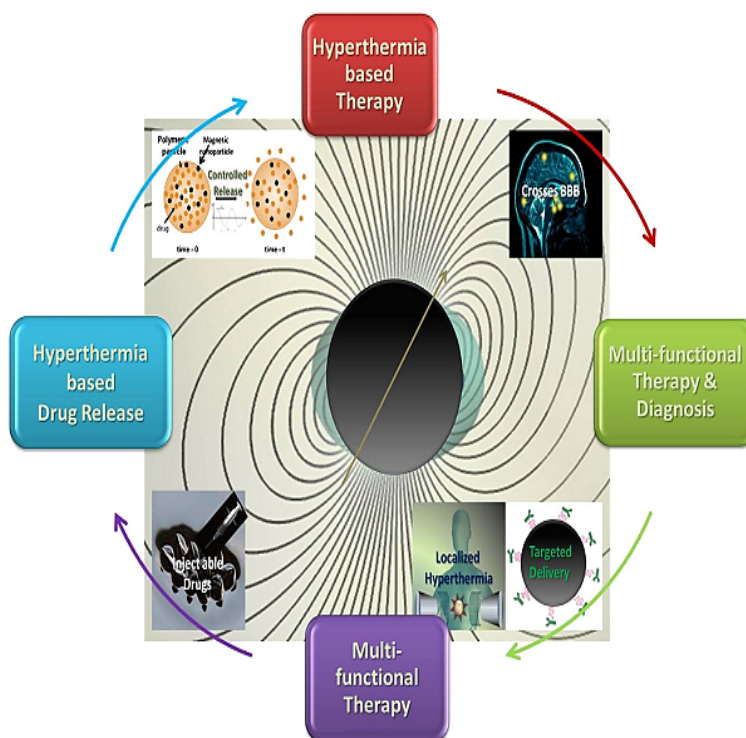
Figure 1.3 Magnetic nanomaterials based hyperthermia therapy applications. Reprinted from [89] - Reproduced with permission from Elsevier Ltd.

Such targeted magnetic hyperthermia treatment can potentially revolutionize cancer therapy regimen by drastically reducing the side effects, which are usually found with chemotherapy. The heating rate of MNPs in magnetic hyperthermia is found to be dependent on numerous factors like concentration of nanoparticles, nanoparticle core size and shape of nanoparticles, surface chemistry of nanoparticles, applied frequency and field intensity of the instrument, and time [90]. Moreover, magnetic nanoparticles have also been successfully used as commercial contrasting agents in MRI imaging [91]. However, there are very few reports of treating bacterial infections by using magnetic hyperthermia [103-105].

One such study performed by Thomas *et al.* used magnetic hyperthermia in presence of carboxylic-acid functionalized MNPs as alternative treatment option for killing *Staphylococcus aureus* cells [106]. They exposed the bacterial cells to AC magnetic field in presence of relatively high concentration of MNPs (up to 50 mg/ml). 10^7-log reduction in bacterial counts was observed within 4 minutes of magnetic hyperthermia treatment in presence of 50 mg/ml concentration of MNPs. In another similar work, Park and co-workers studied the inactivation rate of *Pseudomonas aeruginosa* biofilms in presence of commercially available superparamagnetic iron oxide nanoparticles (SPIONs) and AC magnetic fields [104]. ~4-log reduction in biofilm was achieved through 8 minutes of magnetic hyperthermia treatment using concentration of 60 mg/ml MNPs. They attributed this reduction to disintegration of bacterial cell

membrane at elevated temperatures, which are attained during the hyperthermia treatment. It should be duly noted that in both the above mentioned research studies, the killing of bacterial cells was mainly achieved by sheer increase in the bulk temperature through high concentrations of MNPs and AC magnetic fields. Also, none of the above studies utilized any specific targeting molecule/ligand for targeted hyperthermia therapy.

Magnetically Mediated Energy Delivery (MagMED)

According to conventional theories, applying external alternate magnetic fields in presence of MNPs would result in macroscopic temperature rise and hence aptly referred to as magnetic hyperthermia therapy. The main drawback of this therapy is that to actually get a clinically relevant temperature increase in the living systems mainly *in vitro* and *in vivo* models, large concentrations of MNPs is needed. As majority of the on-going clinical studies utilizing magnetic hyperthermia therapy through MNPs is for cancer treatment, it is not feasible to directly deliver such a large payload of nanoparticles to the desired location in the body via commonly administered routes, e.g., intravenous, intranasal, transdermal, intrathecal, etc. which could substantially increase the temperature of the body region/tissue.

One possible way to reduce the concentration of MNPs to get desired results in terms of killing cancer cells or tumors is to actually make MNPs in such a way that they can be completely internalized by these cells and can target the intracellular pathways providing selective killing without actually rising the overall temperature of the system. In such cases, it would be incorrect to use the term magnetic hyperthermia. Hence, a few

research groups (Dr. Carlos Rinaldi, University of Florida; Dr. O. Thompson Mefford, Clemson University) coined the term 'magnetically mediated energy delivery' (MagMED) to explain the instances where apoptosis of cancer cells was achieved in presence of MNPs and alternate magnetic fields without a major change in the overall temperature of the system [100].

Recent experimental studies have shed new insights on explaining how local temperature rise is attained during MagMED treatment without bulk temperature increases in tissue environment. A study by Huang *et al.* showed that it is possible to remotely activate calcium ion channels in neural cells through alternate magnetic fields with minimal changes in bulk temperature of the tissues [107]. They synthesized manganese ferrite nanoparticles functionalized with streptavidin, which can selectively bind to TRPV1 receptors in neural cells. Finally, they grafted thermal responsive fluorophores on the outer surface of nanoparticles and used alternate magnetic fields to thermally activate ion channels. Through this study, the authors were able to show ~20°C increase in local temperature on the surface of nanoparticles without bulk temperature rise based on the changes in the fluorescence intensity of the fluorophores that were present on the nanoparticles surface.

In another study, Creixell and co-workers performed MagMED experiments in which they observed 99.9% reduction in viability of breast cancer cells in presence of iron-oxide nanoparticles [108]. They functionalized dextran-coated iron-oxide nanoparticles with epidermal growth factor (EGF) targeting ligands that can preferentially attach only to cancer cells. After MagMED therapy, they noticed that the

targeted nanoparticles were greatly internalized by the breast cancer cells compared to non-targeted ones and resulted in reduction in cell-viability of those cells. During this study, they did not notice any measurable increase in temperature when AMF was applied. An extension of the above study by the same research group tried to elucidate the underlying mechanism by which MNPs present in intracellular regions can prove toxic to cancer cells in presence of AMF without bulk temperature increase [109]. The same targeted group of nanoparticles were mixed with breast cancer cells and in presence of AMF, the internalized MNPs could selectively induce lysosomal membrane permeabilization of breast cancer cells. The authors suggested that increased lysosomal permeabilization could result in cellular death of breast cancer cells through increase in reactive oxygen species (ROS) and lysosomal cathepsins production in presence of AMF.

In all of the above reported MagMED studies, the exact mechanisms of intracellular events that are responsible for apoptosis of cancer cells in presence of AMF and MNPs are still not fully understood. Some of the possible ways through which these events are currently explained are: 1) highly localized increase of temperature on the surface of nanoparticles can disrupt several signaling pathways in cells; 2) application of AMF in presence of MNPs can physically/mechanically damage the cell membrane via Neel and Brownian relaxation processes (rotational or vibrational moments of nanoparticles).

Biocompatibility of Magnetic Nanoparticles

In last two decades, there has been tremendous increase in the usage of engineered nanomaterials for various industrial products and the demand is rapidly increasing. Analysts have forecasted that nanomaterial based industrial products will drive the global economic markets by more than 100 billion dollars per annum between the years 2011-2015 [110]. The flexibility to engineer different types of nanomaterials with desired physico-chemical properties has made it possible to use these nanomaterials in numerous biomedical applications. In fact, nanomaterials based treatment therapies for cancer diagnosis and therapy, drug delivery and imaging are already in clinical trial stages [111-117]. However, several factors regarding biocompatibility and toxicity of these nanomaterials still need to be addressed in detail. There is a complex relationship between the morphology, size and chemical properties of these nanomaterials that would eventually determine its toxicity in living organisms and the environment [110, 118-120]. The magnetic properties displayed by magnetic nanoparticles have been extensively utilized in wide range of biomedical applications like MRI imaging, drug delivery, pathogen detection, magnetic cell-separation or magnetic hyperthermia [80, 121-123]. Magnetic nanoparticles have also increased the overall efficacy of anticancer drugs and its presence has also reversed multidrug resistance commonly found in cancer cells [124]. To render magnetic nanoparticles biocompatible, they need to be coated with suitable polymers, which would keep them stable in biological environment. Depending on the overall size of the nanoparticle system, the stabilizing polymer and the type of chemical group present on the polymer end, MNPs can behave and interact differently with the

23

proteins present in the biological environment. Although magnetic nanoparticles have been reported to have excellent biocompatibility [125-127], they might exert toxicity to the host cell depending on their size, surface chemistry and its ability to interact with the proteins present in body fluids. Numerous *in vitro* and *in vivo* studies have demonstrated differential toxicity of MNPs [78, 79, 124, 128-131]. The different toxicity mechanisms observed in determining safe dosage levels of MNPs in these studies include impaired mitochondrial function, cytotoxicity, cell apoptosis, DNA damage and genotoxicity, immunotoxicity, oxidative stress, disordered cell morphology, cytoskeleton damage, cell-membrane damage etc. [131-136]. Therefore, an in-depth and thorough analysis of toxicological profile of MNPs are warranted to make sure that they are biocompatible in living systems before using them clinical settings.

Objectives

MNPs bio-functionalized with different polymers and molecules have been researched widely for diverse biomedical applications. The kind of targeted moiety attached onto surface of MNPs determines the kind of interactions it would have with bacterial and mammalian cells. These interactions are greatly dependent on kind of synthesis procedures used for making MNPs, size of MNPs, type of polymer used as stabilizing agent and finally on the type of cell with which MNPs interacts both in *in vitro* and *in vivo* conditions. The main goal of this dissertation was to synthesize proof-of-concept bacterial adhesin specific MNPs that are bio-functionalized with specific glycoconjugate molecule (GM3), and which can selectively interact with *EC* K99 strain

24

in absence/presence of AMF. The first aim deals with synthesizing mono-anchored GM3-MNPs that are stabilized with heterobifunctional PEO polymer and evaluating its interactions with *EC* K99. The second aim explores the feasibility of using multi-anchored GM3-MNPs in conjunction with AMF for targeted killing of *EC* K99 both in pure and mixed culture environment and trying to explain the possible mechanisms through which *EC* K99 is destroyed. And the last aim investigates the biocompatibility and interaction of our novel MNPs system with normal human colon cells CCD-18Co by employing various toxicity assays. The results obtained in this project will greatly help in providing a unique non-antibiotic platform for treating bacterial infections via MNPs and AMF with minimum toxicity to host-tissue.

References:

1. Neu, H.C., *The crisis in antibiotic resistance.* Science, 1992. **257**(5073): p. 1064-1073.
2. Doern, G.V., *Antimicrobial use and the emergence of antimicrobial resistance with Streptococcus pneumoniae in the United States.* Clinical infectious diseases : an official publication of the Infectious Diseases Society of America, 2001. **33 Suppl 3**: p. S187-192.
3. Mulligan, M.E., *et al.*, *Methicillin-resistant Staphylococcus aureus: a consensus review of the microbiology, pathogenesis, and epidemiology with implications for prevention and management.* The American journal of medicine, 1993. **94**(3): p. 313-228.
4. Cetinkaya, Y., P. Falk, and C.G. Mayhall, *Vancomycin-resistant enterococci.* Clinical Microbiology Reviews, 2000. **13**(4): p. 686-707.
5. Walsh, C., *Molecular mechanisms that confer antibacterial drug resistance.* Nature, 2000. **406**(6797): p. 775-781.
6. *Threat Report 2013*. 2013 September 16 2013 [cited 2013 September 16 2013]; Available from: http://www.cdc.gov/drugresistance/threat-report-2013/.
7. Ofek, I., I. Kahane, and N. Sharon, *Toward anti-adhesion therapy for microbial diseases.* Trends in Microbiology, 1996. **4**(8): p. 297-299.

8.   Naruse, Y., *Theoretical concept of physical antibiotics using nanoparticles.* Japanese Journal of Applied Physics, 2005. **44**: p. 3330.

9.   Sondi, I. and B. Salopek-Sondi, *Silver nanoparticles as antimicrobial agent: a case study on E. coli as a model for Gram-negative bacteria.* Journal of Colloid and Interface Science, 2004. **275**(1): p. 177-182.

10.   Ofek, I., D. Mirelman, and N. Sharon, *Adherence of Escherichia coli to human mucosal cells mediated by mannose receptors.* Nature, 1977. **265**(5595): p. 623-625.

11.   Karlsson, K., *Bacterium-host protein-carbohydrate interactions and pathogenicity.* Biochemical Society Transactions, 1999. **27**(4): p. 471.

12.   Beachey, E.H., *Bacterial adherence: adhesin-receptor interactions mediating the attachment of bacteria to mucosal surface.* The Journal of Infectious Diseases, 1981. **143**(3): p. 325-345.

13.   Sharon, N. and I. Ofek, *Safe as mother's milk: carbohydrates as future anti-adhesion drugs for bacterial diseases.* Glycoconj J, 2000. **17**(7-9): p. 659-664.

14.   Ofek, I. and R.J. Doyle, *Bacterial adhesion to cells and tissues.* 1994: Chapman & Hall New York.

15.   Sharon, N. and H. Lis, *Lectins as cell recognition molecules.* Science, 1989. **246**(4927): p. 227-234.

16.   Duguid, J. and D. Old, *Adhesive properties of Enterobacteriaceae*, in *Bacterial adherence.* 1980, Springer. p. 185-217.

17.   Krogfelt, K.A., *Bacterial adhesion: genetics, biogenesis, and role in pathogenesis of fimbrial adhesins of Escherichia coli.* Reviews of Infectious Diseases, 1991. **13**(4): p. 721-735.

18.   Sharon, N. and H. Lis, *Carbohydrates in cell recognition.* Scientific American, 1993. **268**(1): p. 82-90.

19.   Varki, A., *Selectin ligands.* Proceedings of the National Academy of Sciences of the United States of America, 1994. **91**(16): p. 7390-7397.

20.   Varki, A., *Biological roles of oligosaccharides: all of the theories are correct.* Glycobiology, 1993. **3**(2): p. 97-130.

21.   Mammen, M., G. Dahmann, and G.M. Whitesides, *Effective inhibitors of hemagglutination by influenza virus synthesized from polymers having active ester groups. Insight into mechanism of inhibition.* Journal of Medicinal Chemistry, 1995. **38**(21): p. 4179-4190.

22.   Mammen, M., S.-K. Choi, and G.M. Whitesides, *Polyvalent interactions in biological systems: implications for design and use of multivalent ligands and inhibitors.* Angewandte Chemie International Edition, 1998. **37**(20): p. 2754-2794.

23.   Sharon, N., *Bacterial lectins, cell-cell recognition and infectious disease.* FEBS Letters, 1987. **217**(2): p. 145-157.

24.   Sharon, N., *Carbohydrates as future anti-adhesion drugs for infectious diseases.* Biochimica et biophysica acta, 2006. **1760**(4): p. 527-37.

25.   Merritt, E.A. and W. Hol, *AB5 toxins.* Current Opinion in Structural Biology, 1995. **5**(2): p. 165-171.

26. Kitov, P.I., *et al.*, *Shiga-like toxins are neutralized by tailored multivalent carbohydrate ligands.* Nature, 2000. **403**(6770): p. 669-672.

27. Karmali, M.A., *et al.*, *The association between idiopathic hemolytic uremic syndrome and infection by verotoxin-producing Escherichia coli.* The Journal of Infectious Diseases, 1985. **151**(5): p. 775-782.

28. Todar, K., *Todar's online textbook of bacteriology.* 2006: University of Wisconsin-Madison Department of Bacteriology.

29. Black, R.E., *Epidemiology of travelers' diarrhea and relative importance of various pathogens.* Reviews of infectious diseases, 1990. **12 Suppl 1**: p. S73-9.

30. Mouricout, M.A. and R.A. Julien, *Pilus-mediated binding of bovine enterotoxigenic Escherichia coli to calf small intestinal mucins.* Infection and Immunity, 1987. **55**(5): p. 1216-1223.

31. Barigye, R., *et al.*, *Prevalence and antimicrobial susceptibility of virulent and avirulent multidrug-resistant Escherichia coli isolated from diarrheic neonatal calves.* American Journal of Veterinary Research, 2012. **73**(12): p. 1944-1950.

32. de Verdier, K., *et al.*, *Antimicrobial resistance and virulence factors in Escherichia coli from Swedish dairy calves.* Acta Veterinaria Scandinavica, 2012. **54**(1): p. 2-2.

33. Güler, L., K. Gündüz, and Ü. Ok, *Virulence factors and antimicrobial susceptibility of Escherichia coli isolated from calves in Turkey.* Zoonoses and Public Health, 2008. **55**(5): p. 249-257.

34. Gonzalez, E.A. and J. Blanco, *Colonization antigens, antibiotic resistance and plasmid content of enterotoxigenic Escherichia coli isolated from piglets with diarrhoea in galicia (North-Western Spain).* Veterinary Microbiology, 1986. **11**(3): p. 271-283.

35. Smith, H.W. and M.A. Linggood, *Further observations on Escherichia coli enterotoxins with particular regard to those produced by atypical piglet strains and by calf and lamb strains: the transmissible nature of these enterotoxins and of a K antigen possessed by calf and lamb strains.* Journal of Medical Microbiology, 1972. **5**(2): p. 243-250.

36. Nagy, B., H.W. Moon, and R.E. Isaacson, *Colonization of porcine intestine by enterotoxigenic Escherichia coli: selection of piliated forms in vivo, adhesion of piliated forms to epithelial cells in vitro, and incidence of a pilus antigen among porcine enteropathogenic E. coli.* Infection and Immunity, 1977. **16**(1): p. 344-352.

37. Nagy, B., *et al.*, *Immunization of suckling pigs against enteric enterotoxigenic Escherichia coli infection by vaccinating dams with purified pili.* Infection and Immunity, 1978. **21**(1): p. 269-274.

38. Isaacson, R.E., B. Nagy, and H.W. Moon, *Colonization of porcine small intestine by Escherichia coli: colonization and adhesion factors of pig enteropathogens that lack K88.* The Journal of Infectious Diseases, 1977. **135**(4): p. 531-539.

39. Isaacson, R.E., *et al.*, *In vitro adhesion of Escherichia coli to porcine small intestinal epithelial cells: pili as adhesive factors.* Infection and Immunity, 1978. **21**(2): p. 392-397.

40.   Kyogashima, M., V. Ginsburg, and H.C. Krivan, *Escherichia coli K99 binds to N-glycolylsialoparagloboside and N-glycolyl-GM3 found in piglet small intestine.* Archives of Biochemistry and Biophysics, 1989. **270**(1): p. 391-397.

41.   Mouricout, M., *et al.*, *Glycoprotein glycans that inhibit adhesion of Escherichia coli mediated by K99 fimbriae: treatment of experimental colibacillosis.* Infection and Immunity, 1990. **58**(1): p. 98-106.

42.   Karlsson, K.A., *Meaning and therapeutic potential of microbial recognition of host glycoconjugates.* Molecular Microbiology, 1998. **29**(1): p. 1-11.

43.   Zopf, D. and S. Roth, *Oligosaccharide anti-infective agents.* Lancet, 1996. **347**(9007): p. 1017-1021.

44.   Ofek, I., D.L. Hasty, and N. Sharon, *Anti-adhesion therapy of bacterial diseases: prospects and problems.* FEMS Immunology and Medical Microbiology, 2003. **38**(3): p. 181-191.

45.   Sharon, N. and I. Ofek, *Fighting infectious diseases with inhibitors of microbial adhesion to host tissues.* Critical reviews in Food Science and Nutrition, 2002. **42**(3 Suppl): p. 267-72.

46.   Choi, S.K., M. Mammen, and G.M. Whitesides, *Monomeric inhibitors of influenza neuraminidase enhance the hemagglutination inhibition activities of polyacrylamides presenting multiple C-sialoside groups.* Chemistry and Biology, 1996. **3**(2): p. 97-104.

47.   Firon, N., *et al.*, *Aromatic alpha-glycosides of mannose are powerful inhibitors of the adherence of type 1 fimbriated Escherichia coli to yeast and intestinal epithelial cells.* Infection and Immunity, 1987. **55**(2): p. 472-476.

48.   Chaturvedi, P., *et al.*, *Milk oligosaccharide profiles by reversed-phase HPLC of their perbenzoylated derivatives.* Analytical Biochemistry, 1997. **251**(1): p. 89-97.

49.   Ernst, B. and J.L. Magnani, *From carbohydrate leads to glycomimetic drugs.* Nature Reviews Drug Discovery, 2009. **8**(8): p. 661-677.

50.   Burtscher, C. and S. Wuertz, *Evaluation of the use of PCR and reverse transcriptase PCR for detection of pathogenic bacteria in biosolids from anaerobic digestors and aerobic composters.* Applied and Environmental Microbiology, 2003. **69**(8): p. 4618-4627.

51.   Van Dyck, E., *et al.*, *Detection of Chlamydia trachomatis and Neisseria gonorrhoeae by enzyme immunoassay, culture, and three nucleic acid amplification tests.* Journal of Clinical Microbiology, 2001. **39**(5): p. 1751-1756.

52.   Velusamy, V., *et al.*, *An overview of foodborne pathogen detection: in the perspective of biosensors.* Biotechnology Advances, 2010. **28**(2): p. 232-254.

53.   Leonard, P., *et al.*, *Advances in biosensors for detection of pathogens in food and water.* Enzyme and Microbial Technology, 2003. **32**(1): p. 3-13.

54.   Shinde, S.B., C.B. Fernandes, and V.B. Patravale, *Recent trends in in-vitro nanodiagnostics for detection of pathogens.* Journal of Controllded Release, 2012. **159**(2): p. 164-80.

55.   Lin, C.C., *et al.*, *Selective binding of mannose-encapsulated gold nanoparticles to type 1 pili in Escherichia coli.* Journal of the American Chemical Society, 2002. **124**(14): p. 3508-3509.

56. El-Boubbou, K., C. Gruden, and X. Huang, *Magnetic glyco-nanoparticles: a unique tool for rapid pathogen detection, decontamination, and strain differentiation.* Journal of the American Chemical Society, 2007. **129**(44): p. 13392-13393.

57. Huang, C.C., *et al.*, *Synthesis of fluorescent carbohydrate-protected Au nanodots for detection of Concanavalin A and Escherichia coli.* Analytical Chemistry, 2009. **81**(3): p. 875-882.

58. Joralemon, M.J., *et al.*, *Synthesis, characterization, and bioavailability of mannosylated shell cross-linked nanoparticles.* Biomacromolecules, 2004. **5**(3): p. 903-913.

59. Kim, B.S., *et al.*, *Carbohydrate-coated nanocapsules from amphiphilic rod-coil molecule: binding to bacterial type 1 pili.* Chemical Communications, 2005(15): p. 2035-2037.

60. Qu, L., *et al.*, *Visualizing adhesion-induced agglutination of Escherichia coli with mannosylated nanoparticles.* Journal of Nanoscience & Nanotechnology, 2005. **5**(2): p. 319-322.

61. Liu, L.H., *et al.*, *Photoinitiated coupling of unmodified monosaccharides to iron oxide nanoparticles for sensing proteins and bacteria.* Bioconjugate Chemistry, 2009. **20**(7): p. 1349-1355.

62. Kaittanis, C., *et al.*, *Identification of molecular-mimicry-based ligands for cholera diagnostics using magnetic relaxation.* Bioconjugate Chemistry, 2011. **22**(2): p. 307-314.

63. Schofield, C.L., R.A. Field, and D.A. Russell, *Glyconanoparticles for the colorimetric detection of cholera toxin.* Analytical Chemistry, 2007. **79**(4): p. 1356-1361.

64. Kulkarni, A.A., *et al.*, *Glycan encapsulated gold nanoparticles selectively inhibit shiga toxins 1 and 2.* Bioconjugate Chemistry, 2010. **21**(8): p. 1486-1493.

65. Chien, Y.Y., *et al.*, *Globotriose-functionalized gold nanoparticles as multivalent probes for Shiga-like toxin.* Chembiochem : A European Journal of Chemical Biology, 2008. **9**(7): p. 1100-1109.

66. Lin, C.-C., *et al.*, *Selective binding of mannose-encapsulated gold nanoparticles to type 1 pili in Escherichia coli.* Journal of the American Chemical Society, 2002. **124**(14): p. 3508-3509.

67. Marradi, M., M. Martin-Lomas, and S. Penades, *Glyconanoparticles polyvalent tools to study carbohydrate-based interactions.* Advances in Carbohydrate Chemistry & Biochemistry, 2010. **64**: p. 211-290.

68. Sunasee, R., *et al.*, *Therapeutic potential of carbohydrate-based polymeric and nanoparticle systems.* Expert Opinion on Drug Delivery, 2014. **11**(6): p. 867-884.

69. El-Boubbou, K., C. Gruden, and X. Huang, *Magnetic glyco-nanoparticles: a unique tool for rapid pathogen detection, decontamination, and strain differentiation.* Journal of the American Chemical Society, 2007. **129**(44): p. 13392-13393.

70. Qu, L.W., *et al.*, *Galactosylated Polymeric Nanoparticles: Synthesis and Adhesion Interactions with Escherichia coli.* Journal of Biomedical Nanotechnology, 2005. **1**(1): p. 61-67.

71. Park, S., *et al.*, *Probing cell-surface carbohydrate binding proteins with dual-modal glycan-conjugated nanoparticles.* Journal of the American Chemical Society, 2015. **137**(18): p. 5961-5968.

72. Stone, R., *et al.*, *Targeted magnetic hyperthermia.* Therapeutic Delivery, 2011. **2**(6): p. 815-838.

73. Lu, A.H., E.L. Salabas, and F. Schuth, *Magnetic nanoparticles: synthesis, protection, functionalization, and application.* Angewandte Chemie, 2007. **46**(8): p. 1222-1244.

74. Laurent, S., *et al.*, *Magnetic iron oxide nanoparticles: synthesis, stabilization, vectorization, physicochemical characterizations, and biological applications.* Chemical Reviews, 2008. **108**(6): p. 2064-2110.

75. Park, J., *et al.*, *Ultra-large-scale syntheses of monodisperse nanocrystals.* Nature Materials, 2004. **3**(12): p. 891-895.

76. Petri-Fink, A. and H. Hofmann, *Superparamagnetic Iron Oxide Nanoparticles (SPIONs): From Synthesis to In Vivo Studies - A Summary of the Synthesis, Characterization, In Vitro, and In Vivo Investigations of SPIONs With Particular Focus on Surface and Colloidal Properties.* NanoBioscience, IEEE Transactions on, 2007. **6**(4): p. 289-297.

77. Amstad, E., M. Textor, and E. Reimhult, *Stabilization and functionalization of iron oxide nanoparticles for biomedical applications.* Nanoscale, 2011. **3**(7): p. 2819-43.

78. Shubayev, V.I., T.R. Pisanic, 2nd, and S. Jin, *Magnetic nanoparticles for theragnostics.* Advanced Drug Delivery Reviews, 2009. **61**(6): p. 467-477.

79. Reddy, L.H., *et al.*, *Magnetic nanoparticles: design and characterization, toxicity and biocompatibility, pharmaceutical and biomedical applications.* Chemical Reviews, 2012. **112**(11): p. 5818-5878.

80. Gao, J., H. Gu, and B. Xu, *Multifunctional magnetic nanoparticles: design, synthesis, and biomedical applications.* Accounts of Chemical Research, 2009. **42**(8): p. 1097-1107.

81. Ulbrich, K., *et al.*, *Targeted Drug Delivery with Polymers and Magnetic Nanoparticles: Covalent and Noncovalent Approaches, Release Control, and Clinical Studies.* Chemical Reviews, 2016. **116**(9): p. 5338-5431.

82. Abuchowski, A., *et al.*, *Effect of covalent attachment of polyethylene glycol on immunogenicity and circulating life of bovine liver catalase.* Journal of Biological Chemistry, 1977. **252**(11): p. 3582-3586.

83. Li, W., *et al.*, *Current drug research on PEGylation with small molecular agents.* Progress in Polymer Science, 2013. **38**(3–4): p. 421-444.

84. Sun, C., *et al.*, *PEG-mediated synthesis of highly dispersive multifunctional superparamagnetic nanoparticles: their physicochemical properties and function in vivo.* ACS Nano, 2010. **4**(4): p. 2402-2410.

85. Harris, J.M. and R.B. Chess, *Effect of pegylation on pharmaceuticals*. Nature Reviews Drug Discovery, 2003. **2**(3): p. 214-221.

86. Roberts, M.J., M.D. Bentley, and J.M. Harris, *Chemistry for peptide and protein PEGylation*. Advanced Drug Delivery Reviews, 2002. **54**(4): p. 459-476.

87. Veronese, F.M. and G. Pasut, *PEGylation, successful approach to drug delivery*. Drug Discovery Today, 2005. **10**(21): p. 1451-1458.

88. Jeong, U., *et al.*, *Superparamagnetic Colloids: Controlled Synthesis and Niche Applications*. Advanced Materials, 2007. **19**(1): p. 33-60.

89. Gilchrist, R.K., *et al.*, *Selective inductive heating of lymph nodes*. Annals of surgery, 1957. **146**(4): p. 596-606.

90. Kumar, C.S. and F. Mohammad, *Magnetic nanomaterials for hyperthermia-based therapy and controlled drug delivery*. Advanced Drug Delivery Reviews, 2011. **63**(9): p. 789-808.

91. Kumar, C.S., *Nanomaterials for medical diagnosis and therapy*. Vol. 10. 2007: Wiley-VCH.

92. Rudolf, H., *et al.*, *Magnetic particle hyperthermia: nanoparticle magnetism and materials development for cancer therapy*. Journal of Physics: Condensed Matter, 2006. **18**(38): p. S2919.

93. Rudolf, H., D. Silvio, and R. Michael, *Effects of size distribution on hysteresis losses of magnetic nanoparticles for hyperthermia*. Journal of Physics: Condensed Matter, 2008. **20**(38): p. 385214.

94. Maier-Hauff, K., *et al.*, *Efficacy and safety of intratumoral thermotherapy using magnetic iron-oxide nanoparticles combined with external beam radiotherapy on patients with recurrent glioblastoma multiforme*. Journal of Neuro-Oncology, 2011. **103**(2): p. 317-324.

95. Johannsen, M., *et al.*, *Morbidity and quality of life during thermotherapy using magnetic nanoparticles in locally recurrent prostate cancer: Results of a prospective phase I trial*. International Journal of Hyperthermia, 2007. **23**(3): p. 315-323.

96. Maier-Hauff, K., *et al.*, *Intracranial Thermotherapy using Magnetic Nanoparticles Combined with External Beam Radiotherapy: Results of a Feasibility Study on Patients with Glioblastoma Multiforme*. Journal of Neuro-Oncology, 2007. **81**(1): p. 53-60.

97. Kumar, C.S., *Nanomaterials for cancer therapy*. Vol. 6. 2006: Wiley-VCH Weinheim, Germany.

98. Cherukuri, P., E.S. Glazer, and S.A. Curley, *Targeted hyperthermia using metal nanoparticles*. Advanced Drug Delivery Reviews, 2010. **62**(3): p. 339-345.

99. Pankhurst, Q.A., *et al.*, *Applications of magnetic nanoparticles in biomedicine*. Journal of physics D: Applied physics, 2003. **36**(13): p. R167.

100. Kozissnik, B., *et al.*, *Magnetic fluid hyperthermia: Advances, challenges, and opportunity*. International Journal of Hyperthermia, 2013. **29**(8): p. 706-714.

101. Sonvico, F., *et al.*, *Folate-conjugated iron oxide nanoparticles for solid tumor targeting as potential specific magnetic hyperthermia mediators: synthesis,*

physicochemical characterization, and in vitro experiments. Bioconjugate Chemistry, 2005. **16**(5): p. 1181-1188.

102. Jordan, A., *et al.*, *Magnetic fluid hyperthermia (MFH): Cancer treatment with AC magnetic field induced excitation of biocompatible superparamagnetic nanoparticles.* Journal of Magnetism and Magnetic Materials, 1999. **201**(1): p. 413-419.

103. Thomas, L.A., *et al.*, *Carboxylic acid-stabilised iron oxide nanoparticles for use in magnetic hyperthermia.* Journal of Materials Chemistry, 2009. **19**(36): p. 6529-6535.

104. Park, H., *et al.*, *Inactivation of Pseudomonas aeruginosa PA01 biofilms by hyperthermia using superparamagnetic nanoparticles.* Journal of Microbiological Methods, 2011. **84**(1): p. 41-45.

105. Kim, M.H., *et al.*, *Magnetic nanoparticle targeted hyperthermia of cutaneous Staphylococcus aureus infection.* Annals of Biomedical Engineering, 2013. **41**(3): p. 598-609.

106. Thomas, L.A., *et al.*, *Carboxylic acid-stabilised iron oxide nanoparticles for use in magnetic hyperthermia.* Journal of Materials Chemistry, 2009. **19**(36): p. 6529-6535.

107. Huang, H., *et al.*, *Remote control of ion channels and neurons through magnetic-field heating of nanoparticles.* Nature Nanotechnol, 2010. **5**(8): p. 602-606.

108. Creixell, M., *et al.*, *EGFR-targeted magnetic nanoparticle heaters kill cancer cells without a perceptible temperature rise.* ACS Nano, 2011. **5**(9): p. 7124-7129.

109. Domenech, M., *et al.*, *Lysosomal membrane permeabilization by targeted magnetic nanoparticles in alternating magnetic fields.* ACS Nano, 2013. **7**(6): p. 5091-5101.

110. Wiesner, M.R., *et al.*, *Assessing the risks of manufactured nanomaterials.* Environmental Science & Technology, 2006. **40**(14): p. 4336-4345.

111. Plotkin, M., *et al.*, *18F-FET PET for planning of thermotherapy using magnetic nanoparticles in recurrent glioblastoma.* International Journal of Hyperthermia, 2006. **22**(4): p. 319-325.

112. Heuck, C.J., *et al.*, *Myeloma is characterized by stage-specific alterations in DNA methylation that occur early during myelomagenesis.* Journal of Immunology, 2013. **190**(6): p. 2966-2975.

113. Feldman, E.J., *et al.*, *Pharmacokinetics of CPX-351; a nano-scale liposomal fixed molar ratio formulation of cytarabine:daunorubicin, in patients with advanced leukemia.* Leukemia Research, 2012. **36**(10): p. 1283-1289.

114. Ko, Y.-J., *et al.*, *Nanoparticle albumin-bound paclitaxel for second-line treatment of metastatic urothelial carcinoma: a single group, multicentre, phase 2 study.* The Lancet Oncology, 2013.

115. Yilmaz, A., *et al.*, *Magnetic resonance imaging (MRI) of inflamed myocardium using iron oxide nanoparticles in patients with acute myocardial infarction - Preliminary results.* International Journal of Cardiology, 2013. **163**(2): p. 175-182.

116.   Ando, M., *et al.*, *Phase I and pharmacokinetic study of nab-paclitaxel, nanoparticle albumin-bound paclitaxel, administered weekly to Japanese patients with solid tumors and metastatic breast cancer.* Cancer Chemotherapy and Pharmacology, 2012. **69**(2): p. 457-465.

117.   Kato, K., *et al.*, *Phase II study of NK105, a paclitaxel-incorporating micellar nanoparticle, for previously treated advanced or recurrent gastric cancer.* Investigational New Drugs, 2012. **30**(4): p. 1621-1627.

118.   Firme, C.P., 3rd and P.R. Bandaru, *Toxicity issues in the application of carbon nanotubes to biological systems.* Nanomedicine, 2010. **6**(2): p. 245-256.

119.   Marquis, B.J., *et al.*, *Analytical methods to assess nanoparticle toxicity.* The Analyst, 2009. **134**(3): p. 425-439.

120.   Zhu, M., *et al.*, *Physicochemical properties determine nanomaterial cellular uptake, transport, and fate.* Accounts of Chemical Research, 2013. **46**(3): p. 622-631.

121.   Dave, S.R. and X. Gao, *Monodisperse magnetic nanoparticles for biodetection, imaging, and drug delivery: a versatile and evolving technology.* Wiley Interdisciplinary Reviews: Nanomedicine and Nanobiotechnology, 2009. **1**(6): p. 583-609.

122.   Hahn, P.F., *et al.*, *First clinical trial of a new superparamagnetic iron oxide for use as an oral gastrointestinal contrast agent in MR imaging.* Radiology, 1990. **175**(3): p. 695-700.

123.   Kaittanis, C., S. Santra, and J.M. Perez, *Emerging nanotechnology-based strategies for the identification of microbial pathogenesis.* Advanced Drug Delivery Reviews, 2010. **62**(4-5): p. 408-423.

124.   Szalay, B., *et al.*, *Potential toxic effects of iron oxide nanoparticles in in vivo and in vitro experiments.* Journal of Applied Toxicology, 2012. **32**(6): p. 446-453.

125.   Markides, H., M. Rotherham, and A.J. El Haj, *Biocompatibility and Toxicity of Magnetic Nanoparticles in Regenerative Medicine.* Journal of Nanomaterials, 2012.

126.   Baratli, Y., *et al.*, *Impact of iron oxide nanoparticles on brain, heart, lung, liver and kidneys mitochondrial respiratory chain complexes activities and coupling.* Toxicology In Vitro, 2013. **27**(8): p. 2142-2148.

127.   Kumar, C.S.S.R., *Nanomaterials for Medical Diagnosis and Therapy.* 2007: Wiley.

128.   Sengupta, J., *et al.*, *Physiologically important metal nanoparticles and their toxicity.* Journal of Nanoscience and Nanotechnology, 2014. **14**(1): p. 990-1006.

129.   Mahmoudi, M., *et al.*, *Toxicity evaluations of superparamagnetic iron oxide nanoparticles: cell "vision" versus physicochemical properties of nanoparticles.* ACS Nano, 2011. **5**(9): p. 7263-7276.

130.   Singh, N., *et al.*, *Potential toxicity of superparamagnetic iron oxide nanoparticles (SPION).* Nano Reviews, 2010. **1**.

131.   Griffiths, S.M., *et al.*, *Dextran coated ultrafine superparamagnetic iron oxide nanoparticles: compatibility with common fluorometric and colorimetric dyes.* Analytical Chemistry, 2011. **83**(10): p. 3778-3785.

132.   Wahajuddin and S. Arora, *Superparamagnetic iron oxide nanoparticles: magnetic nanoplatforms as drug carriers.* Int J Nanomedicine, 2012. **7**: p. 3445-3471.

133.   Zhang, H., *et al.*, *Use of metal oxide nanoparticle band gap to develop a predictive paradigm for oxidative stress and acute pulmonary inflammation.* ACS Nano, 2012. **6**(5): p. 4349-4368.

134.   Laurent, S., *et al.*, *Superparamagnetic iron oxide nanoparticles for delivery of therapeutic agents: opportunities and challenges.* Expert Opinion on Drug Delivery, 2014. **11**(9): p. 1449-1470.

135.   Nel, A.E., *et al.*, *Understanding biophysicochemical interactions at the nano–bio interface.* Nature Materials, 2009. **8**(7): p. 543-557.

136.   Feliu, N., *et al.*, *In vivo degeneration and the fate of inorganic nanoparticles.* Chemical Society Reviews, 2016. **45**(9): p. 2440-2457.

Chapter 2

Synthesis and Application of Glycoconjugate-Functionalized Magnetic Nanoparticles as Potent Anti-adhesion Agents for Reducing Enterotoxigenic *Escherichia coli* Infections

1. Introduction:

There has been a recent uprising in the emergence of new multi-drug resistant bacterial strains in the environment, which has resulted in increased morbidity and mortality throughout the world [1-3]. As a result, alternative therapeutic options that are non-antibiotic based are urgently needed to treat such bacterial infections. There have been considerable ongoing scientific interests in understanding multivalent carbohydrate-lectin interactions for various purposes like receptor mimicking, inhibiting bacterial growth and as novel anti-adhesion agents for treating bacterial infections [4-8]. Functionalizing multivalent carbohydrate molecules onto the surface of different nanomaterials offers numerous advantages, e.g., higher affinity constants (K_a) and enthalpy of binding (ΔH) [9, 10], than their monovalent forms in studying ligand-receptor

interactions [11]. Nonetheless, there have been limited reports of using such carbohydrate-functionalized nanomaterials as specific anti-bacterial and anti-adhesion agents. Due to high surface/volume ratio of nanoparticles, it is relatively easy to attach various carbohydrate moieties onto their surface, which has found useful applications in rapid pathogen/toxin detection and its inhibition [12-14]. In several studies, gold nanoparticles [15], magnetic nanoparticles [16], carbon nanotubes [17, 18], polymeric nanoparticles [19-21], and diamond nanoparticles [22] were bio-functionalized with various carbohydrate sugars and used as mimicking agents of host-cell surface receptors that selectively interacted with the adhesin molecules of various *E. coli* strains and resulted in rapid agglutination [20] and reduction in colony forming units (CFUs) of these *E. coli* strains [21]. The unique magnetic properties and biocompatibility displayed by magnetic nanoparticles have been extensively utilized in wide range of biomedical applications like MRI imaging [23], pathogen detection [24], drug-delivery [25], and magnetic hyperthermia [26]. Keeping MNPs stable in biological environments is important in their biomedical applications. Numerous polymer anchor groups like amines [27], alcohols [28], phosphates [29], and carboxylic acids [30] have been utilized to render colloidal stability to MNPs in highly protein-rich biological environments. Of late, anchor groups based on catechols have been extensively researched to provide stable platform for synthesizing multifunctional MNPs [31-34].

Bacterial pathogens utilize two primary mechanisms to adhere onto the host-cell namely carbohydrate-protein recognition and protein-protein interaction [35]. Bacterial adhesin molecules, which take part in carbohydrate-protein interaction, bind bacterial

pathogens onto the host-cell tissue through specific glycolipid or glycoprotein receptors [36]. Enterotoxigenic *Escherichia coli* (ETEC) infection is one of the most common cause of traveler's diarrhea in humans and also in neonatal farm animals like calves, pigs and lambs [37]. Recently, numerous studies have reported increases in multi-drug resistance of ETEC associated with antibiotic treated animal feed [38-41]. Majority of the fimbrial adhesins isolated from ETEC that infected farm animals expressed one or more unique adhesins. These adhesins also act as antigens/virulence factors [41]. *EC* K99 is the main causative agent of bloody diarrhea in young calves, lambs and pigs, a condition also known as colibacillosis. This strain bears K99 antigens, which also act as fimbriae facilitating the adherence of *EC* K99 onto the ileal villus epithelium of calf and pigs and help in initiation of infection [42, 43]. The adhesins of *EC* K99 specifically attach to small intestinal mucus and recognize sialic acid derivatives present on glycolipid receptors [4, 44]. Hence, if this attachment is disrupted, then there is high probability of preventing bacterial infection.

The use of bacterial adhesin-specific glycoconjugate functionalized nanoparticles for prevention/treatment of infections offers several advantages in that it can be designed to target only a specific strain or a specific group of pathogens; it does not impose selection pressure on bacteria exposed to it, hence, minimizing the emergence of resistant bacteria; it is more stable and less expensive than antibodies-based targeting systems, etc. In our previous lab research, we have demonstrated that gold nanoparticles bio-functionalized with specific sialic-acid sequences can cause rapid aggregation of *EC* K99 [45]. Here, we extend our work and further study the intricate details of glycoconjugate

receptor binding specificity of this sequence molecule (Neu5Ac(α2-3)Gal(β1-4)-Glcβ-sp) coated on MNPs (GM3-MNPs) towards *EC* K99 by employing various microscopic techniques and bioassays and show that these MNPs can effectively act as novel non-toxic anti-adhesion agents in reducing ETEC infections.

2. Experimental Section:

***Synthesis of Heterobifunctional Polyethylene Oxide (alkyne-PEO-nitroDOPA)*:** The chemical synthesis of heterobifunctional polyethylene oxide polymer having alkyne at one end and nitroDOPA on the other end is schematically shown in figure 2.1. This complex polymer was synthesized by Roland Stone (PhD student in Dr. O. Thompson Mefford's group, Clemson University). More details regarding the intricate experimental steps involved in synthesizing this polymer and its characterization can be found in the publication, Stone *et al.* 2014 [46].

***Synthesis of Magnetic Nanoparticles*:** The 7.2nm magnetic nanoparticles, synthesized using thermal decomposition of iron(III) acetylacetonate (2mmol), 1,2-hexadecanediol (10mmol), olylamine (4mmol), benzyl ether (20ml), and 6nm iron oxide seeds were added and stirred under a nitrogen flow and brought to 200°C for 1hr to get rid of any moisture. Finally the reaction was brought to reflux for 30mins under a nitrogen head. The particles were purified by precipitation of ethanol and characterized using TEM and DLS.

***Modification of Magnetic Nanoparticles*:** The magnetic nanoparticles were modified by first dissolving alkyne-PEO-nitroDOPA (200 mg, 0.04mmol) into 10ml of

chloroform followed by the slow addition of 1ml (2mg/ml) of magnetic nanoparticles, which were also dispersed in chloroform, while sonicating over 30 mins. The solution was allowed to stir overnight. The particles were then purified by precipitation with hexane, centrifuged to separate particles from solvent. They were then dispersed in ethanol and subsequently precipitated using hexane and separated via centrifugation to collect particles. Finally, the particles were dispersed in deionized water and dialyzed for 3 days.

Synthesis of Magnetic Nanoparticles Functionalized with GM3 Glycoconjugate: The particles with an alkyne surface were then modified using 'click chemistry' with glycoconjugate (Neu5Ac(α2-3)-Gal(β1-4)Glcβ-sp) and azide, 1 : 4 respectively using a copper catalyst for 24 hours in the absence of light. The particles were then dialyzed for 3 days to remove any unbound glycoconjugate, catalyst, and any byproducts of the reaction.

Dynamic Light Scattering (DLS) and Zeta-Potential: DLS was performed on the PEO-coated and GM3-coated magnetic nanoparticles to determine their hydrodynamic radius. The nanoparticle suspensions were diluted in water and placed into a cuvette. Three readings were taken at 25°C using Malvern Zetasizer Nano ZS to determine the intensity average size distribution and z-average diameter. Zeta-potential measurements of these nanoparticle suspensions were also determined using the same instrument. The suspensions were diluted with water and added into zeta-cell and three measurements were taken at 25°C.

Inductively Coupled Plasma Mass Spectroscopy (ICP-MS): The nanoparticle concentration in PEO-MNPs and GM3-MNPs was determined by performing ICP-MS (Thermo-Scientific MS XSeries 2). The nanoparticle suspensions were treated with 2% nitric acid solution in a 15 ml centrifuge tube and subsequently measurements were taken.

Fourier Transform Infrared Spectroscopy (FTIR): FTIR assisted microscopy was done using a Thermo-Nicolet Magna 550 FTIR spectrometer equipped with a Thermo-NicPlan FTIR microscope. Scan number was 16 for each sample including background. Background was collected on a clean germanium plate. Samples were prepped by taking the water suspensions/solution and casting a small drop on a germanium plate. The samples were then set under a heat lamp for 10-15 minutes to dry, resulting in a thin film from which spectrum could be collected using an FTIR microscope.

Fluorescence Microscopy Aggregation Assay: Both *EC* K99 (ATCC 13762) and non-virulent strain *E. coli* O157:H7 6980-2 (*EC* 6980-2; control strain) were transformed with plasmids pGREEN and pGFPuv respectively by electroporation[47]. The green-fluorescent protein (GFP) expressing *E. coli* strains were grown in tryptic soy broth/tryptic soy agar (TSB/TSA) supplemented with ampicillin (100 μg/ml). Freshly grown *E. coli* cultures were used for aggregation assays. After growth, the bacterial cells were centrifuged thrice and re-suspended in 1X sterile phosphate buffered saline (PBS). Approximately, 5×10^7 CFU of bacterial cells were prepared based on optical density (OD_{600}) readings. PEO-

MNPs (40 μg/ml) and GM3-MNPs (40 μg/ml) were mixed with both *EC* K99 and *EC* 6980-2 and this mixture was incubated at room temperature for 30 minutes with gentle shaking. Based on previous method [21], fluorescence microscopy assays were performed at the end of incubation time to visualize nanoparticles-mediated bacterial aggregation.

TEM Imaging of GM3-MNPs and EC K99: TEM imaging was performed to evaluate the specific binding interactions between GM3-MNPs and *EC* K99. GM3-MNPs were added to EC K99 (5×10^7 CFU/ml, suspended in 1X PBS) in an eppendorf tube for 30 minutes at room temperature with gentle shaking. The mixture was centrifuged at 7000 x g for 5 minutes to spin down the bacterial cells along with adherent GM3-MNPs. The supernatant containing unbound GM3-MNPs was removed and the pellet was washed thrice with 1X PBS in repeated centrifugation cycles. This mixture was then fixed in cacodylate-buffered glutaraldehyde (3.5%, pH ~7.4) for 10 -12 hours at 4°C. Subsequently, 3 μl of this mixture was dropped onto a carbon-coated copper grid and allowed to air-dry for 30 minutes. Later, the grids were stained with 2% uranyl acetate solution (3 μl) for 5 minutes and blotted dry with filter-paper (Whatman #4). TEM images were taken on Hitachi H7600 at 120 kV power and magnification ranging from 10000X to 100000X.

CFU Aggregation Assay: In order to determine the extent of GM3-MNPs induced bacterial aggregation, a CFU reduction assay was carried out as previously described [21]. Briefly, both the *E. coli* strains were standardized to a concentration of 5×10^7 CFU in 1X PBS. These bacterial suspensions were then

mixed with different amounts of PEO-MNPs and GM3-MNPs (40 μg/ml and 100 μg/ml) and the mixture was allowed to incubate at room temperature for 30 minutes with gentle shaking. Serial dilutions of these mixtures were made and 50 μl of sample from each dilution tube was transferred onto a sterile, empty petri plate in triplicates. Then, 20 ml of molten TSA (maintained at 45°C) supplemented with ampicillin (100 μg/ml) was carefully poured into the petri plates. The plates were gently rotated to ensure proper mixing of sample and TSA. Finally, after the TSA in the plates solidified, the plates were incubated at 37°C overnight. Next day, the colonies on the plates were counted and CFU reduction was compared to control plates.

*ATP Assay***:** To confirm that the reduction in CFU of *EC* K99 was achieved only due to GM3-MNPs induced bacterial aggregation and not because of inherent toxicity of these nanoparticles, an ATP determination assay [48] was performed using BacTiter-Glo™ microbial cell viability kit (Promega, Madison, WI) following manufacturer's protocol.

*Cytotoxicity Assay***:** To further validate the non-toxic nature of our nanoparticles system, we performed a preliminary cytotoxicity assay on human colon (normal) cell-line CCD-18Co and determined its cell-viability rate after exposing to GM3-MNPs for 24 hours. CCD-18Co Human colon cells (normal) were procured from American Type Culture Collection (ATCC) and grown on 50 cm^2 tissue-culture flask (Corning, NY) in the presence of Eagle's Minimum Essential Medium (EMEM) at 37°C in a humidified atmosphere of 5% CO_2 and 95% air. EMEM was supplemented with 2 mM L-Glutamine,

non-essential amino acids, fetal bovine serum (final concentration – 10%), 100 UI/ml penicillin G, and 100 μg/ml streptomycin. For determining the cytotoxicity of GM3-MNPs, cells between passage generation of 12 and 20 were used. 1.5×10^4 cells/well were seeded (in triplicates) in 96-well culture-plates at 37°C in a humidified atmosphere of 5% CO_2 and 95% air. After 24 hours, varying concentration of GM3-MNPs were added to the cells and incubated for further 24 hours. Next day, MTS assay (CellTiter 96® Aqueous One Solution Cell Proliferation Assay, Promega, USA) was performed according to manufacturer's protocol and the plate was read at 490 nm optical density to measure the absorbance of the formazan product using a microplate reader (Thermo Scientific Multiskan™ FC).

3. Results and Discussion:

In this chapter, we report the synthesis of MNPs coated with heterobifunctional polyethylene oxide (PEO-MNPs) having nitroDOPA as a stable anchoring agent and bio-functionalized with sialic-acid glycoconjugate (Neu5Ac(α2-3)Gal(β1-4)Glcβ-sp) (GM3-MNPs) via 'click chemistry'(Figure 2.1). These GM3-MNPs can effectively act as multivalent ligands, which specifically interact with adhesins present on the *EC* K99.
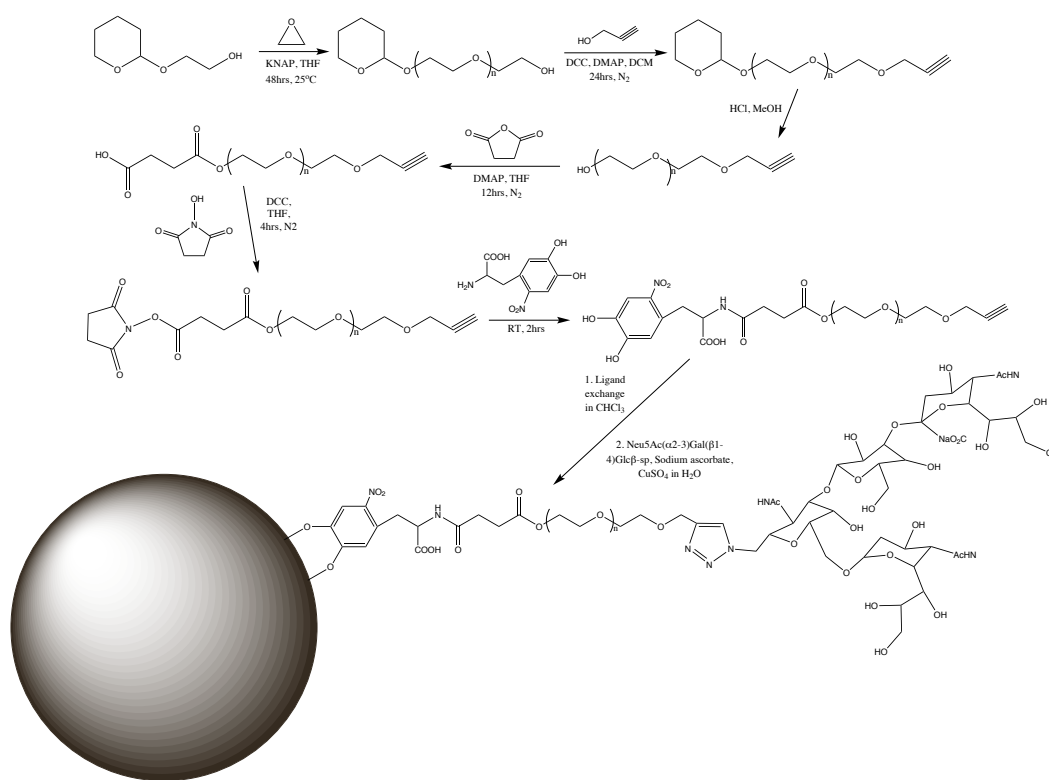
Figure 2.1 Synthesis of heterobifunctional polyethylene oxide coated magnetic nanoparticles bio-functionalized with sialic-acid derivative (Neu5Ac(α2-3)Gal(β1-4)Glcβ-sp).

A heterobifunctional polyethylene oxide (PEO), with a molecular weight of 6300 g/mol, with a protected alcohol on one end and an alcohol on the other was synthesized by the anionic polymerization of ethylene oxide (EO) using tetrahydropyranol as an initiator. The alcohol end group was then modified with an alkyne via a substitution reaction using propargyl bromide (1:4 respectively). Once modified, the protected alcohol group was deprotected with an acid and subsequently purified. Finally, using *N*-hydroxysuccinimide (NHS) and *N,N'*-dicyclohexylcarbodiimide (DCC) coupling, the heterobifunctional PEO was modified with nitrated 3,4 dihydroxy-L-phenylanaline (nitroDOPA) to yield a macromolecule with functionality that can be utilized for 'click chemistry' and provide enhanced binding to an iron oxide surface, as described in

previous work by Stone *et al.*[46], where synthetic details the polymer formation and relevant NMR data can be found. NitroDOPA was selected as the binding group for our system because of its enhanced binding to metal oxides [49].

The aforementioned macromolecule was then used to modify MNPs, synthesized using a modified version of a procedure by Sun *et al.*,[50] via ligand-exchange by slowly adding magnetic nanoparticles dispersed in hexanes to a solution of the macromolecule in chloroform while sonicating. After 12 hours, allowing for significant ligand exchange, the polymer-particle complex was then purified by extraction into DI water and then dialyzed against DI water in 12-14,000 g mol-1 MWCO dialysis membranes for three days to remove any impurities. The use of nitroDOPA containing PEO polymer has recently been shown to be the most effective anchoring chemistry in the ligand exchange of oleic acid coated particles [51]. The resulted particles with attached glycoconjugate (GM3-MNPs) were characterized by dynamic light scattering (DLS) (Table 2.1), zeta-potential (Table 2.1) and FT-IR spectroscopy (Figure 2.2 and 2.3). The absence of azide peak at 2113 cm^{-1} in Figure 2.2 (D) represents the successful conjugation of glycoconjugate moiety onto the polymer-coated magnetic nanoparticles through cycloaddition. The nanoparticle concentration in PEO-MNPs and GM3-MNPs was determined by means of inductively coupled plasma mass spectroscopy (ICP-MS).

Type of MNPs	DLS (Z – Avg) (d. nm)	Zeta-Potential
PEO-MNPs	77.31	-12.1
GM3-MNPs	80.46	-42.0

Table 2.1 DLS and Zeta-Potential measurements of MNPs after functionalizing PEO polymer and GM3 molecule.
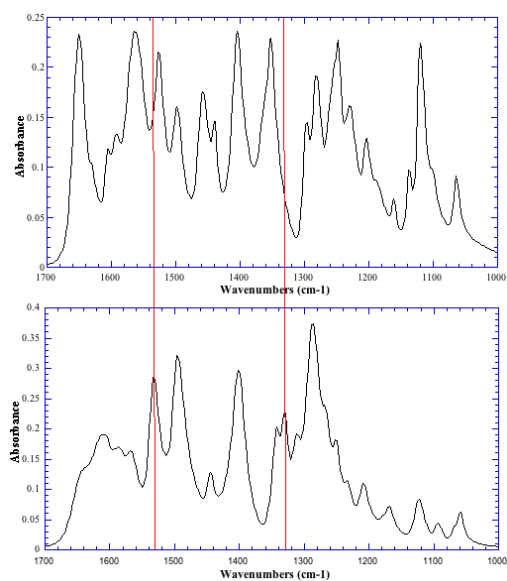
Figure 2.2 FTIR of DOPA (Top) and NitroDOPA (Bottom). Symmetric and asymmetric stretching from the NO_2 peaks at 1330 and 1532 cm^{-1}. Reprinted from (46) - Reproduced by permission of The Royal Society of Chemistry.
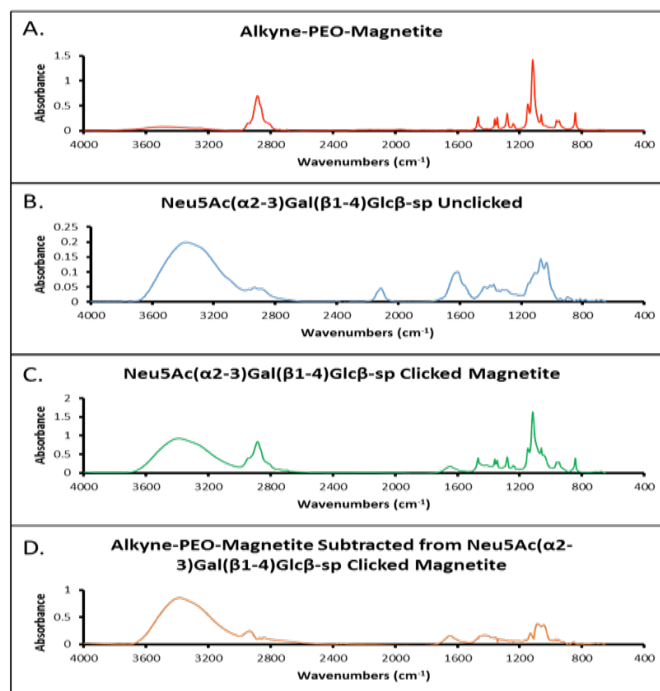
Figure 2.3 FTIR spectroscopy of A.) Magnetite particles modified with the alkyne PEO stabilizer, B.) The Neu5Ac(α2-3)Gal(β1-4)Glcβ-sp targeting moiety prior to "clicking", C.) The resulting complex of magnetic nanoparticles with the

Neu5Ac(α2-3)Gal(β1-4)Glcβ-sp moiety, and D.) The resulting spectrum of subtracting spectrum C by A indicating the successful conjugation of the Neu5Ac(α2-3)Gal(β1-4)Glcβ-sp to targeting molecule.

Clearly, large aggregates of *EC* K99 were observed in the presence of GM3-MNPs (Figure 2.4). No visible aggregation was found when *EC* K99 was mixed with PEO-MNPs (Figure 2.4 c). Moreover, *EC* 6980-2 did not form aggregates when mixed with PEO-MNPs and GM3-MNPs (Figures 2.4 a and b). This shows that both *E. coli* strains clearly have different sugar binding specificities and that *EC* K99 exhibits binding specificity only to GM3-MNPs.
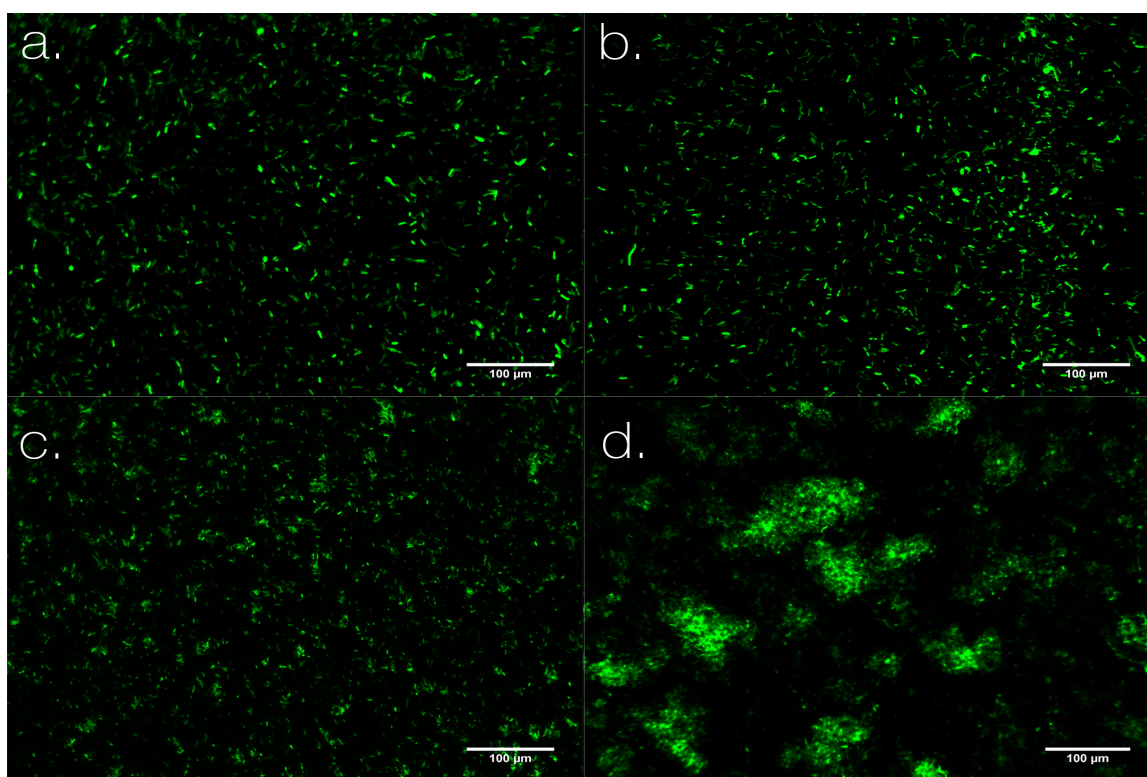
Figure 2.4 Fluorescent microscopy images of *EC* 6980-2 and *EC* K99 in presence of PEO-MNPs and GM3-MNPs. (a) and (b) *EC* 6980-2, in the presence of PEO-MNPs and GM3-MNPs respectively; (c) and (d) *EC* K99, in the presence of PEO-MNPs and GM3-MNPs respectively. Magnification – 400X and scale bar – 100 µm.

Furthermore, transmission electron microscopy (TEM) analysis of the mixture containing GM3-MNPs and *EC* K99 was done to observe intricate details of bacterial aggregation. The samples for TEM analysis were prepared according to a modified multi-step protocol [21, 52]. Large clusters of bacterial cells were observed due to strong interactions between GM3-MNPs and *EC* K99 (Figure 2.5 a and b). The GM3-MNPs were found covering the entire surface of *EC* K99. Because of significant binding of multiple GM3-MNPs onto individual bacterial cells and other GM3-MNPs acting as linking agents to interact with other bacterial cells, we observed significantly large agglutination of *EC* K99.
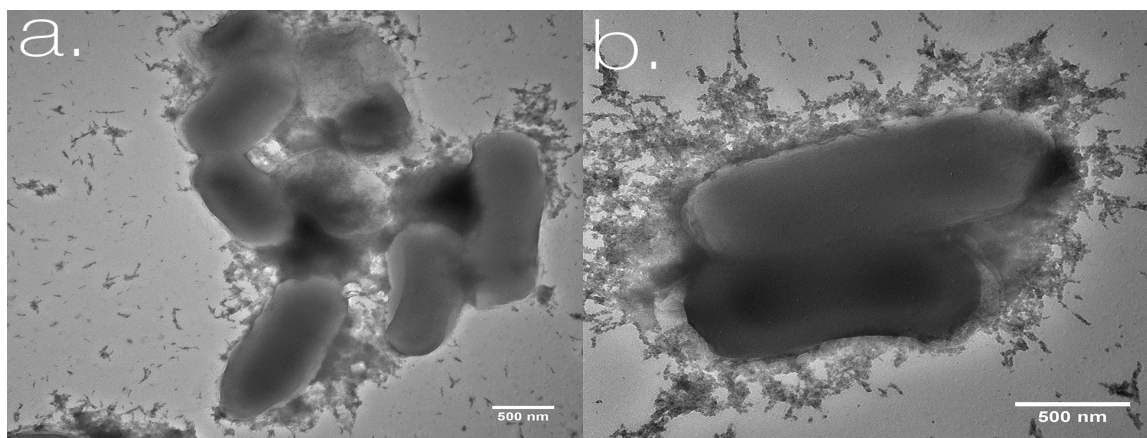
Figure 2.5 TEM images of GM3-MNPs induced bacterial aggregation of *EC* K99. Magnification of (a) and (b) are 30000X and 60000X, respectively. Scale bar is 500 nm.

Entero-pathogenic *E. coli* strains have different sugar binding affinities depending on the type of adhesins present on their outer cell-surface [53]. It is known that *EC* K99 has S type of fimbrial proteins that specifically recognizes and binds only to Neu5Ac(α2-3)Gal(β1-4)Glcβ-sp sialic-acid sequences [4]. The pilus of *EC* K99 is primarily made up of FanC, major fimbrial sub-unit gene product, which is responsible for recognizing and

48

attaching the bacterium to the sialic-acid ganglioside receptors present on the host-cell [54]. On the other hand, *EC* 6980-2 have adhesin molecules that consist of galactose-binding proteins on its outer surface which can attach to galactose receptors [17] present on the host-cell and hence *EC* 6980-2 was not able to form bacterial aggregates when mixed with GM3-MNPs. Based on these sugar-binding specificities, the above mentioned 2 different *E. coli* strains were selected for this study.

As shown in figure 2.6 A, approximately 2-log reduction in CFU of *EC* K99 was observed in the presence of GM3-MNPs (40 μg/ml). This reduction was due to GM3-MNPs induced bacterial aggregation. Also, 1-log reduction of *EC* K99 was observed at 100 μg/ml concentration of GM3-MNPs. Interestingly, there was no reduction in CFU of *EC* 6980-2 in the presence of either GM3-MNPs or PEO-MNPs (Figure 2.6 B). These results correlate with those obtained in fluorescence microscopy assay showing that bacterial cells of *EC* K99 aggregating in clusters of several 100s of bacterial cells in the presence of GM3-MNPs. Surprisingly, *EC* K99 in the presence of GM3-MNPs (100 μg/ml) resulted only in 1-log reduction in CFU since the nanoparticle-bacteria ratio was different. Luo and co-workers [21] obtained similar results when they incubated *E. coli* ORN178 in the presence of different concentrations of mannose-functionalized polymeric nanoparticles. Thus, it is imperative to attain appropriate nanoparticle-bacteria ratio for getting maximum reduction in CFU mediated by nanoparticles-induced bacterial aggregation.
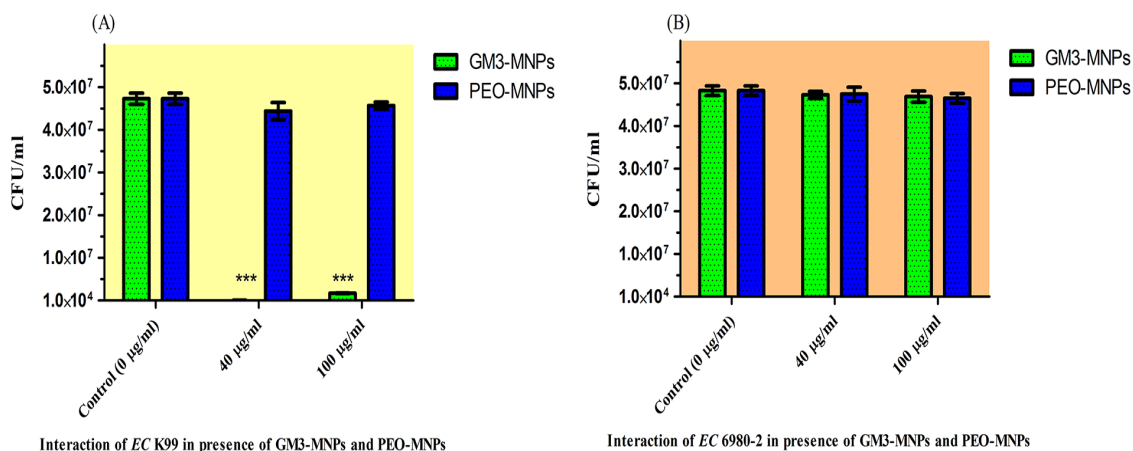
Figure 2.6 (**a**) CFU/ml assay of *EC* K99 in the presence of different concentrations of GM3-MNPs and PEO-MNPs and (**b**) CFU/ml assay of *EC* 6980-2 in the presence of different concentrations of GM3-MNPs and PEO-MNPs. Data expressed as Mean ± SD (n = 3); Statistical Analysis – Two-Way Analysis of Variance (ANOVA) (*** - P<0.0001).

Intracellular ATP levels of both the *E. coli* strains were recorded by measuring their relative luminescence in the presence/absence of GM3-MNPs (40 μg/ml) and PEO-MNPs (40 μg/ml). Figures 2.7 A and B shows that there is no significant difference in intracellular ATP levels of both *E. coli* strains in the presence of nanoparticles. Also, another important feature to determine the toxicity of nanoparticles is to look for any cell-membrane damage and morphological changes in the bacterial cell-membrane structure [52]. Results of TEM imaging of *EC* K99 in the presence of GM3-MNPs showed no visible bacterial cell-membrane damage suggesting the non-toxic nature of our nanoparticles. These results suggest that the reduction in CFU of *EC* K99 was achieved only because of GM3-MNPs induced bacterial aggregation and not due to nanoparticle toxicity.

(A)

(B)

Intracellular ATP levels of *EC* K99 in presence of GM3-MNPs (40 µg/ml) and PEO-MNPs (40 µg/ml)

Intracellular ATP levels of *EC* 6980-2 in presence of GM3-MNPs (40 µg/ml) and PEO-MNPs (40 µg/ml)
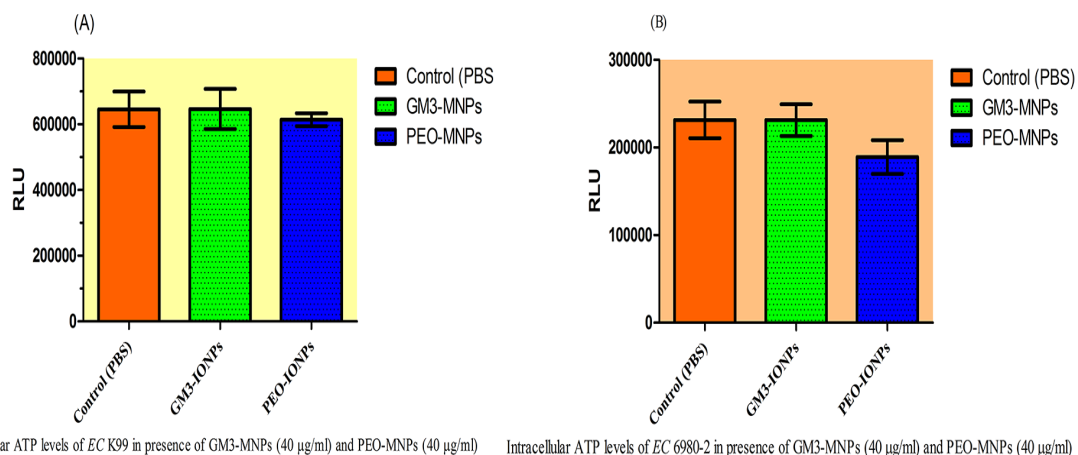
Figure 2.7 Intracellular ATP Assay **(a)** Relative Luminescent Units (RLU) of *EC* K99 when incubated with GM3-MNPs and PEO-MNPs **(b)** RLU of *EC* 6980-2 when incubated with GM3-MNPs and PEO-MNPs. Data expressed as Mean ± SD (n = 3); Statistical Analysis – One-Way Analysis of Variance (ANOVA); (P>0.05).

To further validate the non-toxic nature of our nanoparticles system, we performed a preliminary cytotoxicity assay on human colon (normal) cell-line CCD-18Co and determined its cell-viability rate after exposing to GM3-MNPs for 24 hours. The potential cytotoxicity of GM3-MNPs was measured by performing MTS assay. As seen in figure 2.8, there was no significant reduction in cell-viability rate of CCD-18Co cells in the presence of varying concentrations of GM3-MNPs. These results suggest that our novel glycoconjugate-functionalized nanoparticle system is highly biocompatible.

Cell-viability of CCD-18Co cells in presence of GM3-MNPs
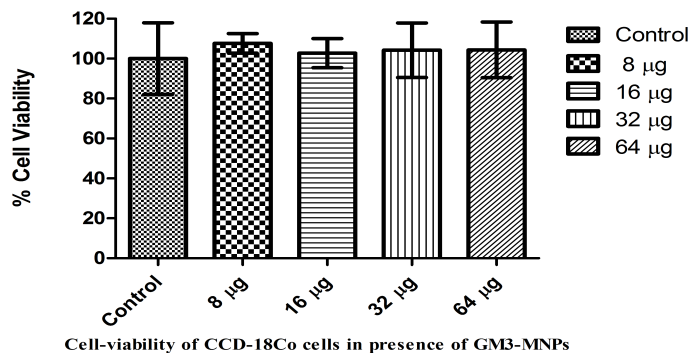
Figure 2.8 Cytotoxicity assay to determine cell-viability of CCD-18Co cells in presence of different concentrations of GM3-MNPs. Data expressed as Mean ± SD (n = 3); Statistical Analysis – One-Way Analysis of Variance (ANOVA); (P>0.05).

4. Conclusion:

In conclusion, we successfully synthesized heterobifunctional polymer coated magnetic nanoparticles that have nitroDOPA as a stable anchoring agent and were bio-functionalized with sialic-acid glycoconjugate (Neu5Ac(α2-3)Gal(β1-4)Glcβ-sp) (GM3-MNPs) using click chemistry. The GM3-MNPs were characterized by employing different techniques and their adhesin specificity was determined using aggregation assays. Our GM3-MNPs specifically interacted only with ETEC strain *EC* K99 as confirmed through fluorescence microscopy and transmission electron microscopy. Also, a 2-log reduction in CFU of *EC* K99 was achieved due to GM3-MNPs induced bacterial aggregation. Moreover, intracellular ATP assays demonstrated that the 2-log reduction in CFU of *EC* K99 was not due to inherent toxicity of the nanoparticles. Thus, our proof-of-concept nanoparticle system can effectively serve as novel non-antibiotic multivalent carriers, which could find applications in detection and capturing of pathogenic multi-

drug resistant bacterial strains from active physiological body fluids. Our systems can especially reduce/treat gastro-intestinal tract infections caused by ETEC pathogens in farm animals and humans since specific bacterial-nanoparticle aggregates can be effectively flushed out from the body system because of high peristaltic flows without disturbing the normal gut microflora that is usually destroyed when antibiotics are used. This system can also be employed as potent anti-adhesion agents that can block/inhibit specific cellular responses by competitively preventing the attachment of bacterial pathogens onto specific eukaryotic cell-surface receptors and thereby reducing the infection load. Furthermore, this nanoparticle system can also be utilized for targeted magnetic hyperthermia treatment of bacterial infections, especially those that are resistant to multiple antibiotics. In future work, nanoparticles with multi-anchored functional groups will be utilized to improve stability of nanoparticles in biological fluids and to enhance their bindings to specific pathogens. Their therapeutic values, i.e., selective killing of pathogens via hyperthermia mediated by glycoconjugate-functionalized magnetic nanoparticles, will be evaluated both *in vitro* in cell-line and *in vivo* in small animal systems. In addition, potential toxicities associated with the use of these nanoparticles will be characterized using various biological assays, e.g., cytotoxicity, genotoxicity, immunogenicity assays, etc.

References:

1.   Walsh, C., *Antibiotics: actions, origins, resistance*. 2003: American Society for Microbiology (ASM).
2.   Levy, S.B. and B. Marshall, *Antibacterial resistance worldwide: causes, challenges and responses*. Nature Medicine, 2004. **10**: p. S122-S129.

3.   Jones, K.E., *et al.*, *Global trends in emerging infectious diseases.* Nature, 2008. **451**(7181): p. 990-993.

4.   Sharon, N., *Carbohydrates as future anti-adhesion drugs for infectious diseases.* Biochimica et Biophysica Acta, 2006. **1760**(4): p. 527-537.

5.   Ernst, B. and J.L. Magnani, *From carbohydrate leads to glycomimetic drugs.* Nature Reviews Drug Discovery, 2009. **8**(8): p. 661-677.

6.   Tra, V.N. and D.H. Dube, *Glycans in pathogenic bacteria–potential for targeted covalent therapeutics and imaging agents.* Chemical Communications, 2014. **50**(36): p. 4659-4673.

7.   Zopf, D. and S. Roth, *Oligosaccharide anti-infective agents.* Lancet, 1996. **347**(9007): p. 1017-1021.

8.   Karlsson, K.A., *Meaning and therapeutic potential of microbial recognition of host glycoconjugates.* Molecular Microbiology, 1998. **29**(1): p. 1-11.

9.   Dam, T.K., *et al.*, *Binding of Multivalent Carbohydrates to Concanavalin A and Dioclea grandiflora Lectin THERMODYNAMIC ANALYSIS OF THE "MULTIVALENCY EFFECT".* Journal of Biological Chemistry, 2000. **275**(19): p. 14223-14230.

10.   Luque, I. and E. Freire, *Structural parameterization of the binding enthalpy of small ligands.* Proteins: Structure, Function, and Bioinformatics, 2002. **49**(2): p. 181-190.

11.   Marradi, M., I. Garcia, and S. Penades, *Carbohydrate-based nanoparticles for potential applications in medicine.* Progress in Molecular Biology and Translational Science, 2011. **104**: p. 141-173.

12.   Marradi, M., *et al.*, *Glyconanoparticles as multifunctional and multimodal carbohydrate systems.* Chemical Society Reviews, 2013. **42**(11): p. 4728-4745.

13.   Marradi, M., M. Martin-Lomas, and S. Penades, *Glyconanoparticles polyvalent tools to study carbohydrate-based interactions.* Advances in Carbohydrate Chemistry and Biochemistry, 2010. **64**: p. 211-290.

14.   Bernardi, A., *et al.*, *Multivalent glycoconjugates as anti-pathogenic agents.* Chemical Society Reviews, 2013. **42**(11): p. 4709-4727.

15.   Lin, C.-C., *et al.*, *Selective binding of mannose-encapsulated gold nanoparticles to type 1 pili in Escherichia coli.* Journal of the American Chemical Society, 2002. **124**(14): p. 3508-3509.

16.   El-Boubbou, K., C. Gruden, and X. Huang, *Magnetic glyco-nanoparticles: a unique tool for rapid pathogen detection, decontamination, and strain differentiation.* Journal of the American Chemical Society, 2007. **129**(44): p. 13392-13393.

17.   Gu, L., *et al.*, *Single-walled carbon nanotubes displaying multivalent ligands for capturing pathogens.* Chemical Communications, 2005(7): p. 874-876.

18.   Gu, L., *et al.*, *Single-walled carbon nanotube as a unique scaffold for the multivalent display of sugars.* Biomacromolecules, 2008. **9**(9): p. 2408-2418.

19.   Qu, L.W., *et al.*, *Galactosylated Polymeric Nanoparticles: Synthesis and Adhesion Interactions with Escherichia coli.* Journal of Biomedical Nanotechnology, 2005. **1**(1): p. 61-67.

20. Qu, L., *et al.*, *Visualizing adhesion-induced agglutination of Escherichia coli with mannosylated nanoparticles.* Journal of Nanoscience and Nanotechnology, 2005. **5**(2): p. 319-322.

21. Luo, P.J.G., *et al.*, *Quantitative Analysis of Bacterial Aggregation Mediated by Bioactive Nanoparticles.* Journal of Biomedical Nanotechnology, 2005. **1**(3): p. 291-296.

22. Barras, A., *et al.*, *Glycan-functionalized diamond nanoparticles as potent E. coli anti-adhesives.* Nanoscale, 2013. **5**(6): p. 2307-2316.

23. Dave, S.R. and X. Gao, *Monodisperse magnetic nanoparticles for biodetection, imaging, and drug delivery: a versatile and evolving technology.* Wiley Interdisciplinary Reviews: Nanomedicine and Nanobiotechnology, 2009. **1**(6): p. 583-609.

24. Kaittanis, C., S. Santra, and J.M. Perez, *Emerging nanotechnology-based strategies for the identification of microbial pathogenesis.* Advanced Drug Delivery Reviews, 2010. **62**(4-5): p. 408-423.

25. Arruebo, M., *et al.*, *Magnetic nanoparticles for drug delivery.* Nano Today, 2007. **2**(3): p. 22-32.

26. Kumar, C.S. and F. Mohammad, *Magnetic nanomaterials for hyperthermia-based therapy and controlled drug delivery.* Advanced Drug Delivery Reviews, 2011. **63**(9): p. 789-808.

27. Aslam, M., *et al.*, *Synthesis of amine-stabilized aqueous colloidal iron oxide nanoparticles.* Crystal Growth & Design, 2007. **7**(3): p. 471-475.

28. Lin, H., *et al.*, *Preparation of magnetic poly (vinyl alcohol)(PVA) materials by in situ synthesis of magnetite in a PVA matrix.* Journal of Applied Polymer Science, 2003. **87**(8): p. 1239-1247.

29. Sahoo, Y., *et al.*, *Alkyl phosphonate/phosphate coating on magnetite nanoparticles: a comparison with fatty acids.* Langmuir, 2001. **17**(25): p. 7907-7911.

30. Vadala, M., *et al.*, *Heterobifunctional poly (ethylene oxide) oligomers containing carboxylic acids.* Biomacromolecules, 2008. **9**(3): p. 1035-1043.

31. Gu, H., *et al.*, *Synthesis and cellular uptake of porphyrin decorated iron oxide nanoparticles—a potential candidate for bimodal anticancer therapy.* Chemical Communications, 2005(34): p. 4270-4272.

32. Amstad, E., *et al.*, *Surface functionalization of single superparamagnetic iron oxide nanoparticles for targeted magnetic resonance imaging.* Small, 2009. **5**(11): p. 1334-1342.

33. Saville, S.L., *et al.*, *Investigation of the stability of magnetite nanoparticles functionalized with catechol based ligands in biological media.* Journal of Materials Chemistry, 2012. **22**(47): p. 24909-24917.

34. Amstad, E., *et al.*, *Ultrastable iron oxide nanoparticle colloidal suspensions using dispersants with catechol-derived anchor groups.* Nano Letters, 2009. **9**(12): p. 4042-4048.

35. Ofek, I. and R.J. Doyle, *Bacterial adhesion to cells and tissues.* 1994: Chapman & Hall New York.

36. Sharon, N., *Bacterial lectins, cell-cell recognition and infectious disease.* FEBS Letters, 1987. **217**(2): p. 145-157.

37. Black, R.E., *Epidemiology of travelers' diarrhea and relative importance of various pathogens.* Reviews of Infectious Diseases, 1990. **12 Suppl 1**: p. S73-9.

38. Barigye, R., *et al.*, *Prevalence and antimicrobial susceptibility of virulent and avirulent multidrug-resistant Escherichia coli isolated from diarrheic neonatal calves.* American Journal of Veterinary Research, 2012. **73**(12): p. 1944-1950.

39. de Verdier, K., *et al.*, *Antimicrobial resistance and virulence factors in Escherichia coli from Swedish dairy calves.* Acta Veterinaria Scandinavica, 2012. **54**(1): p. 2-2.

40. Güler, L., K. Gündüz, and Ü. Ok, *Virulence factors and antimicrobial susceptibility of Escherichia coli isolated from calves in Turkey.* Zoonoses Public Health, 2008. **55**(5): p. 249-257.

41. Nagy, B. and P.Z. Fekete, *Enterotoxigenic Escherichia coli (ETEC) in farm animals.* Veterinary Research, 1999. **30**(2-3): p. 259-284.

42. Nagy, B., H.W. Moon, and R.E. Isaacson, *Colonization of porcine intestine by enterotoxigenic Escherichia coli: selection of piliated forms in vivo, adhesion of piliated forms to epithelial cells in vitro, and incidence of a pilus antigen among porcine enteropathogenic E. coli.* Infection and Immunity, 1977. **16**(1): p. 344-352.

43. Isaacson, R.E., *et al.*, *In vitro adhesion of Escherichia coli to porcine small intestinal epithelial cells: pili as adhesive factors.* Infection and Immunity, 1978. **21**(2): p. 392-397.

44. Kyogashima, M., V. Ginsburg, and H.C. Krivan, *Escherichia coli K99 binds to N-glycolylsialoparagloboside and N-glycolyl-GM3 found in piglet small intestine.* Archives of Biochemistry and Biophysics, 1989. **270**(1): p. 391-397.

45. Vedantam, P., *et al.*, *Binding of Escherichia coli to Functionalized Gold Nanoparticles.* Plasmonics, 2012. **7**(2): p. 301-308.

46. Stone, R., *et al.*, *A Versatile Stable Platform for Multifunctional Applications: Synthesis of NitroDOPA-PEO-Alkyne Scaffolding for Iron Oxide Nanoparticles.* Journal of Materials Chemistry B, 2014. **2**: p. 4789-4793

47. J., S. and R. D.W., *Molecular cloning: a laboratory manual, 3rd edn.* 2001, Cold Spring Harbor Laboratory Press: Cold Spring Harbor.

48. Chakraborti, S., *et al.*, *The molecular basis of inactivation of metronidazole-resistant Helicobacter pylori using polyethyleneimine functionalized zinc oxide nanoparticles.* PloS one, 2013. **8**(8): p. e70776.

49. Amstad, E., *et al.*, *Influence of Electronegative Substituents on the Binding Affinity of Catechol-Derived Anchors to Fe3O4 Nanoparticles.* The Journal of Physical Chemistry C, 2010. **115**(3): p. 683-691.

50. Sun, S., *et al.*, *Monodisperse MFe2O4 (M= Fe, Co, Mn) nanoparticles.* Journal of the American Chemical Society, 2004. **126**(1): p. 273-279.

51. Davis, K.M., *et al.*, *Quantitative measurement of ligand exchange on iron oxide nanoparticles via radiolabeled oleic acid.* Langmuir, 2014. **30**(36): p. 10918-10925

52. Hayden, S.C., *et al.*, *Aggregation and interaction of cationic nanoparticles on bacterial surfaces.* Journal of the American Chemical Society, 2012. **134**(16): p. 6920-6923.

53. Sharon, N. and I. Ofek, *Safe as mother's milk: carbohydrates as future anti-adhesion drugs for bacterial diseases.* Glycoconjugate Journal, 2000. **17**(7-9): p. 659-664.

54. Jay, C.M., *et al.*, *Enterotoxigenic K99 Escherichia coli attachment to host cell receptors inhibited by recombinant pili protein.* Veterinary Microbiology, 2004. **101**(3): p. 153-160.

Chapter 3

Multi-Anchored Glycoconjugate-Functionalized Magnetic

Nanoparticles: A Tool for Selective Killing of Targeted Bacteria via

Alternating Magnetic Fields

1. Introduction:

The emergence of anti-microbial resistance (AMR) has quickly taken hold as one of the greatest threats to modern medicine on a global scale, and the ramifications, if not dealt with in a timely manner, may be catastrophic. Currently, there are more than 160 different kinds of antibiotics available for therapeutic purposes [1]. However, unrestricted and prolonged usage of antibiotics has resulted in rapid emergence of new strains of bacteria that have developed resistance to these drugs and, over time, evolved as multi-drug resistant microorganisms. Infections caused by such bacterial strains have resulted in prolonged hospital stays and an increase in outpatient costs and patient mortality and morbidity throughout the world [2]. In a World Health Organization (WHO) global report on antimicrobial resistance, it is stated that AMR is a complex global public health challenge and that no single or simple strategy will contain the emergence and spread of

AMR infectious organisms [3]. A recent study by the US Center for Disease Control and Prevention estimates that every year, diseases caused by AMR strains of bacteria infect millions of people in the US, and thousands of them die annually due to lack of new antibiotics [4]. The emergence of AMR also has an enormous socio-economic impact. A 2014 report from RAND Europe, estimates the economic cost of AMR to be approximately 3.1% of global output gross domestic product (~2.4 trillion US dollars) [5]. Although recognized as an immediate issue, antibiotic discovery has declined with many major pharmaceutical companies discontinuing their antibiotic development programs over the past decade due to low return on investment and difficulties in identifying new compounds. This reinforces the need for development of novel therapeutic approaches to address the AMR challenges [6-8].

Nanoparticles have been a highly investigated area as their properties differ from their bulk counterparts. Of these materials, iron oxide has found particular prevalence in the biomedical field with use in MRI contrast, drug delivery, cell separation, and cancer therapy [9-11]. When an iron oxide particle is subjected to an alternating magnetic field, a hysteresis loop is completed in which the area relates to the energy release per cycle [12]. By doing this at relatively high frequencies (kHz-MHz), the amount of energy transfer is great enough to affect surrounding cells [13]. This phenomenon was previously referred to as magnetic hyperthermia due to an observed temperature rise. However, recent studies have shown that cell death could be induced in the absence of bulk heating of the environment [13, 14]. In seeking a more descriptive term, we and others prefer to use the phrase magnetically mediated energy delivery (MagMED) [15,

16]. The use of nanoparticles for biological applications requires stringent attention to surface chemistry as it affects reactivity, bio-distribution, and stability [9, 17]. Much research has been put into optimizing surface chemistries for nanomaterials, with poly(ethylene oxide) (PEO) being one of the universally accepted coatings [18]. PEO has been shown to prolong circulation time, greatly improve stability in protein and ion-rich environments, impart secondary functionality, and render stealth from the immune system [18]. Further enhancement in stability may be imparted using a multi-anchored catechol as the iron binding moiety [17, 19]. This is highly necessary as desorption of the polymer coating is an issue with many biomolecules including phosphonates and peptides, which have high affinity for iron oxide [20].

Though numerous groups have reported using alternate magnetic field along with magnetic nanoparticles as an alternative cancer therapy, limited work has been done in the same direction for treating bacterial infections [21-23]. More importantly, to the best of the authors' knowledge, no work exploring the use of nanoparticles for selective killing of targeted pathogen in mixed-bacterial culture settings has been reported. Attachment of bacterial pathogens onto the surface of mammalian cells is one of the foremost events in host-pathogen interactions. Several pathogenic bacteria are able to adhere to specific host-cell receptors via carbohydrate binding proteins, also called adhesins or lectins [24]. These interactions are part of the signal cascade enabling bacteria to recognize the environment they are in and then turn on the cascade of processes leading to infections [25, 26]. If these binding interactions are inhibited/interrupted then the chances of getting infection is greatly reduced [27].

The rapid advancement in the fields of nanotechnology and glycotechnology offers potentially new therapeutic options for treating bacterial infections. Over the last few years, few research groups have studied nanomaterials functionalized with multivalent carbohydrate groups and synthetic glycoconjugates for probing bacterial lectin-carbohydrate interactions [28, 29]. Attaching these molecules onto the surface of nanomaterials has found numerous applications in pathogen detection/targeting,[30] mammalian cell-receptor mimicking [31], drug delivery [32], and in anti-adhesion therapies [33]. Specifically, carbon nanotubes [34, 35], gold nanoparticles [36, 37], diamond nanoparticles [38], polymeric nanoparticles [39], and magnetic nanoparticles [40-43] were reported to be bio-functionalized with different carbohydrate sugars/glycoconjugates and were utilized for studying lectin-carbohydrate interactions in different bacterial species. Given the excellent biocompatibility of using glycoconjugates molecules for functionalizing nanomaterials, not many studies have been carried out that can specifically detect and differentiate bacterial species in a mixed population both *in vitro* and *in vivo*.

Escherichia coli (*E. coli*) is one of the most common types of bacteria naturally occurring in the digestive tract of humans and animals. While most of the *E. coli* strains are harmless to humans and animals, there are few *E. coli* serogroups that are mainly responsible in causing infections. *E. coli* belonging to the enterotoxigenic (ETEC) group is responsible for causing traveler's diarrhea in humans and bloody diarrhea in neonatal calves, pigs and lambs [44-46]. The prevalence of the serogroups and presence of adhesins are considered to be the primary factors that facilitate intestinal colonization of

ETEC. ETEC adhere to small intestinal microvilli membranes *in vivo* via adhesins that recognizes specific carbohydrate receptors and produce enterotoxins that act on enterocytes eventually causing diarrhea [47]. Recently, numerous studies have reported an increase in multi-drug resistance of ETEC strains associated with the inclusion of growth-promoting antibiotics in animal feed [48, 49]. *E. coli* K99 (*EC* K99) is one of the commonly found ETEC strains in newborn farm animals responsible for causing colibacillosis [50]. *EC* K99 has unique adhesins that can specifically recognize and attach to sialic-acid based glycolipid receptors present on the ileal villus epithelium of the small intestine [51, 52]. If these binding interactions are inhibited/interrupted, the chances of getting infection are greatly reduced. Our previous studies have shown that nanoparticles functionalized with specific sialic-acid derivatives resulted in nanoparticles-induced aggregation of *EC* K99 along with excellent biocompatibility [36, 41].

In this study, it is hypothesized that multi-anchored magnetic nanoparticles conjugated with sialic-acid moieties that mimic host-cell receptors specific for *EC* K99 adhesins, would induce rapid clustering of *EC* K99 in the presence of these nanoparticles, and when such bacteria-nanoparticles aggregates are exposed to AMF, it would result in enhanced and selective inactivation/killing of *EC* K99. Our results demonstrate a clinically significant ~3-log reduction in CFU [53] of *EC* K99 in the presence of GM3-MNPs used in conjunction with AMF. To our knowledge, it is for the first time that sialic-acid derived glycoconjugate functionalized magnetic nanoparticles have been employed for specific killing of target bacteria in the presence of AMF. This study serves

as proof-of-concept that a high degree of selective bacterial killing can be obtained without using traditional antibiotics.

2. Experimental Section:

***Synthesis of Magnetite Nanoparticles*:** Magnetite nanoparticles were synthesized via thermal decomposition of an organometallic precursor in a high boiling point organic solvent [54]. Iron (III) acetylacetonate (Alfa Aesar, 99%) (1.074g) was combined in a 3-neck round-bottom with oleic acid (Alfa Aesar, 90%) (15ml) serving as both the solvent and the stabilizing ligand. The vessel was initially purged with N_2 after which flow was adjusted to 0.1 L/min ensuring an inert environment. The vessel was then heated to 350°C and left to react for 3 hours. At 3 hours, the reaction was quenched by removing it from heat, and left to cool under inert atmosphere. The resulting particles were dispersed in minimal hexanes and precipitated using a mixture of 3:1 ethanol (Fisher, Anhydrous) to acetone (Alfa Aesar, 99.5%) (x3). Particles were dispersed in toluene (VWR, 99.5%) and run through an organic based GPC column (Bio-rad S-X polystyrene beads) to further remove excess oleic acid ligand [55]. TEM and size analysis was then done on the particles to ensure size specificity.

Synthesis of Alkyne-PEO-PAA-Dopamine [19]**:** Poly(ethylene oxide) (PEO) synthesis: Ethylene oxide (Sigma Aldrich, 99.9%) distilled into a high pressure Parr reactor. Na-benzylphenone still dried tetrahydrofuran (THF, EMD Millipore, 99.9%) was injected along with a predetermined amount of an anionic initiator potassium bistrimethyl silyl amide (Sigma Aldrich, 1M in THF). The reaction was allowed to run for 72 hours

and was subsequently terminated by opening the reactor to atmosphere. The synthesized PEO was precipitated with diethyl ether (VWR, 99.9%) and washed (3x) by dispersing it in chloroform, precipitating the polymer, centrifuging it at 15,000 RCF for 10 minutes and pouring off the residual supernatant. The PEO was then dried under vacuum overnight. HNMR was performed to calculate molecular weight as well as to confirm the presence of the protected amine end-group.

Under dry N_2 atmosphere, hetero-functional PEO and sodium hydride (Sigma Aldrich, 95%), in slight excess, were dissolved in dry THF. This was allowed to react for 30 minutes before an excess of propargyl bromide (Sigma Aldrich, 80% in toluene) was added drop-wise to the solution over 15 minutes. Once all of the propargyl bromide was added, the solution was allowed to stir for 12 hours at room temperature. The polymer was then purified by dissolution in chloroform and precipitation with diethyl ether (x3) and dried under vacuum for 12 hours. HNMR was performed to confirm the presence of an alkyne.

Deprotection of the trimethyl silyl group was done in 1M hydrochloric acid (VWR) in methanol (VWR, 99+%) and allowed to react for 4 hours. The polymer methanol solution was diluted with DI water and the deprotected PEO was extracted (3x) with 50ml chloroform from which it was precipitated with diethyl ether and dried under vacuum. HNMR was performed to confirm the loss of the trimethylsilyl group.

Coupling of the PEO to the poly(acrylic acid) (PAA, Sigma Aldrich Mn=1,800) was done by dissolving both in dry N,N-dimethylformamide (DMF, Sigma Aldrich, 99.8%) in a 5:1 ratio. To this 1.1 excess (N-(3-dimethylaminopropyl)-N'-ethylcarodiimide hydrochloride

(EDC, TCI, 98%) as well as catalytic amounts of 4-(dimethylamino)pyridine (DMAP, Alfa Aesar, 99+%) were added. The solution was allowed to stir for 12 hours. The solution was filtered, further purified by dissolution in chloroform following precipitation with diethyl ether (x3) and then dried under vacuum. HNMR was done to confirm PEO-PAA coupling.

Attachment of the anchor group: Dopamine hydrochloride (Alfa Aesar, 99%) was dissolved in DMF along with a 10% molar excess of triethylamine (Alfa Aesar, 99%) and allowed to stir for 30 minutes. In a separate round-bottom the PEO-PAA was dissolved in DMF along with EDC and catalytic amounts of DMAP. To this the dopamine hydrochloride solution was added and the combined solution was allowed to stir for 12 hours. The solution was then filtered, purified by dissolution in chloroform then precipitated in diethyl ether. The final product was dried under vacuum and analyzed via HNMR and IR to confirm the presence of the catechol.

Ligand Exchange [17]**:** Both magnetite nanoparticles as well as the PEO-PAA-dopamine were suspended separately in 5ml of chloroform. The particles were at an approximate concentration of 3mg/ml of Fe and the polymer at approximately 40mg/ml. The polymer was then transferred to a scintillation vial capped with a septum and placed in a sonication bath. The bath was turned on and over the course of 15 minutes the magnetic nanoparticle solution was injected into the polymer solution. Once injection was finished, the combined solution was allowed to further sonicate for 15 minutes. The solution was then removed and put on a shaker table for 72 hours. The chloroform was then removed via rotary evaporator and further dried under vacuum. Deionized water (DI

H$_2$O) was then added and the vial was sonicated to help mediate suspension into the water. The water-based particles were then filtered through a 0.2-micron nylon filter to ensure large aggregates were not present. The solutions were then run through a GPC column (Bio-Rad P polyacrylamide beads) to separate excess polymer from the water dispersible particles.

Click Chemistry [56]**:** The Cu(I) catalyzed Huisgen 1,3-dipolar cyclo-addition between the terminal polymer alkyne and the azido-GM3 was done in the aqueous phase with the azido-GM3 being the limiting reagent. A 2 mol% solution of Cu(II) sulfate (Sigma Aldrich, 99%) was combined with equivalent molar amounts of the THPTA (synthesized according to Hong *et al.*) Cu chelating ligand and let to react for 10 minutes [57]. This was then transferred into the aqueous alkyne-particle suspension and the azide-GM3 was then added. After both additions a 10mol% aqueous solution of (+)-sodium L-ascorbate (Sigma Aldrich 98+%) was added to facilitate the reduction of Cu(II) to Cu(I). The click reactions were left at room temperature for 12 hours, and were then purified using size exclusion chromatography [55].

*Dynamic Light Scattering (DLS) and Zeta Potential Measurements***:** DLS was performed on the PEO-coated and GM3-coated magnetic nanoparticles to determine their hydrodynamic radius. The nanoparticle suspensions were diluted in water and placed into a cuvette. Three readings were taken at 25°C using Malvern Zetasizer Nano ZS to determine the intensity average size distribution and z-average diameter. Zeta-potential measurements of these nanoparticle suspensions were also determined using the same

instrument. The suspensions were diluted with water and added into zeta-cell and three measurements were taken at 25°C.

Fourier Transform Infrared Spectroscopy (FTIR): Fourier transform infrared (FTIR) spectroscopy microscopy was done using a Thermo-Nicolet Magna 550 FTIR spectrometer equipped with a Thermo-NicPlan FTIR microscope. 16 Scans were done for both the sample and the background. Samples were prepared by dropping a small amount of the water suspended sample on a germanium plate and left to dry under a heat lamp for 20 minutes. FTIR was done on the resulting films.

Iron Concentration Determination: 50 μl of magnetite suspension was dissolved in concentrated HCl, reduced and complexed with 1,10-phenanthroline (Sigma-Aldrich, 99%). UV-VIS was then performed to determine the amount of iron in the known volume [58, 59].

AMF Treatment of Bacterial Strains in the Presence of MNPs: As reported in our previous study [41], *E. coli* K99 (*EC* K99) was transformed with plasmid pGREEN (Carolina Biological Supply Company, NC, USA) carrying ampicillin-resistance marker gene. Avirulent *E. coli* O157:H7 strain B6914 (*EC* O157) was modified to be rifampicin resistant (100 μg/ml; TCI America, OR, USA) through gradient-plate technique as previously described [60]. *EC* K99 strain was routinely grown in tryptic soy broth/tryptic soy agar (TSB/TSA; EMD Millipore, MA, USA) supplemented with ampicillin (100 μg/ml; TCI America, OR, USA) and *EC* O157 strain was grown in tryptic soy broth/tryptic soy agar (TSB/TSA) supplemented with rifampicin (100 μg/ml). For AMF treatment experiments, bacterial cultures were grown overnight under shaking conditions

67

(250 rpm) at 37°C in TSB supplemented with appropriate antibiotics. Later, the bacterial cells were washed and centrifuged thrice in 1X sterile phosphate buffer saline (PBS). Approximately, 5 x 10^7 CFU of bacterial cells were suspended in 1X PBS based on optical density (OD_{600}) readings. Both the bacterial strains were mixed with different types of MNPs and at different concentrations of MNPs in a sterile microcentrifuge tube and this mixture was incubated at room temperature for 30 minutes under gentle shaking conditions to facilitate the binding interactions between bacterial adhesins and MNPs [41]. At the end of incubation time-period, the mixtures of MNPs and bacteria were transferred to sterile glass vial. This vial was then placed in chamber of the alternate magnetic field generating instrument (EasyHeat Induction Heating System - Ameritherm©) that is covered with 5-turn induction coil, which was connected to polycarbonate recirculating water-bath for maintaining the sample temperature (37°C) [61]. A fiber-optic temperature probe (Neoptix™) was inserted inside this chamber to continuously monitor the temperature. The working conditions of the AMF instrument for the experiments were as follows: 480 Amps current, 207KHz frequency and magnetic field strength of 31 KA/m. The field was measured using an AC magnetic field probe (AMF Life Systems, Auburn Hills, MI). The vial containing the mixture of MNPs and bacteria was then exposed to AMF treatment for different durations (30, 60, and 120 minutes). Different groups of control experiments were as follows: 1) mixture containing only bacterial strains suspended in 1X PBS; 2) mixture containing bacteria and MNPs but no AMF exposure. After AMF treatment, the above-mentioned mixture was serially diluted in 1X sterile PBS and 100 μl of sample from each dilution tube was spread-plated

onto sterile TSA petri plates supplemented with appropriate antibiotics. Later, the TSA plates were incubated overnight at 37°C. Finally, the grown colonies on the TSA plates were counted and compared with control group plates and the reduction in colony counts was expressed as colony forming units per ml.

AMF Treatment of Mixed Bacterial Cultures in the Presence of MNPs: To determine the targeted specificity of GM3-MNPs against *EC* K99 in mixed-culture conditions, both the strains of *EC* K99 (concentration - 5 x 10^7 CFU) and *EC* O157 (concentration - 5 x 10^7 CFU) were mixed in a single microcentrifuge tube. GM3-MNPs (650 μg/ml) were added to this mixture and the tube was incubated for 30 minutes at room temperature under gentle shaking conditions. Later, AMF treatment (time - 120 minutes) was applied to this tube as mentioned earlier. Control groups included 1) adding PEO-MNPs to mixture containing both strains of bacteria in the same tube and exposing/not exposing them to AMF; 2) adding GM3-MNPs to tube containing both bacterial strains but no AMF; 3) AMF exposure to tube containing only bacterial strains and no MNPs. Post-treatment, this mixture was serially diluted in 1X PBS and 100 μl of each dilution was spread plated in triplicates onto TSA plates supplemented with appropriate antibiotics. The petri plates were incubated overnight at 37°C and CFU reduction was compared to control group plates.

Transmission Electron Microscopy (TEM) of Bacterial Strains: TEM imaging of bacteria was performed in order to study the interaction of MNPs and bacterial cell-surface. The samples were prepared according to modified protocol [41, 62]. Post AMF treatment of bacterial cells (MNPs concentration - 650 μg/ml), the mixture samples were

69

removed from the glass vial and centrifuged at 7000 x g for 5 minutes. Later, the supernatant containing unbound MNPs was removed and the pellet was washed with 1x PBS in repetitive centrifugation cycles (3 times). After the final wash, the pellet containing MNPs and bacteria was fixed in cacodylate-buffered glutaraldehyde (3%, pH~7.2; Electron Microscopy Sciences, PA, USA) at 4°C for 12 hours. Subsequently, the sample was again washed in the cacodylate buffer thrice. 5 μl of the sample was dropped onto carbon-coated copper grid and was allowed to air dry for 4 hours. Finally, the sample was stained with 2% uranyl acetate (Electron Microscopy Sciences, PA, USA) solution for 15 seconds and blotted dry with filter paper. TEM images were taken on Hitachi H-7600 at 120 KV accelerating voltage and magnification ranging from 10,000X to 200,000X.

Bacterial Live/Dead Fluorescence Assay: To qualitatively determine the cell membrane integrity of bacterial cells, Live/Dead fluorescence assay were performed using BacLight™ Bacterial Viability Kit (L7007, Molecular Probes, Invitrogen, OR, USA). Freshly grown cells of *EC* K99 and *EC* O157 (5 x 10^7 CFU) in 1X PBS were mixed with PEO-MNPs and GM3-MNPs (Concentration - 650 μg/ml) separately in different microcentrifuge tubes. The mixture was allowed to incubate at room temperature for 30 minutes with gentle mixing after every 5 minutes. The tubes were then exposed to AMF therapy for 120 minutes. The samples were then prepared according to manufacturer's protocol. Later, both fluorescent dyes i.e. SYTO 9 and Propidium Iodide were added to the samples. Finally, the samples were viewed under fluorescence microscope under different filters (SYTO 9 - Excitation/Emission - 485/510 nm;

Propidium Iodide - Excitation/Emission - 485/630 nm) at 400X magnification. The images obtained under different filters were merged in ImageJ software (NIH, USA). Control group samples were not exposed to MNPs/AMF.

Microbial ATP Cell-Viability Assay: To measure the overall intracellular ATP levels of bacterial species (*EC* K99 and *EC* O157) before and after AMF treatment in the presence/absence of MNPs (concentration - 650 μg/ml, AMF treatment time - 120 minutes), microbial BacTiter-Glo™ (Promega, Madison, WI) assay kit was used [23]. The assay was performed according to manufacturer's protocol with a small modification for samples containing MNPs. After AMF treatment of bacteria in the presence of MNPs, the samples were centrifuged at 10,000 x g for 5 minutes. The supernatant containing unbound MNPs was removed and the resultant pellet was washed with 1X PBS thrice in subsequent centrifugation cycles. Finally, the samples were suspended back in 1X PBS and the entire assay was performed in 96-well white-flat bottom plates (Corning®) in triplicates. Also, wells containing MNPs without any bacterial cells were used as control blanks to check for MNPs interference with the assay reagent, if any. At the end of this assay, the plate was read in a micro-plate reader with luminescence capability (Synergy Hybrid H1, Biotek®) and the obtained results were expressed in relative luminescent units (RLUs).

Statistical Analysis: All the statistical analysis was performed using Graphpad Prism software (V 5.0, CA, USA). All the experiments were done in triplicates and data are expressed as Mean±SD. Statistically significant differences between the groups were evaluated by performing ANOVA. *Post hoc* group comparisons were calculated through

Bonferroni post-tests. Results showing P values of ≤ 0.05, <0.01, and <0.001 were considered to be statistically significant.

3. Results and Discussion:

3.1. Synthesis of GM3-MNPs:

Magnetite nanoparticles were synthesized using a one-pot thermal decomposition of iron (III) acetylacetonate and oleic acid [1, 2]. Particles had an average diameter of 23.7 nm with a standard deviation of 1.55 nm (Figure 3.2 A and B). The moment vs. field (MvH) (Figure 3.3) measurement was done on the particles to confirm the super-paramagnetic behavior of the MNPs. Polymer design was based on work by Stone *et al.* where a multi-anchored binding approach showed increased stability in comparison to polymer ligands with a single binding moiety (figure 3.1) [3].
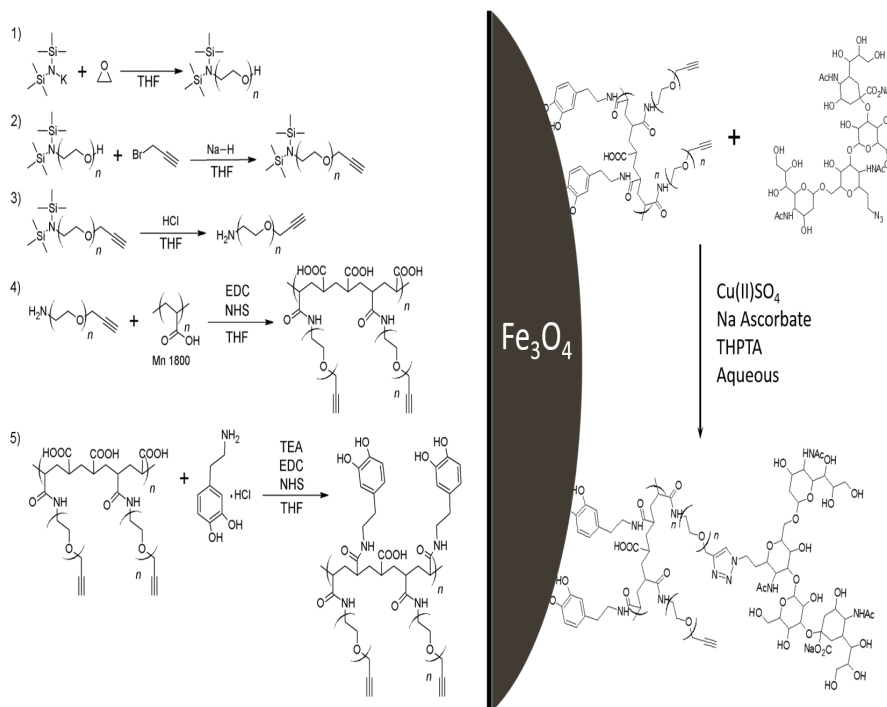
Figure 3.1 Left: 1) Anionic ring opening of ethylene oxide, 2) alkyne functionalization with propargyl bromide, 3) deprotection of primary amine, 4) coupling of PEO to PAA, 5) coupling of dopamine hydrochloride to the PEO-PAA. Right: Click reaction between polymer coated particles and GM3 molecule.
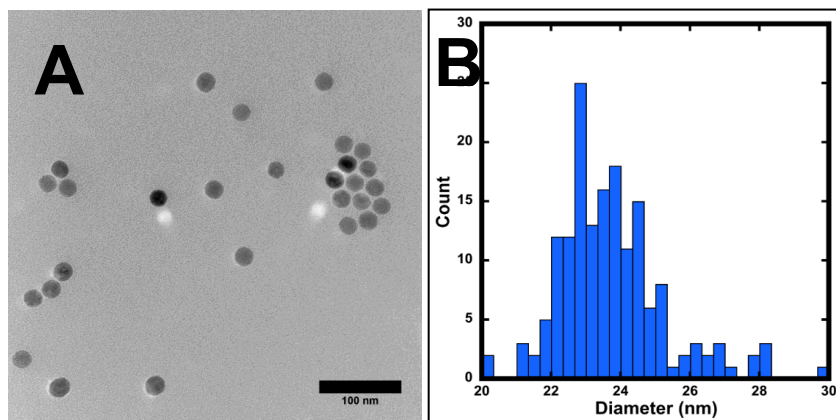
Figure 3.2 Magnetite nanoparticles as synthesized before functionalization with PEO-PAA-dopamine polymer. A – Representative TEM image of the particles. B – Histogram depicting the particle size distribution.
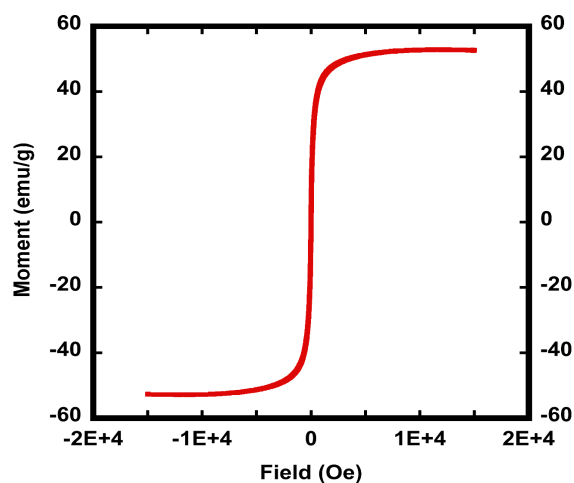
Figure 3.3 Moment vs. Field (MvH) loop showing the superparamagnetic behavior of the magnetite nanoparticles (M_{sat} ~ 53 emu/g Fe).

In this work, however, the chosen catechol was not nitroDOPA but dopamine. HNMR of the polymer was used to confirm both the structure and molecular weight of the PEO-PAA-dopamine macromolecule (Figure 3.4). By using the multi-anchored approach, the stability in salt and protein buffer solutions is retained even when using dopamine as the

anchoring group [4, 5]. Hydrodynamic diameter and zeta potential of the PEO-MNPs before and after click-coupling of GM3 are reported in Table 3.1.
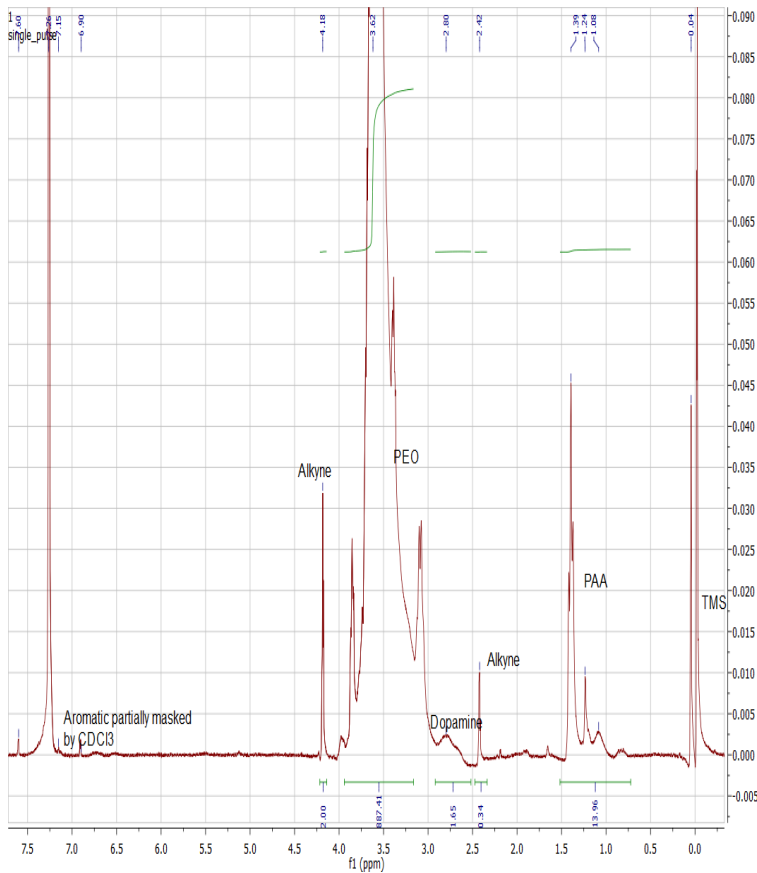
Figure 3.4 HNMR of the final PEO-PAA-dopamine - PAA backbone protons at 1.39 ppm - 1.08 ppm. Alkyne protons at 4.18 ppm and 2.42 ppm. PEO repeat protons at 3.62 ppm. Dopamine aromatic proton signal partially masked by the CDCl$_3$ peak, with alkane protons showing up at 2.8 ppm. Reference was tetramethylsilane at ~0 ppm.

	Hydrodynamic Diameter Z Avg. (nm)	Zeta-potential (mV)
PEO-MNPs	78.8	-8.73
GM3-MNPs	88.8	-7.68

Table 3.1 Dynamic light scattering and zeta-potential measurements - Hydrodynamic diameter and zeta potential as measured by dynamic light scattering before and after GM3 conjugation.

The specific absorption rate (SAR) value for the MNPs was measured to be 53.4 W/g (bulk temperature rise of solution from 37°C to 42°C), which is similar to the value for magnetite reported by Ma *et al* [6]. The increase in the hydrodynamic diameter indicates the GM3 glycoconjugate was successfully coupled to the PEO-MNPs. Attenuated total reflectance Fourier transformed infrared spectroscopy (ATR-FTIR) also confirmed the GM3 coupling went to completion with the disappearance of the azide peak from GM3 at ~2110 cm^{-1} and the appearance of a broad alcohol peak in the GM3-MNPs spectrum from 3620-3170 cm^{-1} (Figure 3.5) [7].
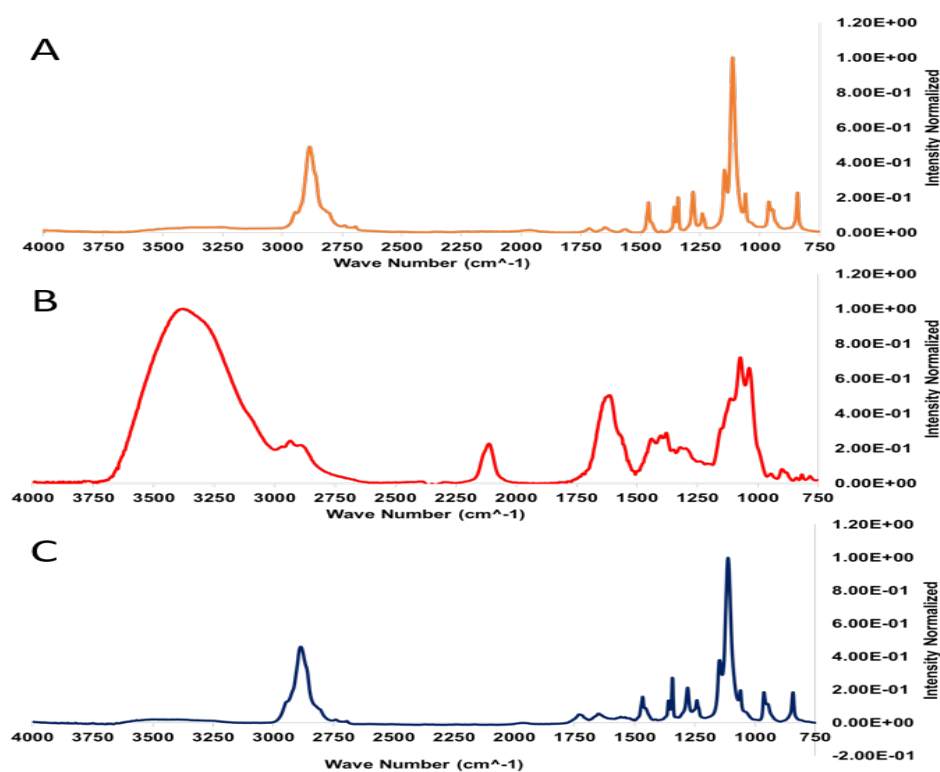
Figure 3.5 FTIR spectra of particles before GM3 conjugation (A), GM3 molecule (B), and after conjugation (C). The lack of the azide peak in C at 2100 cm^{-1} indicates purification of unbound GM3 after conjugation was successful.

3.2 MagMED Inactivation of Bacteria:

The efficacy of GM3-MNPs for specific inactivation of ETEC K99 via MagMED was compared to that of enterohaemorrhagic *Escherichia coli* (EHEC) O157:H7 strain since the two strains showed different receptor-binding specificities and EHEC O157:H7 strains are rarely harbored by pigs [8]. Another *E. coli* strain ORN178 expressing mannose-binding type-1 fimbrial FimH adhesins [9-13] was also evaluated and served as a negative control (data not shown). The MagMED inactivation of bacteria was assessed using a colony forming unit (CFU) reduction assay to determine the number of viable cells (CFUs) remained after treatment.

3.2.1 MagMED Inactivation of *EC* K99:

The efficacy of AMF mediated killing of the target bacteria, *EC* K99, in the presence of GM3-MNPs in a concentration- and time-dependent manner was evaluated. GM3-MNPs were mixed with *EC* K99 and incubated at room temperature for 30 minutes to facilitate the binding between GM3 molecules present on the surface of GM3-MNPs and adhesin molecules of *EC* K99 [7]. PEO-MNPs were used as an internal control group to evaluate the role of the targeting moiety GM3. The magnetic field and frequency used in the AMF therapy remained constant for all treatment groups (31 kA/m and 207kHz). Figure 3.6 A shows the final counts of CFU/ml of *EC* K99 after treatment. The reduction in CFU/ml was found to be both time and MNPs concentration dependent. After 30 minutes of AMF treatment, ~1-log reduction in CFU/ml of *EC* K99 was observed at a particle concentration of 650 µg Fe/ml. After 60 minutes of AMF treatment, a significant

~2-log reduction of *EC* K99 ($p<0.01$) was observed for both 280 µg Fe/ml and 650 µg Fe/ml concentrations of GM3-MNPs. Finally, at the end of 120 minutes of AMF treatment, an extremely significant ~3-log reduction in CFU/ml of *EC* K99 ($p<0.001$) was achieved with particle concentrations of 650 µg Fe/ml. Moreover, no significant killing of *EC* K99 was observed in experimental groups not exposed to AMF (Figure 3.7 A) indicating the non-toxicity of PEO-MNPs and GM3-MNPs to *EC* K99.
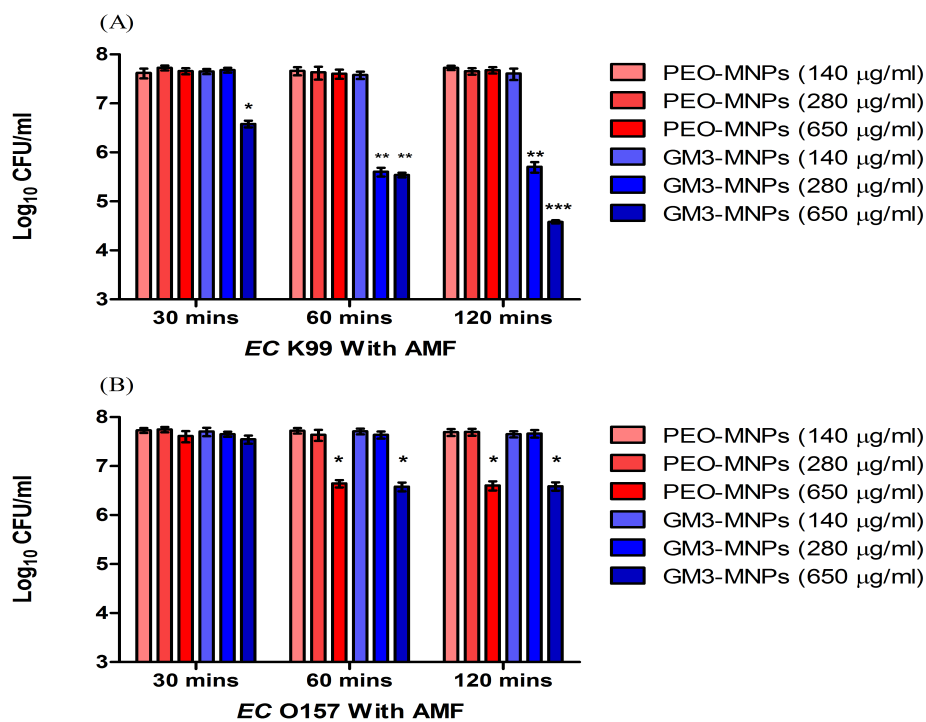
Figure 3.6 Colony Forming Unit (CFU) of *E. coli* strains after AMF treatment at different concentrations of MNPs and different time-intervals; A - CFU/ml of *EC* K99 after AMF treatment; B - CFU/ml of *EC* O157 after AMF treatment. Data is expressed as Mean ± SD (n=3); Statistical analysis – Analysis of Variance (ANOVA); * *p*-value <0.05, ** *p*-value <0.01, and *** *p*-value <0.001

(A)

(B)
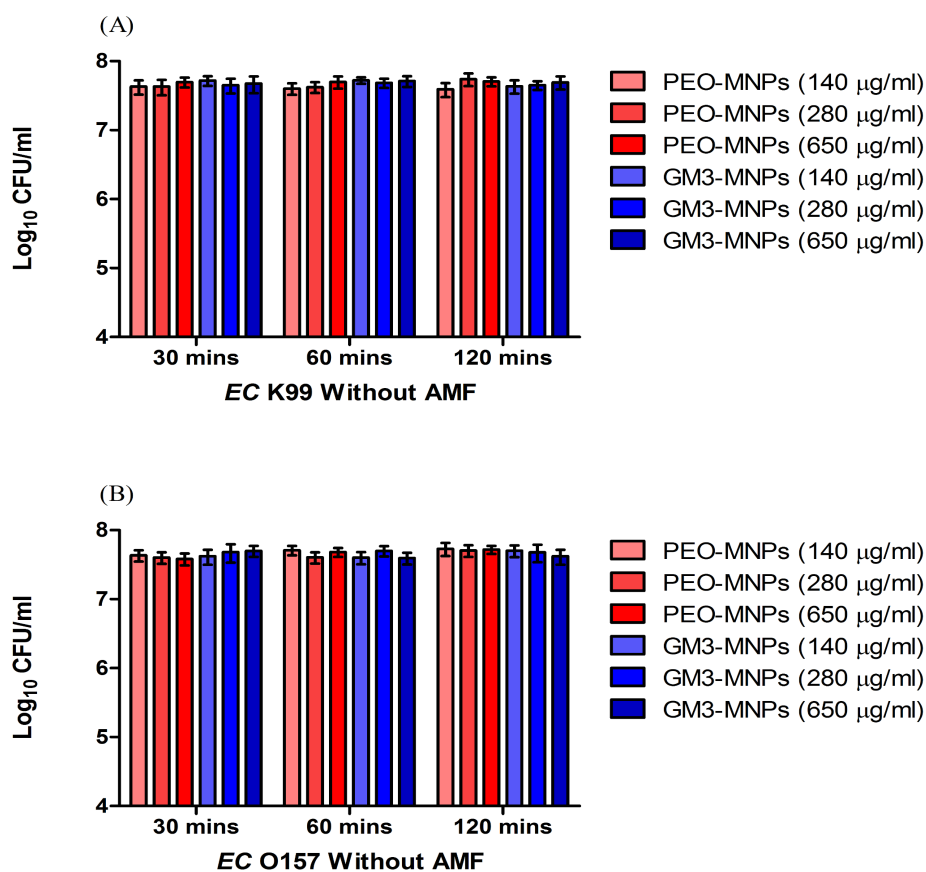
Figure 3.7 CFU/ml assay to determine viability of *E. coli* strains in the absence of AMF at different concentrations of MNPs and at different time-intervals: A - CFU/ml of EC K99 in the absence of AMF; B - CFU/ml of EC O157 in the absence of AMF. Data is expressed as Mean ± SD (n=3); Statistical analysis – Analysis of Variance (ANOVA).

Thus, targeted approach in AMF exposure can explain such effective reduction in CFU/ml of *EC* K99. Several research studies have shown similar results in reduction of bacterial population through antibody-targeted photo-inactivation process via near-infrared laser (NIR) in the presence of nanoparticles in both *in vitro* and *in vivo* settings [14-16]. In our previous work, we have shown that sialic-acid sequences of GM3 molecule (Neu5Ac(α2-3)-Gal-(β1-4)Glcβ-sp) can specifically interact with S-type

fimbrial proteins/adhesins present on the outer surface of *EC* K99 and induce rapid clustering of *EC* K99 [7, 17]. The presence of FanC, a major protein sub-unit present in S-type fimbriae, is primarily responsible for the specific attachment of *EC* K99 onto the ganglioside receptors, which are present on the host-cell surface [18]. Therefore, it is likely that GM3-MNPs-induced bacterial aggregation plays a major role in the applied method. Since GM3-MNPs are attached to or are in extremely near vicinity of *EC* K99, one can expect to see increased delivery of energy from the particles into the bacterial cells. Some reports have also suggested highly localized temperature increase taking place in the biological systems in the presence of MNPs when using AMF [19-21]. For example, Huang *et al.* functionalized the surface of MNPs with fluorophores that act as molecular temperature probes while remotely activating ion channels/neurons in the presence of AMF [22]. Also, the observed drug release due to phase changes in the polymer near the surface of the particle suggests a local temperature increase [23]. In these studies, too, the overall temperature of bulk particle suspensions remained constant or increased marginally. However, the exact mechanisms of how energy from the particle interferes with these pathways are still unknown and are in need of better characterization.

In the present study, the experimental group comprising of 140 µg Fe/ml that underwent AMF treatment did not show significant reduction in CFU/ml of *EC* K99 after 120 minutes of exposure. One possible explanation for this might have to do with the number of particles present in different concentrations of the GM3-MNPs. The lowest concentration group would have the least amount of MNPs. Thus, they might not be able

to efficiently deliver the energy of the MNPs into the bacterial cells. PEO-MNPs at all concentrations and all time-points did not induce significant decrease in the colony counts of *EC* K99.

3.2.2 MagMED Inactivation of *EC* O157:

Figure 3.6 B shows the overall reduction in CFU/ml of *EC* O157 after exposure to AMF in the presence of PEO-MNPs or GM3-MNPs. A ~1-log reduction in CFU/ml was observed with both PEO-MNPs and GM3-MNPs at particle concentration of 650 µg Fe/ml for 60 and 120 minutes. All other MNPs concentrations and time-points showed no significant reduction in colony counts of *EC* O157. No reduction in CFU/ml of *EC* O157 was observed in the absence of AMF (Figure 3.7 B) indicating the non-toxicity of PEO-MNPs and GM3-MNPs to *EC* O157. Several groups have observed certain degree of non-specific electrostatic interactions occurring between bacteria and nanoparticles when mixed with relatively higher concentrations of nanoparticles [24, 25]. Hence, it is possible that due to such non-specific interactions along with high MNPs-to-bacteria ratio, few MNPs might come in contact or close proximity with *EC* O157 resulting in delivery of some magnetic energy into these cells causing a limited ~1-log reduction in CFU. Bacterial control groups exposed to AMF in the absence of MNPs showed no changes in the overall CFU/ml after 120 minutes of exposure (Figure 3.8 A and B) indicating the non-lethal effect of AMF.
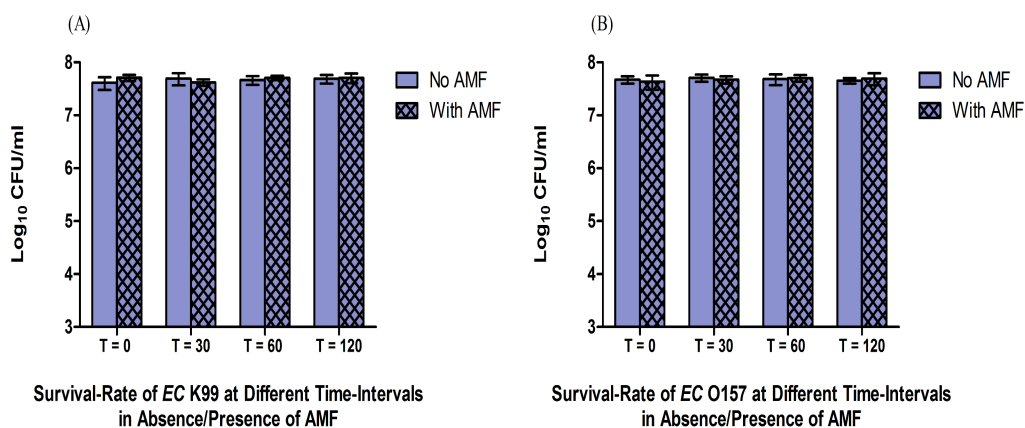
Figure 3.8 Survival rate of *E. coli* strains at 37°C in the absence of MNPs at different time-intervals: A - CFU/ml of *EC* K99 in the absence/presence of AMF; B - CFU/ml of *EC* O157 in the absence/presence of AMF. Data is expressed as Mean ± SD (n=3); Statistical analysis – Analysis of Variance (ANOVA).

Recently, Nguyen *et al.* conducted a similar type of study wherein they showed that iron-oxide nanoparticles could rapidly induce biofilm dispersal in *Pseudomonas aeruginosa* (*P. aeruginosa*) through application of an alternating magnetic field [26]. Their study showed rapid increase in the temperature of buffer solution when nanoparticles were mixed with them and exposed to magnetic field. Similarly, another study reported 4-log reduction in biofilm of *P. aeruginosa* when exposed AC magnetic field in the presence of iron-oxide nanoparticles [27]. The authors have attributed this reduction in biofilm due to quick increase in bulk temperature of the system through magnetic hyperthermia. Thomas *et al.* used magnetic fluid hyperthermia in the presence of carboxylic-acid stabilized iron-oxide nanoparticles and achieved ~7-log reduction in population of *Staphylococcus aureus* [28]. In all of the aforementioned studies, the killing/inactivation of bacterial species/biofilms was attained solely due to drastic

increase in the bulk temperature of the working system through nanoparticles and hyperthermia. It would be worthwhile to note that the aforementioned studies were conducted in the presence of relatively high concentrations of MNPs (ranging from 1 mg/ml to 50 mg/ml) and higher instrument frequencies (e.g., up to 1.05 MHz). Using such high concentrations of MNPs in humans might cause serious concerns with regard to toxicity of MNPs. Also, none of the above listed studies utilized any kind of targeting moiety on nanoparticles for attaining specificity. On the other end, this work demonstrates significant killing of *EC* K99 at much lower concentrations (maximum concentration - 650 µg Fe/ml) and at relatively benign frequencies (i.e., 207 kHz). These results further support our hypothesis that the combination of magnetic fields and presence of GM3-MNPs are responsible for reduction in CFU/ml of *EC* K99 via targeted AMF therapy. The reported CFU reduction within 120 minutes (i.e., 3-log in 2 hours) treatment compares favorably to conventional antibiotic treatments. For examples, Silva *et al.* reported that ciprofloxacin at concentrations corresponding to 1x MIC (Minimal Inhibitory Concentration) reduced *E. coli* population by 1-log over a 24-h study while at 2x and 4x times the MIC value, they observed a ~2.5-log reduction in the first 2 hours and a 4-log reduction after 24 hours of treatment [29]. In a similar study, Drago *et al.* observed no reduction of *E. coli* population at 1x MIC with levofloxacin or ciprofloxacin over a 24-h period while a 2-log and 3-log reduction at 4x MIC was observed 3 hours and 24 hours after treatment, respectively [30]. It is conceivable that with fine-tuned MagMED treatment regimen, it is possible to improve the treatment outcomes of infections caused by multiple-drug resistant bacteria.

As mentioned earlier, a moderate temperature increase (37°C to 42°C) was observed in the bulk particle suspension while measuring SAR values in the presence of magnetic field. To prove that the significant log-reduction of *EC* K99 is not due to temperature increase alone, a CFU/ml assay on both the *E. coli* strains at elevated temperature of 43°C was performed. The bacterial strains were incubated with PEO-MNPs and GM3-MNPs for 120 minutes and this mixture was kept inside the holding chamber of the AMF instrument by maintaining a constant temperature of 43°C for 120 minutes in the absence of magnetic field. As seen in Figure 3.9 A and B, no significant changes in CFU/ml of *EC* K99 and *EC* O157 were observed after exposing the bacteria to MNPs and at elevated temperatures for 120 minutes. This strongly suggests that inactivation of the bacteria cannot be attributed to temperature alone.
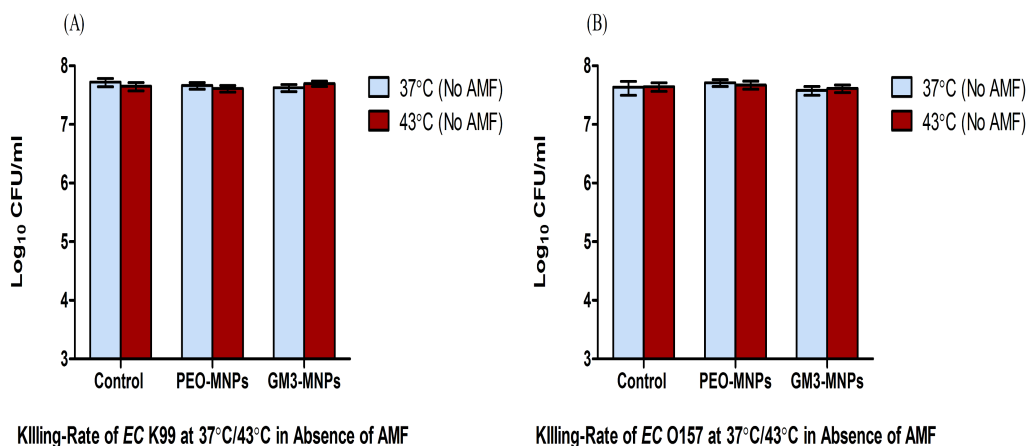
Figure 3.9 Evaluating the effect of temperature increase on killing-rate of *E. coli* strains in the absence of AMF (time - 120 minutes): A - Killing-rate of *EC* K99 at 37°C/43°C in the presence of MNPs (concentration - 650 µg Fe/ml); B - Killing-rate of *EC* O157 at 37°C/43°C in the presence of MNPs (concentration - 650 µg Fe/ml). Data is expressed as Mean ± SD (n=3); Statistical analysis - 2-Way Analysis of Variance (ANOVA).

3.2.3 MagMED Inactivation of *EC* K99 and *EC* O157 in Mixed-Culture:

Pathogens interact with host in a heterogeneous environment; the efficacy of utilizing MagMED for killing of the target bacteria *EC* K99 was evaluated in a mixed-culture condition. Both strains of the *E. coli* cultures were mixed in the same container at equal concentrations and added either the GM3-MNPs or the PEO-MNPs at a maximum concentration of 650 µg Fe/ml. These mixtures underwent the same AMF exposure as described earlier for 120 minutes and the CFU/ml reduction assay was done to determine the inactivation rates of both strains of *E. coli*. As seen in Figure 3.10 A, a significant ~2.5-log reduction ($p<0.001$) in CFU/ml of *EC* K99 in the presence of GM3-MNPs and AMF exposure was observed. The other mixed culture containing PEO-MNPs did not show significant difference in CFU/ml numbers compared to controls in the absence/presence of AMF. In addition, ~1-log reduction ($p<0.05$) in CFU/ml of *EC* O157 was seen when the mixed-cultures were added with PEO-MNPs or GM3-MNPs and underwent AMF treatment for 120 minutes (Figure 3.10 B). This reduction in CFU/ml of *EC* O157 is comparable in both mixed-culture and pure-culture experiments. Compared to CFU/ml assay results of *EC* K99 in pure bacterial culture experiments where a ~3-log reduction was observed, the results obtained from mixed-culture experiments showed a ~2.5-log reduction. This minor difference could be the result of a change in nanoparticle-to-bacterium ratio in mixed-culture experiments. Since the nanoparticle-to-bacterium ratio was reduced by half under mixed-culture settings, the probability of GM3-MNPs interacting with *EC* K99 as well as *EC* O157 is also slightly reduced than in pure culture

settings. To the best of our knowledge, this is the first report wherein killing of targeted bacterial strains via MagMED has been demonstrated in mixed-culture settings.
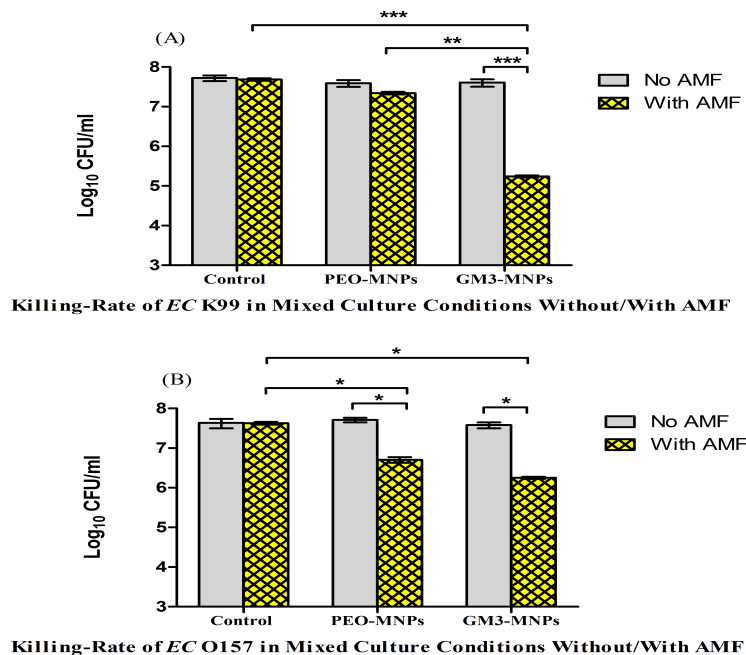
Figure 3.10 Colony Forming Unit (CFU) of *E. coli* strains in mixed-culture conditions exposed to AMF for 120 minutes in the presence of MNPs (650 µg Fe/ml); A - CFU/ml of *EC* K99 after AMF treatment; B - CFU/ml of *EC* O157 after AMF treatment. Data is expressed as Mean ± SD (n=3); Statistical analysis - 2-Way Analysis of Variance (ANOVA); * *p*-value <0.05, ** *p*-value <0.01, and *** *p*-value <0.001.

3.3 Investigating Interactions between GM3-MNPs and *EC* K99 via Transmission Electron Microscopy (TEM):

One of the many causes for inactivation/killing of bacterial cells could be due to physical damages of bacterial cell membrane that results from the presence of different types of nanoparticles [31, 32]. In order to investigate the bacterial-nanoparticle interactions between GM3-MNPs and *EC* K99, TEM analysis on the samples was performed before and after AMF exposure. Since the maximum reduction in CFU/ml of *EC* K99 was achieved in the presence of 650 µg Fe/ml MNPs after 120 minutes, the same

experimental conditions to investigate if AMF exposure can exert any specific morphological changes on the bacterial cell membrane of *EC* K99 was followed. Visualizing TEM images, highly specific interactions taking place between GM3-MNPs and outer membrane of *EC* K99 was observed. Figure 3.11 B shows the extent of GM3-MNPs specifically attached to *EC* K99. The entire cell-surface of the bacteria was covered with GM3-MNPs before applying AMF. There was no visible morphological change seen on the bacterial cell surface of *EC* K99, which could also indicate that the nanoparticle system does not have an apparent inherent toxicity by itself towards bacteria.

E. coli	No AMF		With AMF	
	With PEO MNPs	With GM3 MNPs	With PEO MNPs	With GM3 MNPs
K99	A	B	C	D
O157	E	F	G	H
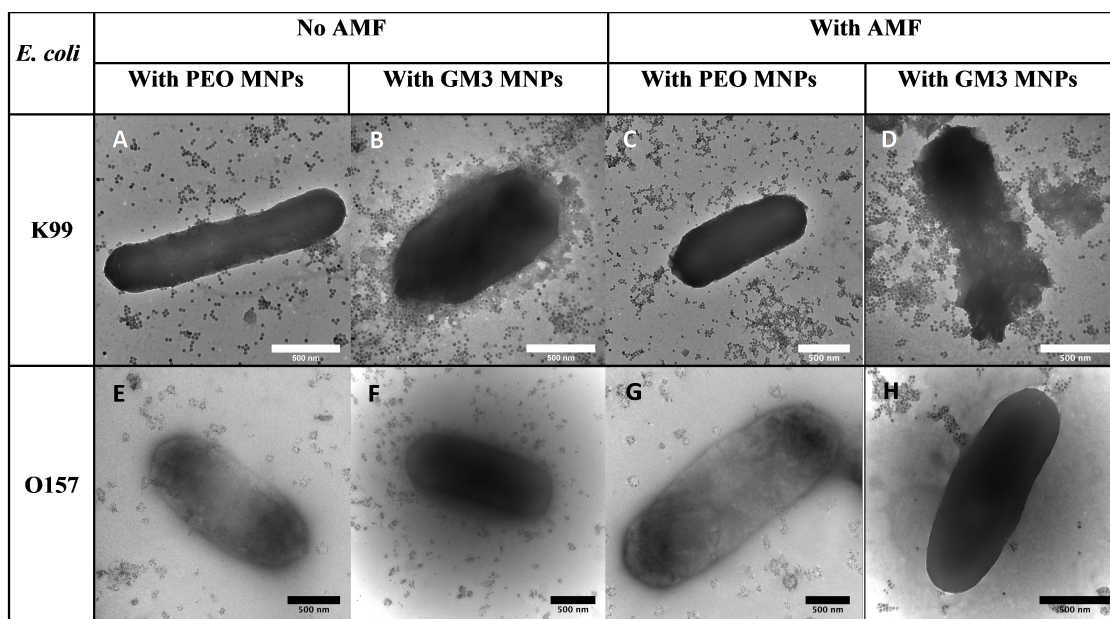
Figure 3.11 TEM images of GM3-MNPs induced bacterial membrane damage of *E. coli* strains: A, B, E, F - Before AMF, and C, D, G, H - after AMF treatment for 120 minutes. Concentration of MNPs - 650 μg Fe/ml. Scale bar is 500 nm.

Also, GM3-MNPs induced bacterial aggregation of *EC* K99 was clearly visible in TEM images (Figure 3.12 B). In contrast, after applying AMF, the cell structure of *EC* K99 was seen to be extremely damaged as seen in Figure 3.10 D. Please also note that the diameters of *EC* K99 were reduced to less than 0.5x0.25 μm from the typical 1x0.5 μm. The nanoparticles were found internalized in cells of *EC* K99 after rupturing the cell membrane. Concurrent findings were also reported in a few studies with regard to destruction of bacterial cell membrane via targeted photo-thermal lysis in the presence of nanoparticles [33, 34]. Even after AMF exposure, GM3-MNPs were found to remain attached onto bacterial cell debris, which suggests strong binding interactions between GM3-MNPs and adhesin molecules of *EC* K99 present on the bacterial cell surface. Interestingly, it was observed that both the polar ends of *EC* K99 were found to be much more deformed and broken (Figure 3.12 A and B). However, not much damage was seen towards the horizontal length of *EC* K99. A large quantity of cell membrane debris was observed in the TEM analysis suggesting that *EC* K99 would have undergone thermal lysis after AMF exposure possibly due to highly localized temperature increase. Moreover, both PEO-MNPs and GM3-MNPs did not show any substantial attachment to *EC* O157 cells (Figure 3.11 E to H). Even the cell membrane morphologies looked similar to control group cells that were exposed to AMF without any MNPs. Thus, the TEM analysis and CFU/ml assays support our initial findings regarding the specific interactions occurring between GM3-MNPs and *EC* K99 and that GM3-MNPs found on bacterial surface of *EC* K99 play an important role in lysing the bacterial cells (bactericidal) when exposed to AMF.
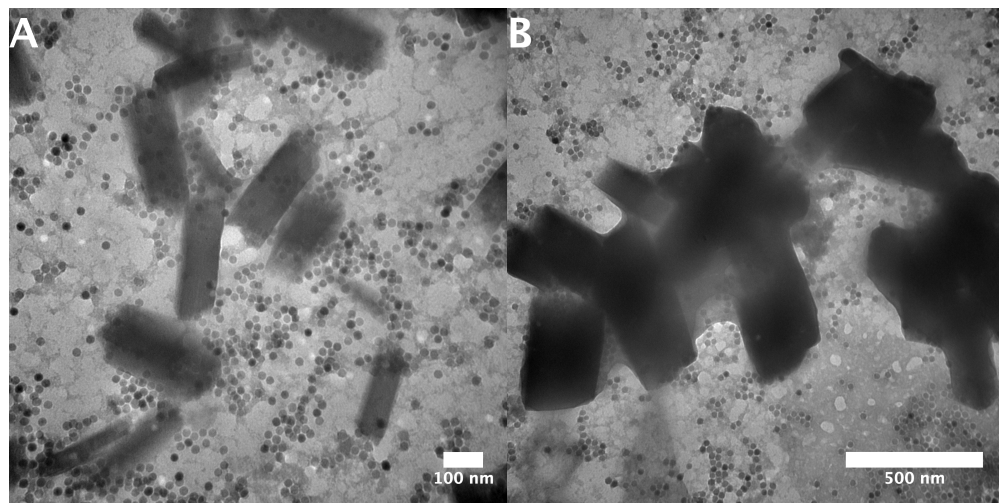
Figure 3.12 TEM imaging of *EC* K99 cells after AMF treatment in the presence of GM3-MNPs: A - *EC* K99 cells showing lysis/breakage of their polar ends (Scale bar - 100 nm); B - *EC* K99 cells showing aggregation and breakage induced by presence of GM3-MNPs and AMF (Scale bar - 500 nm). Magnification ranges between 50,000X to 150,000X.

3.4 Bacterial Live/Dead Fluorescence Assay:

One of the common assays employed to check the membrane integrity of bacterial cells is to use propidium iodide dye [35]. Since the TEM analysis showed extensive membrane damage of *EC* K99 cells after AMF treatment, to further support these results, bacterial live/dead assays were performed. *E. coli* strains, after AMF exposure in the presence of MNPs, were stained using mixture of SYTO 9 and propidium iodide dyes. SYTO 9 is a green-fluorescent dye that stains both live and dead bacterial cells by entering inside them. Conversely, propidium iodide can only permeate those bacterial cells whose cell membrane structures have been compromised and stains them red. For this assay, the bacterial strains were mixed with different types of MNPs. Figure 3.13 shows the results obtained after performing live/dead-staining assays.

E. coli	No AMF		With AMF	
	With PEO MNPs	**With GM3 MNPs**	**With PEO MNPs**	**With GM3 MNPs**
K99	A	B	C	D
O157	E	F	G	H
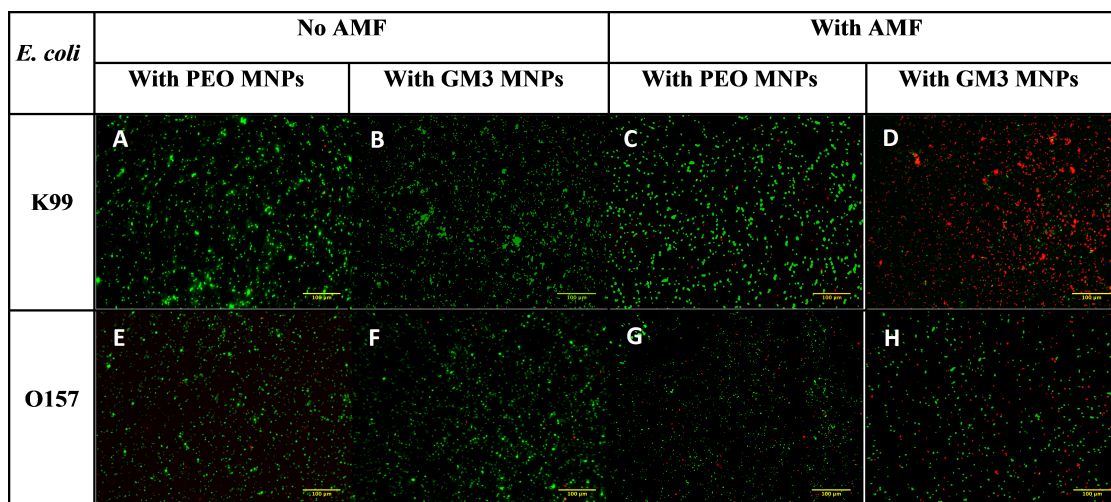
Figure 3.13 Live/Dead Staining Assay using SYTO 9 and Propidium iodide dyes. Both strains *EC* K99 and *EC* O157 are stained with mixture containing the above-mentioned dyes. The bacterial strains were initially mixed with PEO-MNPs and GM3-MNPs (concentration - 650 μg Fe/ml) and then exposed to AMF treatment for 120 minutes. Live bacterial cells appear green in color and dead cells appear red in color. All the images are merged together for both green and red channel filters of the microscope. A, B, E, and F represent *E. coli* cells incubated with MNPs but without AMF treatment. C, D, G, and H represent *E. coli* cells incubated with MNPs in the presence of AMF. Magnification - 400X, Scale bar - 100 μm.

As clearly seen in Figure 3.13 D, more than 95% of *EC* K99 cells were stained red in color after exposure to AMF in the presence of GM3-MNPs. This proves that indeed *EC* K99 cells experienced extensive cell membrane damage due to AMF. Also, ~50% of *EC* O157 cells were stained red which suggests partial membrane damage (Figure 3.13 G-H). In contrast, both *E. coli* strains stained green in color in the presence of MNPs but without exposure to AMF (Figure 3.13 A, B, E, F). The control group of bacterial cells in the absence of both MNPs and AMF also stained green in color (Figure 3.14 A and B). These results further support the non-toxic nature of the nanoparticles. Several research groups obtained similar results for live/dead staining assay when

magnetic nanoparticles were used as antibacterial agents [25, 26, 36]. These results correlate with those obtained in CFU reduction assay wherein *EC* K99 and *EC* O157 showed ~3-log reduction and ~1-log reduction in CFU/ml, respectively, after 120 minutes of AMF treatment in the presence of GM3-MNPs.
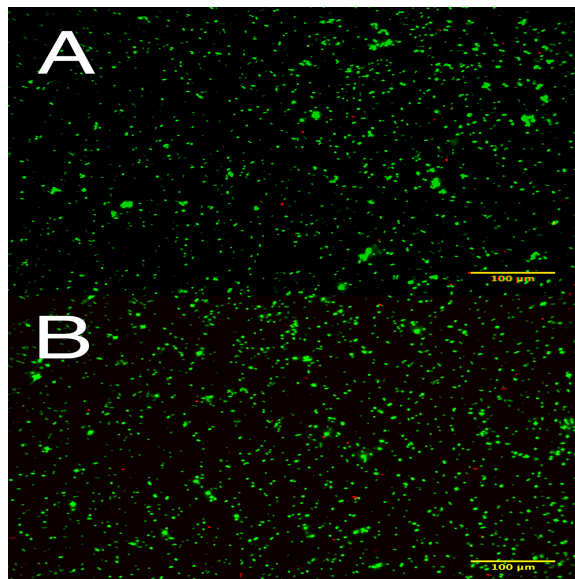
Figure 3.14 Live/Dead Staining Assay using SYTO 9 and Propidium iodide dyes: A - *EC* K99 in the absence of MNPs and no AMF; B - *EC* O157 in the absence of MNPs and no AMF. Magnification - 400X, Scale bar - 100 μm.

3.5 ATP Assay:

The amount of ATP level present in any cell determines its metabolic state. In the presence of toxic materials/chemicals, the metabolic state of the cell can change and the intracellular ATP levels could drop because of toxicity. Higher levels of intracellular ATP levels indicate that the cell is metabolically active and their levels directly correlate to the actual number of bacterial cells present in the solution. Currently, several antibiotics available in the market exert their effects on targeting bacterial membrane

components to eradicate infections [37, 38]. To further demonstrate and explain the effect of AMF exposure on the biochemical metabolism of the inner cell membrane, an ATP assay based on luminescence was conducted to evaluate final ATP levels of *EC* K99 and *EC* O157 after exposing them to AMF for 120 minutes in the presence of different types of MNPs at their highest concentrations (650 μg Fe/ml). As seen in Figure 3.15 A, a substantial decrease in intracellular ATP levels of *EC* K99 ($p < 0.001$) after 120 minutes of AMF treatment can be observed in the presence of GM3-MNPs only while *EC* K99 in the presence of PEO-MNPs with/without AMF did not show significant changes in ATP levels. In contrast, the intracellular levels of *EC* O157 were found to be slightly reduced both in the presence of PEO-MNPs or GM3-MNPs with AMF exposure (Figure 3.15 B). A similar decrease in ATP levels was reported in *P. aeruginosa* when they were subjected to magnetic induction in the presence of iron-oxide nanoparticles [26]. One possible explanation for reduced ATP levels in the presence of AMF exposure can be the decline in membrane potential of bacteria, which could lead to interruption in ATP synthesis mechanisms (e.g., reduced proton motive force), membrane depolarization and eventually cell-death [32, 39, 40].
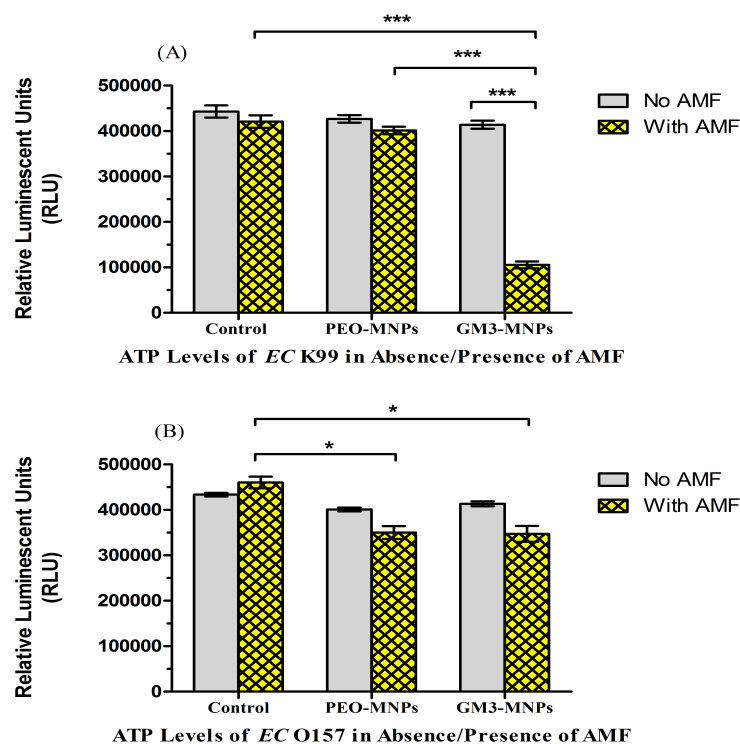
Figure 3.15 Intracellular ATP levels of bacterial strains in the presence of MNPs using BacTiter Glo. A - ATP levels of *EC* K99 after 120 minutes of AMF treatment in the presence of MNPs; B - ATP levels of *EC* O157 after 120 minutes of AMF treatment in the presence of MNPs. Data expressed as Mean ± SD (n = 3); Statistical Analysis - 2-Way Analysis of Variance (ANOVA). * *p*-value <0.05, ** *p*-value <0.01, and *** *p*-value <0.001.

It is worth noting that *EC* O157 when treated with AMF in the presence of PEO-MNPs or GM3-MNPs resulting in similar limited level of cell damage, reductions in viable cells and intracellular ATPs. These results indicated that the changes are independent of the GM3 functional groups present on the surface of MNPs. The susceptibility of *EC* O157 to localized temperature changes due to proximity could be due to a lower thermal decimal reduction time (*D*-value) of *EC* O157 than that of *EC* K99 [41].

4. Conclusion:

Proof-of-concept multi-anchored glycoconjugate GM3-MNPs that have high affinity to adhesin of *EC* K99 were synthesized. The prepared nanoparticle system can specifically interact with adhesin molecules of *EC* K99 and cause agglutination through nanoparticle-bacteria complex. Applying AMF treatment to such complex caused significant reduction in viability of targeted bacteria *EC* K99 in both pure-culture and mixed-cultures settings due to possible highly localized temperature increase. Exposure to such conditions resulting in compromised membrane integrity of *EC* K99 as determined through TEM imaging and Live/Dead staining. Moreover, GM3-MNPs coupled with AMF resulted in significant decrease in the overall intra-cellular ATP levels of the bacterium. Hence, the unique multi-anchored nanoparticle system in the presence of AMF can be effectively used as novel non-antibiotic platform for local and selective inactivation of the target bacteria in biological systems without affecting the viability of nearby cells/tissues. In the event of gastro-intestinal (GI) tract infections caused by ETEC pathogens, administered antibiotics can disrupt/destroy beneficial gut micro-flora in addition to pathogens. It could cause various side effects in the human body along with giving rise to antibiotic-resistant bacterial strains. The presented system can find useful applications in treating such infections in animals and humans and in conditions when administered antibiotics, especially those of the last-line-of-defense drugs, fail to eradicate the infections due to drug-resistance. Future studies will involve optimization of particle parameters including nanoparticle core-size and polymer coatings, as well as a detailed investigation on the effects of field strength and frequency to maximize killing

rate of clinically relevant multi-drug resistant bacterial pathogens. Additionally, biocompatibility of our nanoparticle system will be evaluated in human cell-lines and small animal models.

References:

1.   Neu, H.C., *The crisis in antibiotic resistance.* Science, 1992. **257**(5073): p. 1064-1073.

2.   Jones, K.E., *et al.*, *Global trends in emerging infectious diseases.* Nature, 2008. **451**(7181): p. 990-993.

3.   Organization, W.H., *Antimicrobial resistance: global report on surveillance.* 2014: World Health Organization.

4.   Frieden, T. *Antibiotic Resistance Threats in the United States*. 2013 [cited 2015 6/24/2015]; Available from: http://www.cdc.gov/drugresistance/threat-report-2013/.

5.   Taylor Jirka, M.H., Erez Yerushalmi, Richard Smith, Jacopo Bellasio, Raffaele Vardavas, Teresa Bienkowska-Gibbs and Jennifer Rubin, *Estimating the Economic Costs of Antimicrobial Resistance: Models and Results*, in *Research Reports*. 2014: Santa Monica, Calfornia. p. 113.

6.   Andersson, D.I. and D. Hughes, *Antibiotic resistance and its cost: is it possible to reverse resistance?* Nature Reviews Microbiology., 2010. **8**(4): p. 260-271.

7.   Walsh, C., *Antibiotics: actions, origins, resistance*. 2003: American Society for Microbiology (ASM).

8.   Braykov, N.P., *et al.*, *Trends in resistance to carbapenems and third-generation cephalosporins among clinical isolates of Klebsiella pneumoniae in the United States, 1999–2010.* Infection Control and Hospital Epidemiology, 2013. **34**(3): p. 259-268.

9.   Amstad, E., M. Textor, and E. Reimhult, *Stabilization and functionalization of iron oxide nanoparticles for biomedical applications.* Nanoscale, 2011. **3**(7): p. 2819-2843.

10.   Liu, G., *et al.*, *Applications and Potential Toxicity of Magnetic Iron Oxide Nanoparticles.* Small, 2013. **9**(9-10): p. 1533-1545.

11. Reddy, L.H., *et al.*, *Magnetic nanoparticles: design and characterization, toxicity and biocompatibility, pharmaceutical and biomedical applications.* Chemical Reviews, 2012. **112**(11): p. 5818-5878.

12. Carrey, J., B. Mehdaoui, and M. Respaud, *Simple models for dynamic hysteresis loop calculations of magnetic single-domain nanoparticles: Application to magnetic hyperthermia optimization.* Journal of Applied Physics, 2011. **109**(8): p. 083921.

13. Chiu-Lam, A. and C. Rinaldi, *Nanoscale Thermal Phenomena in the Vicinity of Magnetic Nanoparticles in Alternating Magnetic Fields.* Advanced Functional Materials, 2016. 26(22): p. 3933-3941

14. Creixell, M., *et al.*, *EGFR-targeted magnetic nanoparticle heaters kill cancer cells without a perceptible temperature rise.* ACS Nano, 2011. **5**(9): p. 7124-7129.

15. Hauser, A.K., *et al.*, *Magnetic nanoparticles and nanocomposites for remote controlled therapies.* Journal of Controlled Release, 2015. **219**: p. 76-94.

16. Kozissnik, B., *et al.*, *Magnetic fluid hyperthermia: Advances, challenges, and opportunity.* International Journal of Hyperthermia, 2013. **29**(8): p. 706-714.

17. Saville, S.L., *et al.*, *Investigation of the stability of magnetite nanoparticles functionalized with catechol based ligands in biological media.* Journal of Materials Chemistry, 2012. **22**(47): p. 24909-24917.

18. Harris, J.M., *Introduction to Biotechnical and Biomedical Applications of Poly(Ethylene Glycol)*, in *Poly(Ethylene Glycol) Chemistry: Biotechnical and Biomedical Applications*, J.M. Harris, Editor. 1992, Springer US: Boston, MA. p. 1-14.

19. Stone, R., *et al.*, *Highly stable multi-anchored magnetic nanoparticles for optical imaging within biofilms.* Journal of colloid and interface science, 2015. **459**: p. 175-182.

20. Davis, K., *et al.*, *Quantitative measurement of ligand exchange on iron oxides via radiolabeled oleic acid.* Langmuir, 2014. **30**(36): p. 10918-10925.

21. Thomas, L.A., *et al.*, *Carboxylic acid-stabilised iron oxide nanoparticles for use in magnetic hyperthermia.* Journal of Materials Chemistry, 2009. **19**(36): p. 6529-6535.

22. Park, H., *et al.*, *Inactivation of Pseudomonas aeruginosa PA01 biofilms by hyperthermia using superparamagnetic nanoparticles.* Journal of Microbiological Methods, 2011. **84**(1): p. 41-45.

23.   Nguyen, T.K., *et al.*, *Iron oxide nanoparticle-mediated hyperthermia stimulates dispersal in bacterial biofilms and enhances antibiotic efficacy.* Scientific Reports, 2015. **5**: p. 18385.

24.   Ofek, I. and R.J. Doyle, *Bacterial adhesion to cells and tissues*. Vol. 735. 1994: Springer.

25.   Ofek, I. and N. Sharon, *Adhesins as lectins: specificity and role in infection.* Current Topics in Microbiology and Immunology, 1990. **151**: p. 91-113.

26.   Sharon, N. and H. Lis, *Carbohydrates in cell recognition.* Scientific American, 1993. **268**(1): p. 82-9.

27.   Sharon, N. and I. Ofek, *Safe as mother's milk: carbohydrates as future anti-adhesion drugs for bacterial diseases.* Glycoconjugate Journal, 2000. **17**(7-9): p. 659-664.

28.   Marradi, M., *et al.*, *Glyconanoparticles as multifunctional and multimodal carbohydrate systems.* Chemical Society Reviews, 2013. **42**(11): p. 4728-4745.

29.   Jesus, M. and S. Penadés, *Understanding carbohydrate-carbohydrate interactions by means of glyconanotechnology.* Glycoconjugate journal, 2004. **21**(3-4): p. 149-163.

30.   Wang, Y., *et al.*, *Nanomaterials in carbohydrate biosensors.* TrAC, Trends in Analytical Chemistry, 2014. **58**: p. 54-70.

31.   Kulkarni, A.A., *et al.*, *Glycan encapsulated gold nanoparticles selectively inhibit shiga toxins 1 and 2.* Bioconjugate Chemistry, 2010. **21**(8): p. 1486-1493.

32.   Sunasee, R., *et al.*, *Therapeutic potential of carbohydrate-based polymeric and nanoparticle systems.* Expert Opinion on Drug Delivery, 2014. **11**(6): p. 867-884.

33.   Qu, L., *et al.*, *Visualizing adhesion-induced agglutination of Escherichia coli with mannosylated nanoparticles.* Journal of Nanoscience and Nanotechnology, 2005. **5**(2): p. 319-322.

34.   Gu, L., *et al.*, *Single-walled carbon nanotubes displaying multivalent ligands for capturing pathogens.* Chemical Communications, 2005(7): p. 874-876.

35.   Wang, H., *et al.*, *Unique Aggregation of Anthrax (Bacillus a nthracis) Spores by Sugar-Coated Single-Walled Carbon Nanotubes.* Journal of the American Chemical Society, 2006. **128**(41): p. 13364-13365.

36.   Vedantam, P., *et al.*, *Binding of Escherichia coli to Functionalized Gold Nanoparticles.* Plasmonics, 2012. **7**(2): p. 301-308.

37.   Lin, C.-C., *et al.*, *Selective binding of mannose-encapsulated gold nanoparticles to type 1 pili in Escherichia coli.* Journal of the American Chemical Society, 2002. **124**(14): p. 3508-3509.

38.   Khanal, M., *et al.*, *Inhibition of type 1 fimbriae-mediated Escherichia coli adhesion and biofilm formation by trimeric cluster thiomannosides conjugated to diamond nanoparticles.* Nanoscale, 2015. **7**(6): p. 2325-2335.

39.   Qu, L.W., *et al.*, *Galactosylated Polymeric Nanoparticles: Synthesis and Adhesion Interactions with Escherichia coli.* Journal of Biomedical Nanotechnology, 2005. **1**(1): p. 61-67.

40.   El-Boubbou, K., C. Gruden, and X. Huang, *Magnetic glyco-nanoparticles: a unique tool for rapid pathogen detection, decontamination, and strain differentiation.* Journal of the American Chemical Society, 2007. **129**(44): p. 13392-13393.

41.   Raval, Y.S., *et al.*, *Synthesis and application of glycoconjugate-functionalized magnetic nanoparticles as potent anti-adhesion agents for reducing enterotoxigenic Escherichia coli infections.* Nanoscale, 2015. **7**(18): p. 8326-8331.

42.   Park, S., *et al.*, *Probing cell-surface carbohydrate binding proteins with dual-modal glycan-conjugated nanoparticles.* Journal of the American Chemical Society, 2015. **137**(18): p. 5961-5968.

43.   Liu, L.H., *et al.*, *Photoinitiated coupling of unmodified monosaccharides to iron oxide nanoparticles for sensing proteins and bacteria.* Bioconjugate Chemistry, 2009. **20**(7): p. 1349-1355.

44.   Black, R.E., *Epidemiology of travelers' diarrhea and relative importance of various pathogens.* Rev. Infect. Dis., 1990. **12 Suppl 1**: p. S73-9.

45.   Piddock, L.J., *Multidrug-resistance efflux pumps? not just for resistance.* Nature Reviews Microbiology, 2006. **4**(8): p. 629-636.

46.   Navaneethan, U. and R.A. Giannella, *Mechanisms of infectious diarrhea.* Nature Clinical Practice Gastroenterology & Hepatology, 2008. **5**(11): p. 637-647.

47.   Mouricout, M.A. and R.A. Julien, *Pilus-mediated binding of bovine enterotoxigenic Escherichia coli to calf small intestinal mucins.* Infection and Immunity, 1987. **55**(5): p. 1216-1223.

48.   Barigye, R., *et al.*, *Prevalence and antimicrobial susceptibility of virulent and avirulent multidrug-resistant Escherichia coli isolated from diarrheic neonatal calves.* American Journal of Veterinary Research, 2012. **73**(12): p. 1944-1950.

49.   Güler, L., K. Gündüz, and Ü. Ok, *Virulence factors and antimicrobial susceptibility of Escherichia coli isolated from calves in Turkey.* Zoonoses Public Health, 2008. **55**(5): p. 249-257.

50.   Smith, H.W. and M.A. Linggood, *Further observations on Escherichia coli enterotoxins with particular regard to those produced by atypical piglet strains and by calf and lamb strains: the transmissible nature of these enterotoxins and of a K antigen possessed by calf and lamb strains.* Journal of Medical Microbiology, 1972. **5**(2): p. 243-250.

51.   Nagy, B., H.W. Moon, and R.E. Isaacson, *Colonization of porcine intestine by enterotoxigenic Escherichia coli: selection of piliated forms in vivo, adhesion of piliated forms to epithelial cells in vitro, and incidence of a pilus antigen among porcine enteropathogenic E. coli.* Infection and Immunity, 1977. **16**(1): p. 344-352.

52.   Isaacson, R.E., *et al.*, *In vitro adhesion of Escherichia coli to porcine small intestinal epithelial cells: pili as adhesive factors.* Infection and Immunity, 1978. **21**(2): p. 392-397.

53.   Barry, A.L., *et al.*, *Methods for determining bactericidal activity of antimicrobial agents; approved guideline.* NCCLS document M26-A, 1999. **19**(18).

54.   Park, J., *et al.*, *Ultra-large-scale syntheses of monodisperse nanocrystals.* Nature Materials, 2004. **3**(12): p. 891-895.

55.   Shen, Y., *et al.*, *Purification of quantum dots by gel permeation chromatography and the effect of excess ligands on shell growth and ligand exchange.* Chemistry of Materials, 2013. **25**(14): p. 2838-2848.

56.   Himo, F., *et al.*, *Copper (I)-catalyzed synthesis of azoles. DFT study predicts unprecedented reactivity and intermediates.* Journal of the American Chemical Society, 2005. **127**(1): p. 210-216.

57.   Hong, V., *et al.*, *Analysis and Optimization of Copper‐Catalyzed Azide–Alkyne Cycloaddition for Bioconjugation.* Angewandte Chemie International Edition English, 2009. **121**(52): p. 10063-10067.

58.   Vreeland, E.C., *et al.*, *Enhanced Nanoparticle Size Control by Extending LaMer's Mechanism.* Chemistry of Materials, 2015. **27**(17): p. 6059-6066.

59.   International, A., *Standard Test Method for Iron in Trace Quantities Using the 1,10-Phenanthroline Method*. 2015, ASTM International.

60.   Kim, J., F. Luo, and X. Jiang, *Factors impacting the regrowth of Escherichia coli O157: H7 in dairy manure compost.* Journal of Food Protection®, 2009. **72**(7): p. 1576-1584.

61. Saville, S.L., *et al.*, *The formation of linear aggregates in magnetic hyperthermia: implications on specific absorption rate and magnetic anisotropy.* J Colloid and Interface Science, 2014. **424**: p. 141-151.

62. Hayden, S.C., *et al.*, *Aggregation and interaction of cationic nanoparticles on bacterial surfaces.* Journal of the American Chemical Society, 2012. **134**(16): p. 6920-6923.

63. Sun, S., *et al.*, *Monodisperse MFe2O4 (M= Fe, Co, Mn) nanoparticles.* Journal of the American Chemical Society, 2004. **126**(1): p. 273-279.

64. Mondini, S., *et al.*, *Colloidal stability of iron oxide nanocrystals coated with a PEG-based tetra-catechol surfactant.* Nanotechnology, 2013. **24**(10): p. 105702.

65. Ma, M., *et al.*, *Size dependence of specific power absorption of Fe3O4 particles in AC magnetic field.* Journal of Magnetism and Magnetic Materials, 2004. **268**(1): p. 33-39.

66. Ferens, W.A. and C.J. Hovde, *Escherichia coli O157:H7: Animal Reservoir and Sources of Human Infection.* Foodborne Pathogens and Disease, 2011. **8**(4): p. 465-487.

67. Qu, L., *et al.*, *Galactosylated Polymeric Nanoparticles: Synthesis and Adhesion Interactions with Escherichia coli.* Journal of Biomedical Nanotechnology, 2005. **1**(1): p. 61-67.

68. Maurer, L. and P.E. Orndorff, *Identification and characterization of genes determining receptor binding and pilus length of Escherichia coli type 1 pili.* Journal of Bacteriology, 1987. **169**(2): p. 640-645.

69. Luo, P.G., *et al.*, *Quantitative Analysis of Bacterial Aggregation Mediated by Bioactive Nanoparticles.* Journal of Biomedical Nanotechnology, 2005. **1**(3): p. 291-296.

70. Gu, L., *et al.*, *Single-walled carbon nanotubes displaying multivalent ligands for capturing pathogens.* Chemical Communications, 2005(7): p. 874-876.

71. Qu, L., *et al.*, *Visualizing Adhesion-Induced Agglutination of Escherichia coli with Mannosylated Nanoparticles.* Journal of Nanoscience and Nanotechnology, 2005. **5**(2): p. 319-322.

72. Wang, C. and J. Irudayaraj, *Multifunctional magnetic-optical nanoparticle probes for simultaneous detection, separation, and thermal ablation of multiple pathogens.* Small, 2010. **6**(2): p. 283-289.

73. Ray, P.C., *et al.*, *Nanomaterials for targeted detection and photothermal killing of bacteria.* Chemical Society Reviews, 2012. **41**(8): p. 3193-3209.

74.   Shokri, R., M. Salouti, and R.S. Zanjani, *Anti protein A antibody-gold nanorods conjugate: a targeting agent for selective killing of methicillin resistant Staphylococcus aureus using photothermal therapy method.* Journal of Microbiology, 2015. **53**(2): p. 116-121.

75.   Jay, C.M., *et al.*, *Enterotoxigenic K99+ Escherichia coli attachment to host cell receptors inhibited by recombinant pili protein.* Veterinary microbiology, 2004. **101**(3): p. 153-160.

76.   Dong, J. and J.I. Zink, *Taking the temperature of the interiors of magnetically heated nanoparticles.* ACS Nano, 2014. **8**(5): p. 5199-207.

77.   Dias, J.T., *et al.*, *DNA as a molecular local thermal probe for the analysis of magnetic hyperthermia.* Angewandte Chemie International Edition English, 2013. **52**(44): p. 11526-11529.

78.   Yu, L., *et al.*, *Evaluation of hyperthermia of magnetic nanoparticles by dehydrating DNA.* Scientific Reports, 2014. **4**: p. 7216.

79.   Huang, H., *et al.*, *Remote control of ion channels and neurons through magnetic-field heating of nanoparticles.* Nature Nanotechnology, 2010. **5**(8): p. 602-606.

80.   Riedinger, A., *et al.*, *Subnanometer local temperature probing and remotely controlled drug release based on azo-functionalized iron oxide nanoparticles.* Nano Letters, 2013. **13**(6): p. 2399-2406.

81.   Arakha, M., *et al.*, *Antimicrobial activity of iron oxide nanoparticle upon modulation of nanoparticle-bacteria interface.* Scientific Reports, 2015. **5**: p. 14813.

82.   Silva, F., *et al.*, *Bacteriostatic versus bactericidal activity of ciprofloxacin in Escherichia coli assessed by flow cytometry using a novel far-red dye.* The Journal of Antibiotics, 2011. **64**(4): p. 321-325.

83.   Drago, L., *et al.*, *Activity of levofloxacin and ciprofloxacin against urinary pathogens.* Journal of Antimicrobial Chemotherapy, 2001. **48**(1): p. 37-45.

84.   Zhu, X., *et al.*, *Nanomedicine in the Management of Microbial Infection - Overview and Perspectives.* Nano Today, 2014. **9**(4): p. 478-498.

85.   Zhao, Y., *et al.*, *Synergy of non-antibiotic drugs and pyrimidinethiol on gold nanoparticles against superbugs.* Journal of the American Chemical Society, 2013. **135**(35): p. 12940-12943.

86.   Fan, Z., *et al.*, *Popcorn-Shaped Magnetic Core–Plasmonic Shell Multifunctional Nanoparticles for the Targeted Magnetic Separation and Enrichment, Label-Free*

SERS Imaging, and Photothermal Destruction of Multidrug-Resistant Bacteria. Chemistry - A European Journal , 2013. **19**(8): p. 2839-2847.

87.   Norman, R.S., *et al.*, *Targeted photothermal lysis of the pathogenic bacteria, Pseudomonas aeruginosa, with gold nanorods.* Nano Letters, 2008. **8**(1): p. 302-306.

88.   Boulos, L., *et al.*, *LIVE/DEAD BacLight : application of a new rapid staining method for direct enumeration of viable and total bacteria in drinking water.* Journal of Microbiolical Methods, 1999. **37**(1): p. 77-86.

89.   Durmus, N.G., *et al.*, *Enhanced efficacy of superparamagnetic iron oxide nanoparticles against antibiotic-resistant biofilms in the presence of metabolites.* Advanced Materials, 2013. **25**(40): p. 5706-5713.

90.   Liu, P.-F., *et al.*, *Use of nanoparticles as therapy for methicillin-resistant Staphylococcus aureus infections.* Current Drug Metabolism, 2009. **10**(8): p. 875-884.

91.   Hurdle, J.G., *et al.*, *Targeting bacterial membrane function: an underexploited mechanism for treating persistent infections.* Nature Reviews Microbiology, 2011. **9**(1): p. 62-75.

92.   Adhikari, M.D., *et al.*, *Membrane-directed high bactericidal activity of (gold nanoparticle)-polythiophene composite for niche applications against pathogenic bacteria.* Advanced Healthcare Materials, 2013. **2**(4): p. 599-606.

93.   Wehling, J., *et al.*, *Bactericidal activity of partially oxidized nanodiamonds.* ACS Nano, 2014. **8**(6): p. 6475-6483.

94.   Beal, J.D., C. Moran, and P.H. Brooks. *Fermented Liquid Feed: The potential for eliminating enteropathogens from feed*. in *Fifth International Symposium on the Epidemiology and Control of Foodborn Pathogens in Pork*. 2003.

Chapter 4

Assessing the Biocompatibility of Multi-anchored Glycoconjugate Functionalized Magnetic Nanoparticles in Normal Human Colon Cell-line CCD-18Co

1. Introduction:

In the last two decades, nanotechnology has evolved to be one of the most promising scientific areas, which have a huge potential to drastically change the facet of biomedical world in terms of its applicability. As a result, there has been a continuous rise in the amount of literature reported that deals with the application of nanomaterials to treat various human diseases [1, 2]. Application of nanomaterials in biomedical field, commonly referred to 'Nanomedicine', has attracted huge investments (in billions) in research & development funding both in the US and European counterparts. For example, the annual budget of National Nanotechnology Initiative (NNI) of US government grew exponentially from $0.5 billion in 2001 to $24 billion in 2017 [3, 4]. Some of the widely used nanoparticles for biomedical applications include gold nanoparticles, silver nanoparticles, magnetic nanoparticles, quantum dots, etc. These nanoparticles have been

used for targeted drug and gene delivery (e.g., delivery of anticancer drugs), as antibacterial agents, as vaccines, in various bio-imaging techniques like magnetic resonance imaging (MRI), positron emission tomography (PET) & computerized tomography (CT), and in diagnostics among several other applications [5-9]. Despite the rapid splurge in funding of nanoparticle research aimed for treating several diseases, not much success has been achieved in terms of their effective use in clinical settings [4, 10].

Currently, there exists a huge fundamental gap in translating the laboratory-based results of different nanoparticles that can certainly be used in bench-to-bedside scenarios. Some of the major factors that prevent their clinical use are difficulties in successful synthesis of nanoparticles that have consistent physical and chemical properties, reduced stability of nanoparticles in biological environment, poor understanding of the interactions which occurs between nanoparticles, biomolecules, and body fluids, and lastly the safety and biocompatibility of nanoparticles inside human body [11, 12]. Amongst all of the above stated issues, in this chapter, we will be mainly focusing on how surface functionalization of magnetic nanoparticles can affect its interaction with biological environment. Among various metallic nanoparticles, magnetic nanoparticles (MNPs), on account of their small size, unique magnetic properties and high degree of biocompatibility, have garnered major attention in nanomaterials research due to their multitude biomedical applications, which include but are not limited to targeted drug delivery, magnetic hyperthermia, magnetic resonance imaging, cell separation, cancer therapy, diagnostics and pathogen detection [13-15]. In fact, MNPs are already used clinically as MRI contrast agents for therapeutic purposes [6, 16]. Recent research efforts

have largely concentrated on manipulating the surface chemical properties of MNPs so as to render them high stability in biological rich environment. During the typical synthesis procedure, the resultant MNPs are generally found to be hydrophobic in nature and hence it is colloidically unstable in biological environment, thereby, not suitable in clinical applications [17, 18]. Making such MNPs hydrophilic is of prime importance in order to achieve chemically stable colloidal suspension of MNPs. For this purpose, surface coating of MNPs is essential and functionalizing the core of MNPs by robust monomeric/polymeric stabilizers typically does it. Also, these polymers should be biologically inert in nature so as to provide electrostatic and or stearic repulsion and 'stealth' properties to MNPs in presence of protein-rich environment and at the same time they should be able to circulate in the body for prolonged time duration until they reach their targeted location without triggering body's immune response [19, 20].

Some of the commonly employed monomeric agents that can easily bind to the core of MNPs include carboxylic acids, alcohols, sulfates, phosphates, and amines [18, 21-23]. Polymeric stabilizers utilized for surface stabilization of MNPs usually include binding groups such as polyethylene glycol (PEG)/polyethylene oxide (PEO), alginate, dextran, poly vinyl alcohol (PVA), chitosan, etc. [24-27]. Extensive studies have been done on synthesized MNPs that has PEO polymer as the main stabilizing agent. PEO is one of the universally accepted polymers that have been approved by the FDA. Some of major advantages of attaching PEO onto nanoparticles, which make them extremely suitable for clinical applications, are improved stability of the entire nanoparticle system in biological environment, imparting 'stealth' properties to MNPs and extended blood

circulation time, amphiphilic in nature, soluble in water as well as in many other solvents, can act as carrier molecule in different pharmaceutical products and the ease of manipulating its surface chemistry for wide-spread use in biomedical applications [17, 26, 28, 29]. However, in the presence of high salt & protein concentration, few of the above-mentioned binding groups tend to undergo desorption process and can be easily displaced from the surface of MNPs core (generally made up of iron-oxide). More specifically, anionic phosphates and silicates present in bodily fluids and also on the surface of several peptide molecules have high affinity towards iron-oxide core of MNPs and hence can lead to colloidal instability and rapid aggregation of MNPs [17]. In order to overcome this issue, recent studies have suggest that catechol-based anchor groups can inhibit non-specific interactions of other reactive groups towards the iron-oxide core and this has greatly improved the stability of MNPs in physiological fluids [30-34]. These catechol groups frequently use dopamine-based molecules that can tightly bind to metal oxide cores (especially Fe_3O_4), and can also be effortlessly attached to polymeric agents via different chemistry routes.

Several studies have presented MNPs coated with appropriate polymer stabilizing agents to be highly biocompatible and biodegradable in *in vitro* and *in vivo* [9, 15, 35, 36]. The main advantage of using MNPs for clinical applications is that, compared to other nanoparticles, MNPs can be metabolized and completely removed/excreted from the body through various systemic and cellular iron homeostasis pathways [37, 38]. However, it should be carefully noted that the biocompatibility of MNPs is highly dependent on multitude of factors like core size, final size of MNPs, surface chemistry of

the MNPs, adsorbed proteins on the surface of MNPs, given dosage, biodistribution, and final localization of MNPs in the body among several others [37, 39-41]. In spite of having excellent biocompatibility, numerous *in vitro* and *in vivo* studies have demonstrated differential toxicity of MNPs [24, 38, 41-43]. The different toxicity mechanisms observed in determining safe dosage levels of MNPs in cell-line studies include impaired mitochondrial function, cytotoxicity, cell apoptosis, DNA damage and genotoxicity, immunotoxicity, oxidative stress, disordered cell morphology, cytoskeleton damage, cell-membrane damage, etc. [11, 24, 25, 37, 44, 45]. Other factors that influence the toxicity levels of MNPs in *in vitro* conditions include type of cell-line, concentration of MNPs, incubation time, and cellular uptake [4, 46]. To date, the majority of the cell-line toxicity studies of MNPs have been largely conducted in cancer cell-line models. Some of the commonly used ones are breast, colon, intestinal, lung, and brain cancer cell-lines [5, 6, 47-49]. However, using such cancer cell-lines does not always provide reliable nanotoxicity evaluation of tested nanomaterials since these cell-lines may have been intentionally manipulated with to make them immortal [46, 50]. Also, cancer cells have higher proliferation rate, higher resilience to foreign objects, disorganized and leaky blood vessels, and altered cellular signaling pathways and therefore they do not correctly represent the physiological/biological state of normal cells [46, 51]. Hence, in-depth toxicological studies carried out in normal cell-lines or primary cells are warranted to fully comprehend and determine the possible toxicity mechanisms of MNPs before further testing is done in animal models.

Carbohydrates are important group of molecules that play vital role in numerous biological processes in mammalian systems. Some of the key processes modulated by carbohydrate molecules, include cell-cell communication, molecular signal transduction, cell growth and differentiation, apoptosis, inflammation and immune responses, tumor metastasis etc. [52-54]. Several of these carbohydrate molecules also serve as cell-surface receptors that can recognize viral/bacterial pathogens entering into the cells. Over the last two decades, numerous reports have utilized functionalized nanoparticles (e.g., gold nanoparticles, silver nanoparticles, diamond nanoparticles, magnetic nanoparticles, carbon nanotubes etc.) based on carbohydrate chemistry, which includes monosaccharide, disaccharides, oligosaccharides, and glycan/glycoconjugate molecules [55-58]. These studies have investigated the role of different carbohydrate molecules present on the surface of nanoparticles in studying multivalent carbohydrate-carbohydrate interactions, carbohydrate-lectin interactions for therapeutic purposes. Nanoparticles functionalized with carbohydrate molecules offer many advantages compared to their monovalent forms especially with regard to achieving high affinity constant (K_a) and increased binding enthalpy (ΔH) due to presence of multivalent interactions [59]. On account of their high surface/volume ratio, functionalizing numerous carbohydrate groups onto the surface of nanoparticles is fairly easy and it also drastically increases the biocompatibility of the entire nanoparticle system. Especially, MNPs having different physico-chemical properties and functionalized with carbohydrates have been frequently used in various biomedical applications such as targeted drug delivery, MRI imaging, pathogen

detection, as vaccines, anti-adhesion therapies, bio-sensing applications, cancer treatment, and cell-surface receptor mimicking [55-57, 59].

Few studies have described using nanoparticles functionalized with specific lectins and carbohydrates for targeted drug delivery to colon cells [60-62]. Of late, nanoparticles loaded with different drugs have been used as therapeutic agents for treating inflammatory bowel syndrome (IBS) [63, 64]. Most of these treatment regimens often involve localized and targeted drug release via orally ingested nanoparticles to the colon region of the gastrointestinal tract (GI tract). Such approach increased the overall efficacy of the drugs used in treating IBS by utilizing various nano-drug formulation strategies that enhanced the uptake of drug-loaded nanoparticles into the inflamed/diseased region of the colon. Frequently, in the case for disease diagnosis and evaluation of IBS, GI tract imaging is done via MRI and CT scan [65]. These imaging techniques often include MNPs as theragnostic agents, which can act both as MRI contrast and drug delivery agents. By utilizing nano-platform based imaging techniques, it is possible to monitor the drug-release kinetics of nanoparticles in the GI tract. Most of the *in vitro* studies that have been carried out till date to understand the cellular and molecular interactions of nanoparticles with intestinal cells regularly use Caco-2 cells (human colorectal adenocarcinoma) monolayers [66-69]. However, using Caco-2 cells for such studies do not accurately reflect the physiological conditions of normal colon cells. Even though PEG/PEO polymer used for stabilizing MNPs has been reported to have excellent biocompatibility in numerous cell-lines and animal studies, several research studies have deemed it to be toxic to cells [70-74]. Most of the *in vitro* cell-line

studies evaluating toxicity of PEO-coated nanoparticles typically do not expose the cells above 100-200μg/ml [37, 75]. However, it is important to understand the biological response of cells in presence of sub-lethal and lethal concentrations of nanoparticles. Depending on overall size, surface charge, polymer length and degree of grafting density on nanoparticle surface, PEO can show differential toxicity.

Previous research work has shown that MNPs synthesized with dopamine-anchored heterobifunctional PEO polymer (PEO-MNPs) and bio-functionalized with sialic-acid specific glycoconjugate moiety (Neu5Ac(α2-3)Gal(β1-4)-Glcβ-sp) (GM3-MNPs) can be effectively used as targeted antibacterial agents against enterotoxigenic *Escherichia coli*, which is usually associated with gastroenteritis and can also trigger post-infectious IBS [59, 76]. In this chapter, we will be focusing on evaluating the biocompatibility of both PEO-MNPs and GM3-MNPs in normal human colon cell-line CCD18-Co. According to author's knowledge, this is a first study which encompasses different toxicity assays to better understand the biocompatibility of glycoconjugate functionalized MNPs in normal human colon cells. Understanding the interactions occurring between different MNPs and CCD18-Co cells will eventually help in determining the safe dosage levels of these MNPs to be effectively used as novel drug delivery agents for treating IBS and infections associated with it.

2. Experimental Section:

Synthesis of Magnetite Nanoparticles: Magnetite nanoparticles were synthesized via thermal decomposition of an organometallic precursor in a high boiling point organic solvent [77]. Iron (III) acetylacetonate (Alfa Aesar, 99%) (1.074g) was combined in a 3-neck round-bottom with oleic acid (Alfa Aesar, 90%) (15ml) serving as both the solvent and the stabilizing ligand. The vessel was initially purged with N_2 after which flow was adjusted to 0.1 L/min ensuring an inert environment. The vessel was then heated to 350°C and left to react for 3 hours. At 3 hours, the reaction was quenched by removing it from heat, and left to cool under inert atmosphere. The resulting particles were dispersed in minimal hexanes and precipitated using a mixture of 3:1 ethanol (Fisher, Anhydrous) to acetone (Alfa Aesar, 99.5%) (x3). Particles were dispersed in toluene (VWR, 99.5%) and run through an organic based GPC column (Bio-rad S-X polystyrene beads) to further remove excess oleic acid ligand [78]. TEM and size analysis was then done on the particles to ensure size specificity.

Synthesis of Alkyne-PEO-PAA-Dopamine [79]**:** Poly(ethylene oxide) (PEO) synthesis: Ethylene oxide (Sigma Aldrich, 99.9%) distilled into a high pressure Parr reactor. Na-benzylphenone still dried tetrahydrofuran (THF, EMD Millipore, 99.9%) was injected along with a predetermined amount of an anionic initiator potassium bistrimethyl silyl amide (Sigma Aldrich, 1M in THF). The reaction was allowed to run for 72 hours and was subsequently terminated by opening the reactor to atmosphere. The synthesized PEO was precipitated with diethyl ether (VWR, 99.9%) and washed (3x) by dispersing it in chloroform, precipitating the polymer, centrifuging it at 15,000 RCF for 10 minutes

and pouring off the residual supernatant. The PEO was then dried under vacuum overnight. HNMR was performed to calculate molecular weight as well as to confirm the presence of the protected amine end-group.

Under dry N_2 atmosphere, hetero-functional PEO and sodium hydride (Sigma Aldrich, 95%), in slight excess, were dissolved in dry THF. This was allowed to react for 30 minutes before an excess of propargyl bromide (Sigma Aldrich, 80% in toluene) was added drop-wise to the solution over 15 minutes. Once all of the propargyl bromide was added, the solution was allowed to stir for 12 hours at room temperature. The polymer was then purified by dissolution in chloroform and precipitation with diethyl ether (x3) and dried under vacuum for 12 hours. HNMR was performed to confirm the presence of an alkyne.

Deprotection of the trimethyl silyl group was done in 1M hydrochloric acid (VWR) in methanol (VWR, 99+%) and allowed to react for 4 hours. The polymer methanol solution was diluted with DI water and the deprotected PEO was extracted (3x) with 50ml chloroform from which it was precipitated with diethyl ether and dried under vacuum. HNMR was performed to confirm the loss of the trimethylsilyl group.

Coupling of the PEO to the poly(acrylic acid) (PAA, Sigma Aldrich Mn=1,800) was done by dissolving both in dry N,N-dimethylformamide (DMF, Sigma Aldrich, 99.8%) in a 5:1 ratio. To this 1.1 excess (N-(3-dimethylaminopropyl)-N'-ethylcarodiimide hydrochloride (EDC, TCI, 98%) as well as catalytic amounts of 4-(dimethylamino)pyridine (DMAP, Alfa Aesar, 99+%) were added. The solution was allowed to stir for 12 hours. The solution was filtered, further purified by dissolution in chloroform following precipitation

with diethyl ether (x3) and then dried under vacuum. HNMR was done to confirm PEO-PAA coupling.

Attachment of the anchor group: Dopamine hydrochloride (Alfa Aesar, 99%) was dissolved in DMF along with a 10% molar excess of triethylamine (Alfa Aesar, 99%) and allowed to stir for 30 minutes. In a separate round-bottom the PEO-PAA was dissolved in DMF along with EDC and catalytic amounts of DMAP. To this the dopamine hydrochloride solution was added and the combined solution was allowed to stir for 12 hours. The solution was then filtered, purified by dissolution in chloroform then precipitated in diethyl ether. The final product was dried under vacuum and analyzed via HNMR and IR to confirm the presence of the catechol.

Ligand Exchange [32]**:** Both magnetite nanoparticles as well as the PEO-PAA-dopamine were suspended separately in 5ml of chloroform. The particles were at an approximate concentration of 3mg/ml of Fe and the polymer at approximately 40mg/ml. The polymer was then transferred to a scintillation vial capped with a septum and placed in a sonication bath. The bath was turned on and over the course of 15 minutes the magnetic nanoparticle solution was injected into the polymer solution. Once injection was finished, the combined solution was allowed to further sonicate for 15 minutes. The solution was then removed and put on a shaker table for 72 hours. The chloroform was then removed via rotary evaporator and further dried under vacuum. Deionized water (DI H_2O) was then added and the vial was sonicated to help mediate suspension into the water. The water-based particles were then filtered through a 0.2-micron nylon filter to ensure large aggregates were not present. The solutions were then run through a GPC

column (Bio-Rad P polyacrylamide beads) to separate excess polymer from the water dispersible particles.

Click Chemistry [80]**:** The Cu(I) catalyzed Huisgen 1,3-dipolar cyclo-addition between the terminal polymer alkyne and the azido-GM3 was done in the aqueous phase with the azido-GM3 being the limiting reagent. A 2 mol% solution of Cu(II) sulfate (Sigma Aldrich, 99%) was combined with equivalent molar amounts of the THPTA (synthesized according to Hong *et al.*) Cu chelating ligand and let to react for 10 minutes [81]. This was then transferred into the aqueous alkyne-particle suspension and the azide-GM3 was then added. After both additions a 10mol% aqueous solution of (+)-sodium L-ascorbate (Sigma Aldrich 98+%) was added to facilitate the reduction of Cu(II) to Cu(I). The click reactions were left at room temperature for 12 hours, and were then purified using size exclusion chromatography [78].

Dynamic Light Scattering (DLS) and Zeta Potential Measurements: DLS was performed on the PEO-coated and GM3-coated magnetic nanoparticles to determine their hydrodynamic radius. The nanoparticle suspensions were diluted in water and placed into a cuvette. Three readings were taken at 25°C using Malvern Zetasizer Nano ZS to determine the intensity average size distribution and z-average diameter. Zeta-potential measurements of these nanoparticle suspensions were also determined using the same instrument. The suspensions were diluted with water and added into zeta-cell and three measurements were taken at 25°C.

Furthermore, 50µg/ml concentration of PEO-MNPs and GM3-MNPs were added in a cuvette and incubated at 37°C for different time intervals with Dulbecco's modified

eagle's medium (DMEM) supplemented without/with 10% fetal bovine serum (FBS) to investigate the stability of MNPs in protein and salt rich biological environment. After the incubation time, DLS (at 37°C) was performed on the above mentioned nanoparticles-cell culture suspension to check for any changes in their overall hydrodynamic diameters.

Fourier Transform Infrared Spectroscopy (FTIR): FTIR microscopy was done using a Thermo-Nicolet Magna 550 FTIR spectrometer equipped with a Thermo-NicPlan FTIR microscope. 16 Scans were done for both the sample and the background. Samples were prepared by dropping a small amount of the water suspended sample on a germanium plate and left to dry under a heat lamp for 20 minutes. FTIR was done on the resulting films.

Iron Concentration Determination: 50 μl of magnetite suspension was dissolved in concentrated HCl, reduced and complexed with 1,10-phenanthroline (Sigma-Aldrich, 99%). UV-VIS was then performed to determine the amount of iron in the known volume [82, 83].

Culturing of CCD-18Co Cells: CCD-18Co human colon cells (normal) were procured from American Type Culture Collection (ATCC) and routinely grown on 50 cm^2 tissue-culture flask in the presence of Eagle's Minimum Essential Medium (EMEM) at 37°C in a humidified atmosphere of 5% CO_2 and 95% air. EMEM was supplemented with 2 mM L-Glutamine, non-essential amino acids, fetal bovine serum (final concentration - 10%), 100 UI/ml penicillin G, and 100μg/ml streptomycin. Fresh EMEM complete medium was added to growing cells every 2 days. For determining the

114

biocompatibility of MNPs, cells between passage generation of 12 and 25 were used. All the media chemicals, 96-well plates and culture flasks required for growing the cells were obtained from Corning, USA.

Cytotoxicity of MNPs to CCD-18Co Cells [59]: The potential cytotoxicity of both PEO-MNPs and GM3-MNPs towards CCD-18Co cells was determined by performing MTS assay (CellTiter 96® Aqueous One Solution Cell Proliferation Assay, Promega, USA). For this assay, approximately 1.5×10^4 cells/well (100μl) were seeded (in triplicates) in transparent flat-bottom 96-well culture-plates at 37°C in a humidified atmosphere of 5% CO_2 and 95% air. After 24 hours, fresh growth medium containing varying concentrations (10μg/ml, 50μg/ml, 100μg/ml, 250μg/ml, and 500μg/ml of Fe) of PEO-MNPs and GM3-MNPs was added to the cells and the cells were incubated for further 24 and 48 hours. After the required incubation time period, cells were washed twice with sterile tissue-culture grade PBS. 100μl of fresh EMEM culture medium (without serum) was added to the wells and MTS assay was performed according to manufacturer's protocol. Later, the plate was read at 490 nm optical density to measure the absorbance of the formazan product using a microplate reader (Thermo Scientific Multiskan™ FC) and percentage cell-viability rate of CCD-18Co cells in presence of MNPs was determined.

Intracellular Adenosine Triphosphate (ATP) Levels of CCD-18Co Cells in Presence of MNPs [84, 85]: Intracellular ATP levels of CCD-18Co cells were measured in presence of both PEO-MNPs and GM3-MNPs to determine if their presence interrupted/inhibited ATP synthesis in the cells. Approximately 1.5×10^4 cells/well

115

(100μl) were seeded (in triplicates) in white flat-bottom 96-well culture-plates at 37°C in a humidified atmosphere of 5% CO_2 and 95% air. After 24 hours, fresh growth medium containing varying concentrations (10μg/ml, 50μg/ml, 100μg/ml, 250μg/ml, and 500μg/ml of Fe) of PEO-MNPs and GM3-MNPs was added to the cells and the cells were incubated for further 24 and 48 hours. After the required incubation time period, cells were washed twice with sterile tissue-culture grade PBS. 100μl of fresh EMEM culture medium (without serum) was added to the wells and CellTiter-Glo® 2.0 assay (Promega, USA) was performed according to manufacturer's protocol with minor modification in incubation time period. After adding the CellTiter-Glo 2.0 reagent to the cells, the plate was gently mixed and later incubated at room temperature for 20 minutes. At the end of this assay, the plate was read in a micro-plate reader with luminescence capability (Synergy Hybrid H1, Biotek®) and the obtained results were expressed in relative luminescent units (RLUs).

Cell Membrane Integrity of CCD-18Co cells in Presence of MNPs [24, 86]**:** Approximately 1.5×10^4 cells (600μl) were seeded (in duplicates) in 4-well chamber slide (Corning, USA) at 37°C in a humidified atmosphere of 5% CO_2 and 95% air. After 24 hours, fresh growth medium containing maximum concentration of PEO-MNPs and GM3-MNPs (i.e. 500μg/ml of Fe) were added to the cells and they were further incubated for 24 and 48 hours. Later, the cells were washed thrice with sterile tissue-culture grade PBS and finally the cells were re-suspended back in sterile tissue-culture grade PBS. Now, live/dead® viability assay (Invitrogen, USA) was performed to determine the extent of cell-membrane damage of CCD-18Co cells in presence of MNPs. Both the staining

116

dyes (Ethidium homodimer-1 and Calcein) were mixed together in a sterile microcentrifuge tube along with sterile tissue-culture grade PBS. The final concentrations of the dyes were 20μM and 10μM respectively when added to the chamber slides containing CCD-18Co cells. The chamber slide was then incubated at room temperature for 40 minutes. The stained cells were then observed under fluorescent microscope with appropriate fluorescent filter cubes (calcein - excitation/emission: 485/530 nm; ethidium homodimer-1 - excitation/emission: 530/645 nm) at 100X and 200X magnification. Later, the images obtained under different fluorescent filters were merged in ImageJ software (NIH, USA).

Intracellular Glutathione (GSH) Levels of CCD-18Co Cells in Presence of MNPs [69, 87]**:** Approximately 1.5×10^4 cells/well (100μl) were seeded (in triplicates) in white flat-bottom 96-well culture-plates at 37°C in a humidified atmosphere of 5% CO_2 and 95% air. After 24 hours, fresh growth medium containing varying concentrations (10μg/ml, 50μg/ml, 100μg/ml, 250μg/ml, and 500μg/ml of Fe) of PEO-MNPs and GM3-MNPs was added to the cells and cells were incubated for further 24 and 48 hours. After the required incubation time period, cells were washed twice with sterile tissue-culture grade PBS. Intracellular GSH levels were measured by utilizing GSH-Glo™ Glutathione assay kit (Promega, USA). All the subsequent steps in this experiment were done according to manufacturer's protocol with a minor modification in incubation times. After adding the GHS-Glo reagent to the cells, the plate was gently mixed and incubated at room temperature for 40 minutes. Subsequently, after adding luciferin detection reagent to the cells, the plate was further incubated for 20 minutes. At the end of this assay, the

plate was read in a micro-plate reader (Synergy Hybrid H1, Biotek®) and luminescence intensity of the each well obtained was expressed in relative luminescent units (RLUs).

Intracellular Caspase 3/7 levels of CCD-18Co cells in Presence of MNPs [88, 89]**:** Approximately 1.5×10^4 cells/well (100μl) were seeded (in triplicates) in white flat-bottom 96-well culture-plates at 37°C in a humidified atmosphere of 5% CO_2 and 95% air. After 24 hours, fresh growth medium containing varying concentrations (10μg/ml, 50μg/ml, 100μg/ml, 250μg/ml, and 500μg/ml of Fe) of PEO-MNPs and GM3-MNPs was added to the cells and cells were incubated for further 24 and 48 hours. After the required incubation time period, intracellular caspase 3/7 protein levels were determined through Caspase-Glo® 3/7 assay kit (Promega, USA). The experiment was performed according to manufacturer's protocol and the plate was incubated for 2.5 hr at room temperature after adding the Caspase-Glo 3/7 reagent. Later, the plate was read in a micro-plate reader (Synergy Hybrid H1, Biotek®) and luminescence intensity of the each well obtained was expressed in relative luminescent units (RLUs).

Statistical Analysis: All the statistical analysis was performed using GraphPad Prism software (V 7.0, CA, USA). All the experiments were done in triplicates and data are expressed as Mean±SD. Statistically significant differences between the groups were evaluated by performing ANOVA. Post hoc group comparisons were calculated through Tukey's multiple comparisons test. Results showing p-values of ≤0.05, <0.01, and <0.001 were considered to be statistically significant.

3. Results and Discussion:

3.1. Synthesis of GM3-MNPs

Magnetite nanoparticles were synthesized using a one-pot thermal decomposition of iron (III) acetylacetonate and oleic acid [82, 90]. Particles had an average diameter of 23.7 nm with a standard deviation of 1.55 nm (Figure 4.2 A and B). The moment vs. field (MvH) (Figure 4.3) measurement was done on the particles to confirm the super-paramagnetic behavior of the MNPs. Polymer design was based on work by Stone *et al.* where a multi-anchored binding approach showed increased stability in comparison to polymer ligands with a single binding moiety (Figure 4.1) [79].
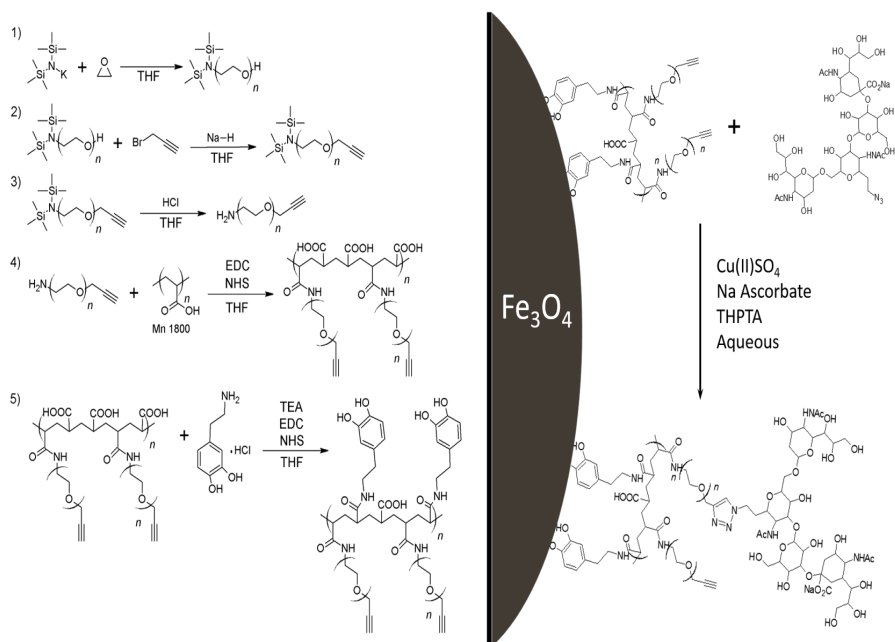
Figure 4.1 Left: 1) Anionic ring opening of ethylene oxide, 2) alkyne functionalization with propargyl bromide, 3) deprotection of primary amine, 4) coupling of PEO to PAA, 5) coupling of dopamine hydrochloride to the PEO-PAA. Right: Click reaction between polymer coated particles and GM3 molecule.
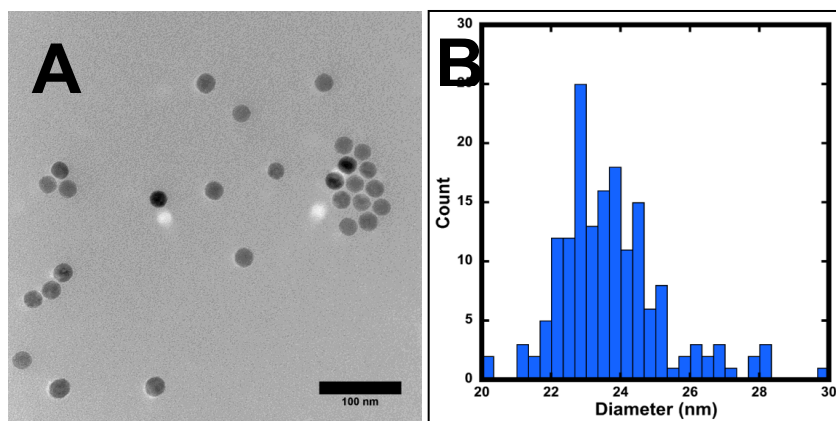
Figure 4.2 Magnetite nanoparticles as synthesized before functionalization with PEO-PAA-dopamine polymer. A – Representative TEM image of the particles. B – Histogram depicting the particle size distribution.
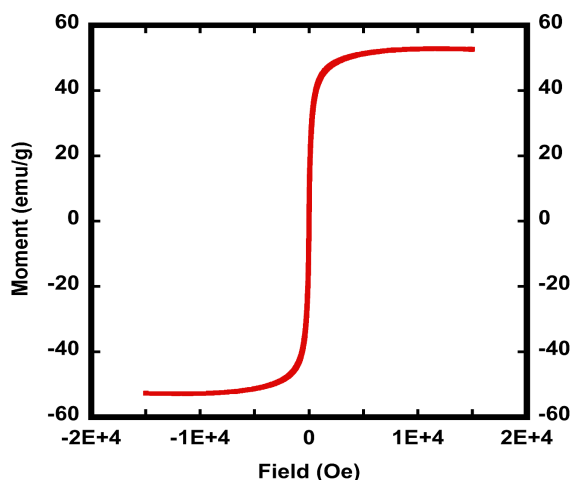
Figure 4.3 Moment vs. Field (MvH) loop showing the superparamagnetic behavior of the magnetite nanoparticles (M_{sat} ~ 53 emu/g Fe).

In this work, however, the chosen catechol was not nitroDOPA but dopamine. HNMR of the polymer was used to confirm both the structure and molecular weight of the PEO-PAA-dopamine macromolecule (Figure 4.4). By using the multi-anchored approach, the stability in salt and protein buffer solutions is retained even when using dopamine as the anchoring group [32, 33]. Hydrodynamic diameter and zeta potential of

the PEO-MNPs before and after click-coupling of GM3 are reported in Table 4.1.
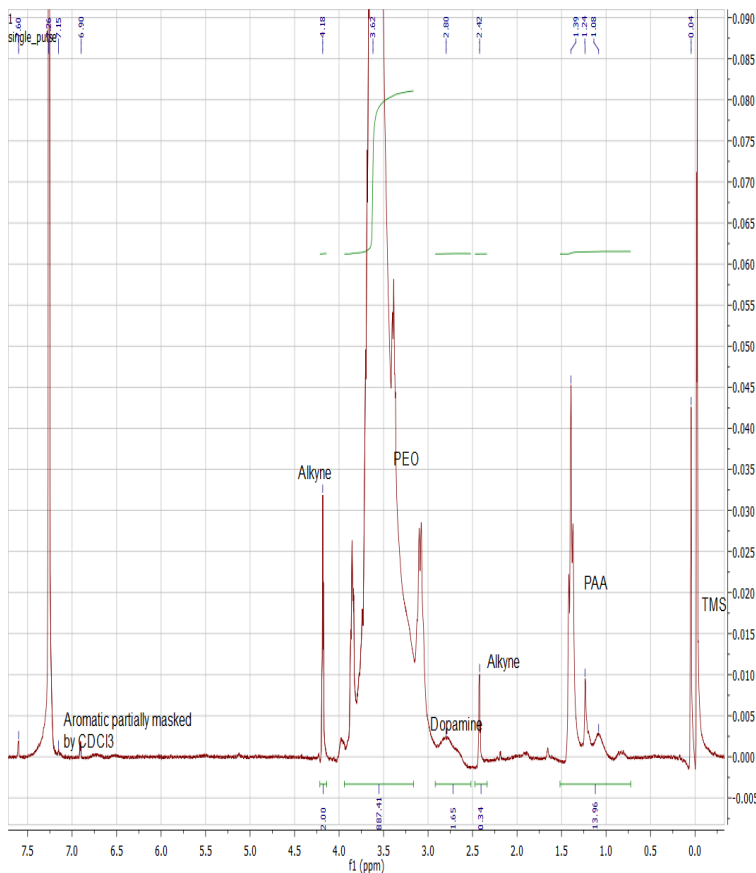
Figure 4.4 HNMR of the final PEO-PAA-dopamine - PAA backbone protons at 1.39 ppm - 1.08 ppm. Alkyne protons at 4.18 ppm and 2.42 ppm. PEO repeat protons at 3.62 ppm. Dopamine aromatic proton signal partially masked by the CDCl$_3$ peak, with alkane protons showing up at 2.8 ppm. Reference was tetramethylsilane at ~0 ppm.

	Hydrodynamic Diameter Z Avg. (nm)	Zeta-potential (mV)
PEO-MNPs	78.8	-8.73
GM3-MNPs	88.8	-7.68

Table 4.1 Dynamic light scattering and zeta-potential measurements - Hydrodynamic diameter and zeta potential as measured by dynamic light scattering before and after GM3 conjugation.

The increase in the hydrodynamic diameter indicates the GM3 glycoconjugate was successfully coupled to the PEO-MNPs. Attenuated total reflectance Fourier transformed infrared spectroscopy (ATR-FTIR) also confirmed the GM3 coupling went to completion

with the disappearance of the azide peak from GM3 at ~2110 cm^{-1} and the appearance of

a broad alcohol peak in the GM3-MNPs spectrum from 3620-3170 cm^{-1} (Figure 4.5) [59].
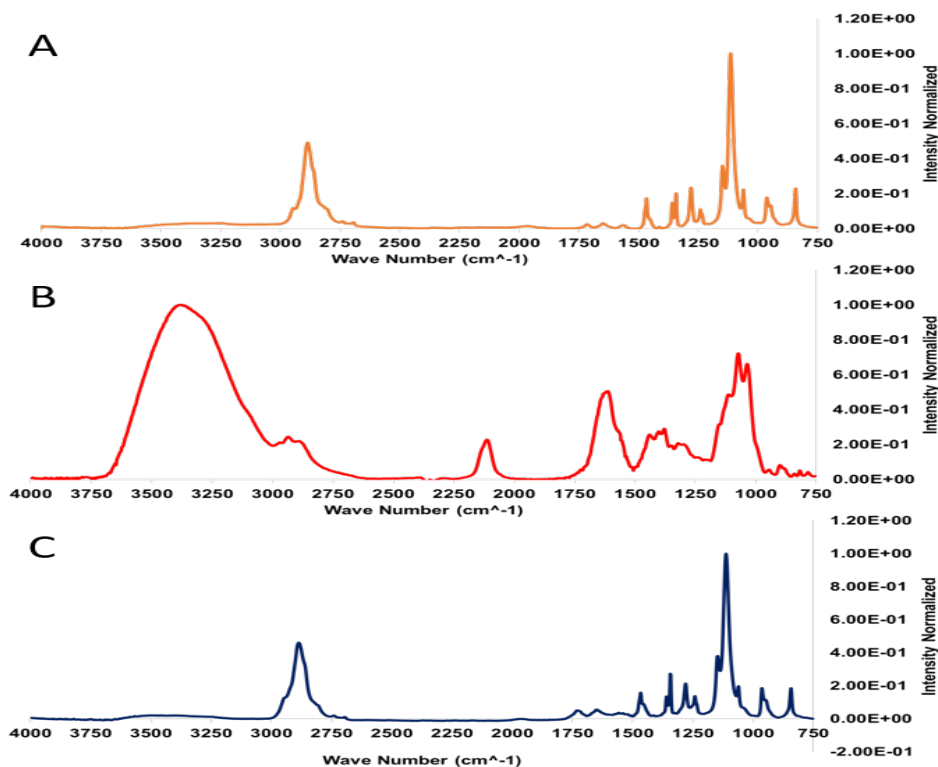
Figure 4.5 FTIR spectra of particles before GM3 conjugation (A), GM3 molecule (B), and after conjugation (C). The lack of the azide peak in C at 2100 cm^{-1} indicates purification of unbound GM3 after conjugation was successful.

The presence of biological medium has an important effect on the overall size diameter and surface charge of the synthesized MNPs. The presence of functional groups on the surface of MNPs also determines the extent to which it interacts with salts and proteins. DLS studies were conducted both on PEO-MNPs and GM3-MNPs over a period of 3 days to evaluate their overall stability in cell-culture medium DMEM in absence/presence of 10% FBS. As seen from table 4.2, the particle size of PEO-MNPs (in

water) instantly increased from 78.8 nm to 173.03 nm (more than doubled) within 5 minutes of incubation in presence of DMEM. After 72 hr, the particle size still remained ~170 nm. The presence of FBS in DMEM did not significantly change the overall diameter of PEO-MNPs during the entire experimental period. However, we did notice a slight reduction in size of PEO-MNPs in presence of DMEM+FBS. In contrast, GM3-MNPs (in water) increased their size from 88.8 nm to 104 nm (an increase of ~18 nm) when mixed and incubated for 5 minutes in presence of DMEM. Here also the overall size of GM3-MNPs did not change drastically over 3 days incubation time-period in presence of DMEM. Interestingly, after mixing GM3-MNPs with media containing DMEM+FBS for 5 minutes, there was no major change in the diameter (88.8 nm to 91.14 nm). However, after 24 hr and beyond, the size increased to ~110 nm in presence of DMEM+FBS. Several studies have reported the formation of 'protein-corona' (protein adsorption) layer on the surface of MNPs when incubated in presence of cell-culture medium containing high salt and protein concentrations [37, 91, 92]. It is due to this protein-corona formation that the overall size of the nanoparticles is increased. Moreover, extended period of protein-corona formation can also affect the colloidal stability of nanoparticle system in the biological media and eventually the nanoparticles tend to lose their colloidal stability and form aggregates due to corona formation.

The presence of different types of chemical functional groups found on polymers and the length of the polymer itself plays an important role as to how and what kind of proteins interact with the nanoparticle surface and become adsorbed on it [4, 45]. In our results, we observed a rapid increase in size diameter of PEO-MNPs within 5 minutes of

incubation with DMEM and once the size was increased, it remained pretty consistent for the next 72 hr. Such kind of phenomenon can be credited to formation of thick layer of 'hard protein-corona', which essentially represents an irreversible change in the amounts of proteins, which are getting adsorbed/released over a period of time on the surface of nanoparticles [93, 94]. Albumin and globulins are most dominant serum proteins found in any cell-culture medium [4]. Major ionic salts that are present in any cell-culture medium include sodium (Na^+), potassium (K^+), chloride (Cl^-), and bicarbonate (HCO_3^-). The PEO-PAA polymer that we used as multi-anchored stabilizing agent for PEO-MNPs have a lot of reactive alkyne groups on its surface that are free and can potentially interact with the above mentioned serum proteins and ionic salts present in DMEM. A study done by Ekkebus *et al.* showed that terminal alkyne groups could selectively react with cysteine amino acid via thiol-alkyne side chain reaction [95]. The size increase of PEO-MNPs when mixed with DMEM could be due to the chemical interactions taking place between the free alkyne groups present on our polymer chains with thiol end-group containing amino acids like cysteine and cystine. Moreover, several coenzymes and cofactors present in DMEM contain thiol groups, which can also interact with alkyne. The above-mentioned chemical reactions taking place between alkyne and thiol-rich compounds might be one of the reasons for formation of protein-corona around PEO-MNPs in DMEM and thereby increasing its overall diameter size by more than 2-fold. In the case of GM3-MNPs, the PEO-PAA polymer with alkyne group underwent 'click reaction' to covalently attach GM3 molecule through alkyne-azide linkage. So, GM3-MNPs would have relatively less amount of free alkyne groups, which can interact with serum proteins

and ionic salts of DMEM and hence less amount of proteins would get adsorbed on its surface and forms a thin layer of protein-corona which would eventually increase the overall size of GM3-MNPs but only to a certain extent (increase of ~18 nm). Furthermore, it is worthwhile to note that presence of multi-anchored DOPA group is also responsible for maintaining colloidal stability of MNPs in biological environment via intact stearic interactions. Recent work of Stone *et al.* (2015) suggested that multi-anchored dopamine groups present on MNPs made them colloidically stable in FBS medium compared to mono-anchored groups that lost their stability by forming large aggregates having size diameter of >500 nm [34].

Hydrodynamic Diameter Z. average (nm) of MNPs in Presence of Cell-Culture Medium for Different Time-Intervals						
	PEO-MNPs (in H$_2$O)	PEO-MNPs + DMEM	PEO-MNPs + DMEM + 10% FBS	GM3-MNPs (in H$_2$O)	GM3-MNPs + DMEM	GM3-MNPs + DMEM + 10% FBS
t = 5 min	78.8 nm	173.03 nm	167.03 nm	88.8 nm	104.00 nm	91.14 nm
t = 24 hr	78.4 nm	171.97 nm	164.70 nm	88.6 nm	106.00 nm	106.00 nm
t = 48 hr	78.1 nm	171.17 nm	165.83 nm	88.1 nm	106.80 nm	109.90 nm
t = 72 hr	78.1 nm	172.50 nm	164.77 nm	88.3 nm	108.00 nm	110.30 nm

Table 4.2 Dynamic light scattering measurements - Hydrodynamic diameter of MNPs as measured by dynamic light scattering in presence of cell-culture medium DMEM.

The presence of nanomaterials in cell-lines is one of the many factors responsible for inducing toxicity in them. Different nanoparticles, when presented with direct contact to cells, can elicit cytotoxic responses inside mitochondria. One of the many in vitro

assays, which determine the damage done to mitochondria in presence of nanoparticles, is to quantify and measure the reductase/dehydrogenase enzymes activity inside the living mitochondria [39, 96]. MTS assay in one of the frequently employed cytotoxicity assay, which measures the amount of tetrazolium salt that is bio-reduced to formazan product by viable cells. This amount can then be detected colorimeterically and formazan produced is directly proportional to the number of living cells. The cytotoxicity of PEO-MNPs and GM3-MNPs to CCD-18Co cells was measured by CellTiter 96® Aqueous One Solution Cell Proliferation Assay [59]. Increasing concentrations of both MNPs were added and the cells were incubated for 24 and 48 hr. As seen from figure 4.6 A, PEO-MNPs were found to be highly cytotoxic to CCD-18Co cells above 100μg/ml concentration after 24 hr of exposure in a dose-dependent manner. <5% cell-viability was observed in the cells exposed to 500μg/ml concentration of PEO-MNPs at the end of 24 hr. Interestingly; GM3-MNPs did not show any significant cytotoxicity at all concentrations. In comparison to 24 hr time-period, PEO-MNPs showed significant cytotoxicity to the cells after 48 hr exposure even at 100μg/ml concentration (Figure 4.6 B). Above this concentration, <5% cell-viability of CCD-18Co cells was seen. To our surprise, cells exposed to GM3-MNPs for 48 hr did not show any significant cytotoxicity. Even the maximum concentration of 500μg/ml of GM3-MNPs showed >90% viability rate. PEO polymer attached to nanoparticle surface is generally found to be biocompatible both in *in vitro* and *in vivo* settings [25, 26, 28]. However, there have been few reports of toxicity of PEO coated nanoparticles. In a recent study conducted by Escamilla-Rivera *et al.*, MNPs coated with PEG were found to have 50% cell-viability at 100μg/ml concentration

126

after 48 hr exposure to THP-1 macrophages [97]. Also, the presence of PAA group on the polymer has been described to have significant toxicity in animal models [71, 98, 99]. It should be also noted that cell-viability rate also depends on the length of PEO tails present on the surface of MNPs as reported by Hafeli *et al.* [100]. Their study showed that by increasing tail length of PEO polymer (from 0.75 kDa to 15 kDa), cell-viability rate of various human cell-lines also increased. Also, the presence of carbohydrate/glycoconjugate molecules on MNPs have been reported to have no significant cytotoxicity to different cell-lines the results of which were similar to what we observed [101-103].
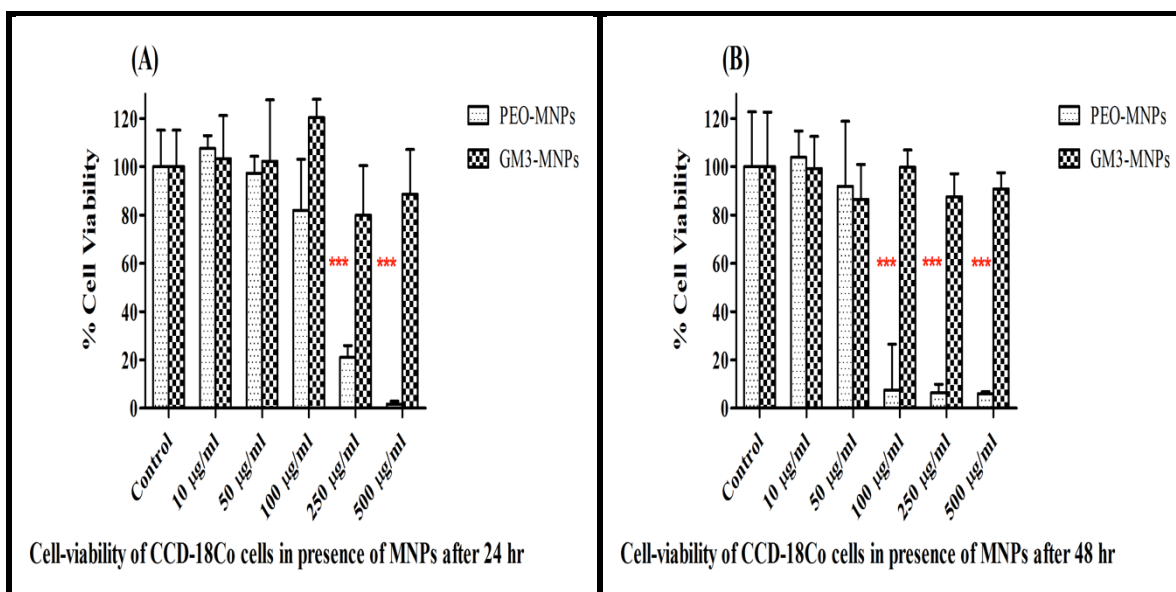
Figure 4.6 Cell-viability cytotoxicity MTS assay: a) CCD-18Co cells exposed to varying concentrations of PEO-MNPs for 24 hr; b) CCD-18Co cells exposed to varying concentrations of GM3-MNPs for 48 hr. Data is expressed as Mean ± SD (n=3); Statistical analysis – Analysis of Variance (ANOVA); * p-value <0.05, ** p-value <0.01, and *** p-value <0.001

The amount of ATP level present in any cell determines its metabolic state. In the presence of any toxic materials/chemicals, the metabolic state of the cell will change and the intracellular ATP levels can drop if there is any significant cytotoxicity to the cells. Higher levels of intracellular ATP commonly indicates that the cell is metabolically active and their level directly correlate to the actual number of living cells. Numerous research studies have reported a significant decrease in intracellular ATP levels of cells in presence of different types of nanoparticles [104-106]. To further understand the inherent cytotoxic mechanisms of MNPs on the inner cell membrane biochemical cycles taking place inside mitochondria, we measured the intracellular ATP levels of CCD-18Co cells based on luminescent assay. The cells were incubated with different concentrations of PEO-MNPs and GM3-MNPs for 24 and 48 hr. As seen from figure 4.7 A and B, the ATP levels of the cells started to decrease substantially when exposed to PEO-MNPs above 100μg/ml concentration. More than 90% reduction in the ATP levels was observed for 250μg/ml and 500μg/ml concentrations of PEO-MNPs. In comparison, cells exposed to GM3-MNPs for 24 hr did not show any significant decrease in ATP levels at all concentrations. When the exposure time was increased to 48 hr, cells in presence of PEO-MNPs showed a rapid decline in intracellular ATP levels beginning from 100μg/ml concentration (Figure 4.7 B). At concentrations above 100μg/ml, a significant reduction (>95%) in ATP levels was seen in presence of PEO-MNPs. Several reports have suggested that the kind of polymer coating and size of MNPs could play an important role in maintaining ATP levels inside the cells. In one such study, MNPs coated with different polymers like DEAE, chitosan and PEI exhibited variation in its cytotoxic

response to human brain microvascular endothelial cell-line with PEI-MNPs showing maximum cytotoxicity [107]. In another study, MNPs functionalized with starch were incubated with murine macrophage cell-line for 48 hr and the authors observed a drastic decrease in ATP levels of the cells [108]. However, presence of GM3-MNPs to the CCD-18Co cells did show a slight decrease (not significant) in ATP levels at concentrations above 250µg/ml, thereby, proving that GM3-MNPs do not cause any detrimental toxic effects on the overall functioning of ATP synthesis mechanisms inside mitochondria in CCD-1Co cells. These results prove that PEO-MNPs can possibly interfere with the ATP synthesis pathways inside the mitochondrial membrane, which can cause reduction in proton motive force and membrane depolarization.
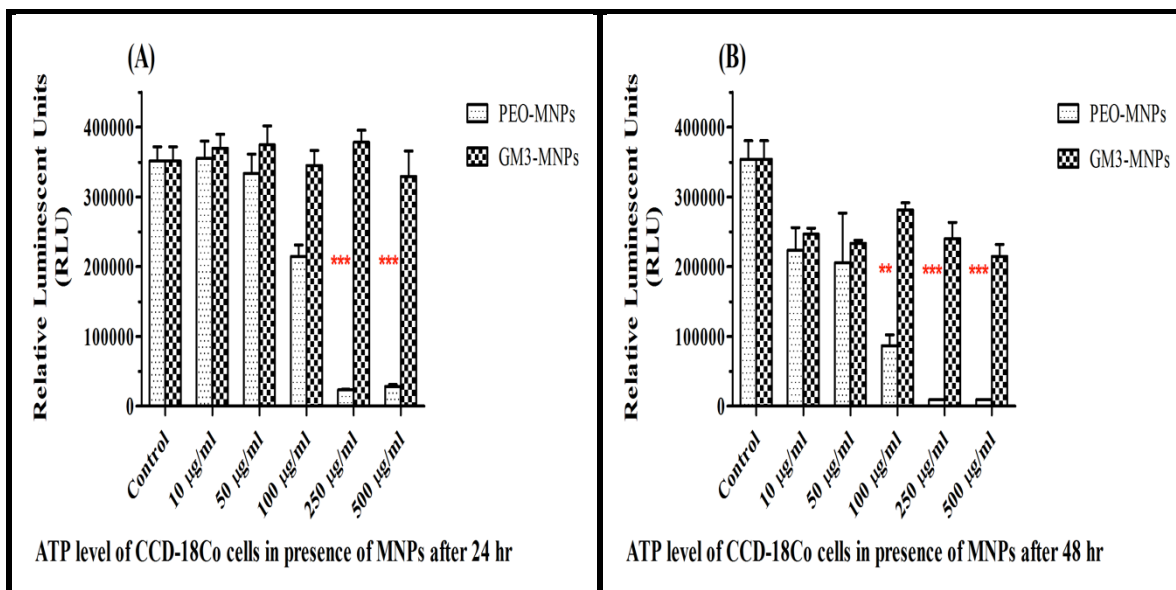
Figure 4.7 Intracellular ATP levels of CCD-18Co cells in the presence of MNPs using CellTiter Glo 2.0 assay. A) ATP levels of cells exposed to PEO-MNPs at increasing concentrations for 24 hr; B) ATP levels of cells exposed to GM3-MNPs at increasing concentrations for 48 hr. Data is expressed as Mean ± SD (n=3); Statistical analysis – Analysis of Variance (ANOVA); * p-value <0.05, ** p-value <0.01, and *** p-value <0.001

Next, we evaluated the potential toxicity of MNPs to CCD-18Co cells by performing membrane integrity assay. It is one of the commonly employed in vitro assays that determine the extent of membrane damage of mammalian cells when exposed to various nanomaterials [75, 96]. Most of these assays utilize a mixture of fluorescent dyes that can interact with specific enzymes present inside the cells depending on their ability to enter the cell. In our study, we exposed the cells only to highest concentration of MNPs (500μg/ml) based on the preliminary cytotoxicity results that we observed. After the predetermined incubation time-period, live/dead viability assay was done in presence of 2 different fluorescent dyes, calcein AM and ethidium homodimer-1. Calcein AM is a cell-permeable dye, which is non-fluorescent to begin with. Once inside the living cell, various intracellular esterases break down this dye and it is retained inside the cells that have intact membrane and can now emit intensely green fluorescence. Contrary, ethidium homodimer-1 dye cannot enter the live cell that has intact membrane. Those cells whose cell-membrane integrity has been compromised only take it up and once inside these damaged cells, it can brightly emit red fluorescence. As seen from figure 4.8 C, CCD-18Co cells exposed to PEO-MNPs after 24 hr showed a distinct change in their morphology and structure compared to control cells, which showed perfect slender and elongated fibrils (Figure 4.8 A). The cells were found to be clumped together in small irregular round/oval shapes. There was partial membrane damage to the cells as evident from limited red fluorescence. After 48 hr exposure, majority of the cells exposed to PEO-MNPs suffered extensive membrane damage (as seen by intense red fluorescence) and the cells also shrunk in size (Figure 4.8 D). We also observed extensive cell-

detachment in CCD-18Co cells in presence of PEO-MNPs. Such cell features are indicative of necrosis/ apoptosis. In comparison, cells incubated with 500 μg/ml of GM3-MNPs for 24 and 48 hr did not show any visible cell-membrane damage (Figure 4.8 E and F). More than 90% viability has seen in these cells. However, we did notice a small change in the overall size and arrangement of the cells. Compared to control group, cells exposed to GM3-MNPs had smaller fibrils. Also, their overall size dimensions (in terms of length and width) slightly reduced. They were also found to be growing at further distance from each other and there was hardly any overlapping of cell fibrils with each other referred to cell retraction. One possible explanation for such morphological change in cells in presence of MNPs might have to do with maintaining of cytoskeleton structures that includes actin and tubulin filaments. Both these structures are essential for proper growth and maintenance of cells as they directly take part in cell-cell communication, transport of nutrients and other vital organelles. Nonetheless, the change in cell morphology in presence of MNPs is something that has been already investigated previously. Few research studies have reported that MNPs functionalized with dextran, citric acid and PEG can effectively disrupt the overall cytoskeleton arrangement in different cell-lines through destruction of actin and microtubules through cell uptake [86, 109, 110]. Also, at high concentrations of MNPs (500 μg/ml and 1000 μg/ml), the overall length and diameter of murine neural progenitor cells and primary human blood outgrowth endothelial cells were found to be condensed and these cells also showed retraction properties (growing but tend to repeal from each other) during their growth cycle which is similar to what we observed in CCD-18Co cells exposed to GM3-MNPs

131

[111]. It also reduced the expression of focal adhesion kinase (FAK) protein, which is suggested to have damaging repercussions on kinase signaling pathways that maintains the cytoskeleton structures. Such disruptions in cytoskeleton pathways can activate pro-apoptosis signaling pathways in the cells, which can lead to cell-death. Thus, the results of our live/dead staining assay suggests that PEO-MNPs can possibly interfere and destroy cell cytoskeleton structures that can stall the regular cell cycle and cause cell-death. Whereas, the presence of GM3 molecule on MNPs can potentially prevent such drastic cytoskeleton toxicity of CCD-18Co cells.

	24 hr	48 hr
Control	A	B
PEO-MNPs	C	D
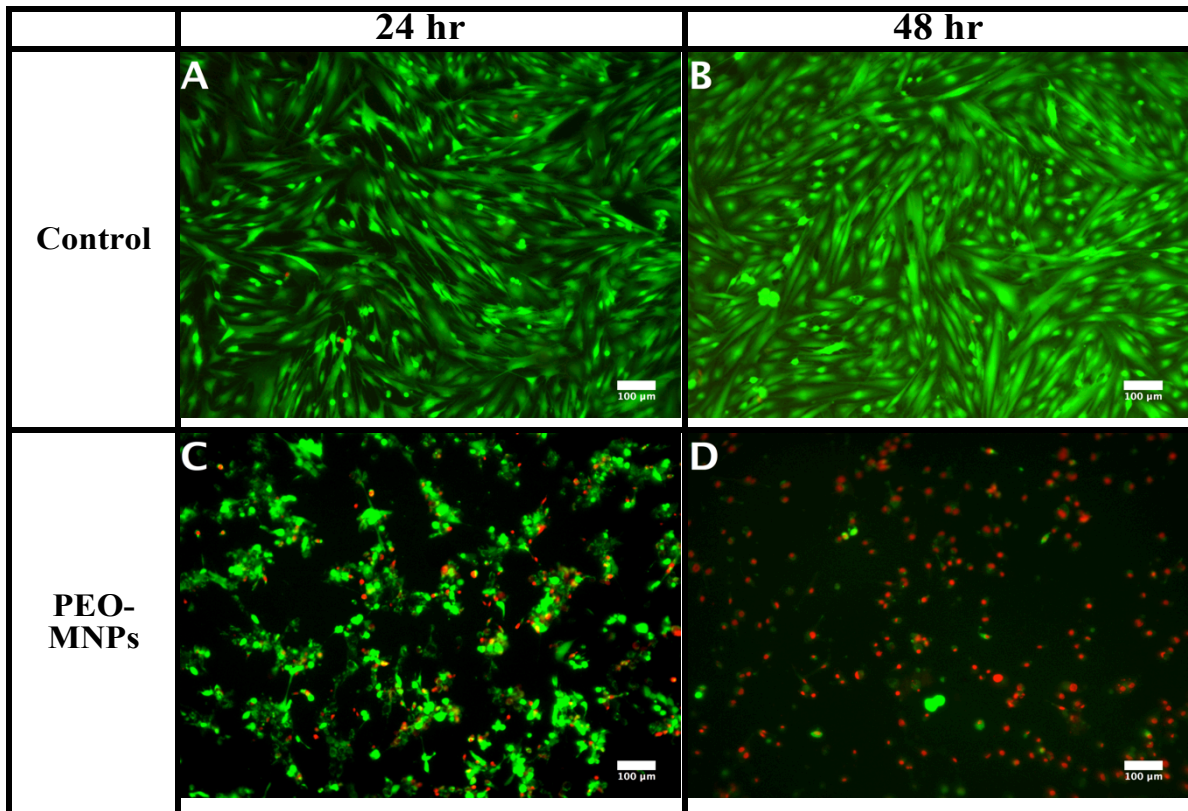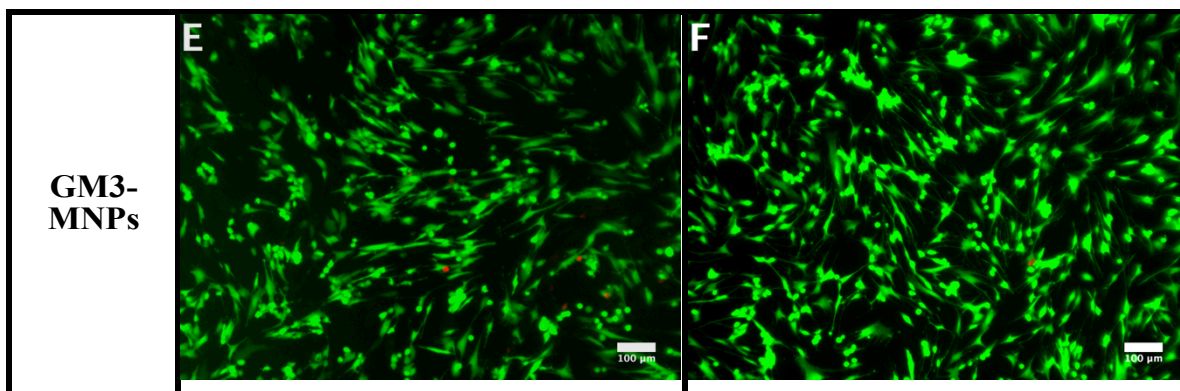
Figure 4.8 Live/Dead staining assay using calcein AM and ethidium homodimer-1 dyes. CCD-18Co cells were incubated in presence of PEO-MNPs and GM3-MNPs for 24 and 48 hr (Concentration - 500μg/ml). Live cells appear green in color and dead cells appear red in color. All the images were merged together for both green and red channel filters of the microscope. A, B - control cells (no MNPs); C, D - cells exposed to PEO-MNPs; E, F - cells exposed to GM3-MNPs. Magnification: 100X; Scale bar - 100μm.

It is known that the amount of reactive oxygen species in the cellular environment gives an indication of the oxidative stress levels. Glutathione (GSH) is an important and powerful antioxidant present in the mammalian cell. It normally exists in oxidized dimer form (GSSH). However, when the cell is experiencing oxidative stress due to presence of reactive oxygen species, free radicals, and toxic metal ions, GSSH is converted into its reduced monomeric form, GSH, which is an indicator of cellular oxidative stress that can lead to cell death or apoptosis [112, 113]. There have been numerous reports of increased oxidative stress in cells exposed/treated with different kinds of nanomaterials especially MNPs [114-116]. So, in order to evaluate whether CCD-18Co cells are undergoing cellular oxidative stress in presence of MNPs, we carried out GSH-glo assay to check for any changes in the overall GSH levels. At the end of 24 hr exposure to PEO-MNPs, the

GSH levels in the cells decreased drastically at concentrations of 250μg/ml and 500μg/ml (Figure 4.9 A). In the case of GM3-MNPs, cells lowered their overall GSH counts only at highest concentration of 500μg/ml. Compared to 24 hr, cells exposed to 48 hr of PEO-MNPs and GM3-MNPs exhibited concentration-dependent decrease in GSH levels starting from 50μg/ml concentration (Figure 4.9 B). Interestingly, even the lowest concentration of 10μg/ml was sufficient enough to cause a substantial decline in cellular GSH levels. The overall reduction in GSH levels obtained in this experiment was not something unexpected. Numerous works have examined the effect of MNPs in disturbing the overall mechanisms of antioxidant pathways in cells [117-119]. The most common *in vitro* and *in vivo* toxicity of MNPs develop due to production of reactive oxygen species (ROS), which include singlet oxygen, hydrogen peroxide, hydroxyl radicals and superoxide anions [114, 120]. MNPs are likely to be taken up by the cells via different endocytic pathways depending on their size and surface chemistry [121]. Once inside the cells, MNPs are typically degraded in the lysosomes into ferrous (Fe^{2+}) ions due to their low pH environment. These Fe^{2+} ions could potentially enter the mitochondrial membrane system through membrane depolarization and interact with different enzymes of the electron transport system especially with NADPH oxidase, oxygen and hydrogen peroxide producing ferric ions (Fe^{3+}) and highly reactive hydroxyl radicals through Fenton chemistry [38, 122]. High levels of ROS species can deteriorate the cellular levels of GSH thereby causing oxidative stress. A study conducted by Watanabe *et al.* reported that exposing MNPs to human alveolar epithelial cells caused DNA damage, increased ROS production and reduced GSH levels even at low concentration of 10μg/ml, which is

similar to what we observed [123]. Similarly, significant increase in ROS levels and simultaneous reduction in GSH levels was observed in human breast cancer cells when exposed to MNPs. Here too, the authors described these effects to be time and concentration-dependent [124]. Based on these results, we can aptly deduce that both type of MNPs systems used in our experiments are responsible for generating increased ROS levels along with reducing intracellular GSH levels in CCD-18Co cells. Further studies needs to be conducted to decide the exact levels of several intracellular ROS (e.g., hydroxyl ions, hydrogen peroxide, singlet oxygen etc.) that are getting boosted due to presence of MNPs to fully elucidate the role of ROS in causing cellular toxicity in presence of MNPs.
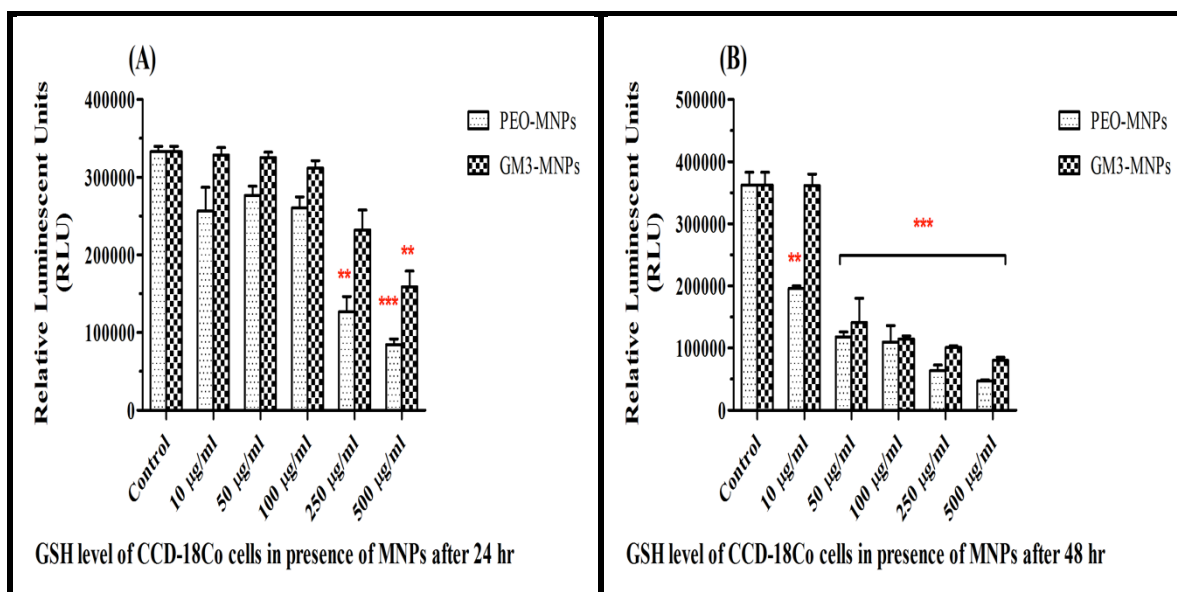
Figure 4.9 Intracellular Glutathione (GSH) levels of CCD-18Co cells in the presence of MNPs using GSH-Glo assay. A) GSH levels of cells exposed to PEO-MNPs at increasing concentrations for 24 hr; B) GSH levels of cells exposed to GM3-MNPs at increasing concentrations for 48 hr. Data is expressed as Mean ± SD (n=3); Statistical analysis – Analysis of Variance (ANOVA); * p-value <0.05, ** p-value <0.01, and *** p-value <0.001

The presence of nanomaterials in biological system has been shown to induce apoptosis in cells by activating various cell-death signaling pathways [43, 125]. In order to determine whether CCD18-Co cells are showing any apoptotic activity in presence of MNPs, we quantitatively measured the levels of caspase3 and caspase7 proteins. These caspase proteins belong to cysteine-aspartic acid protease (caspase) family. This family also includes other caspase proteins like caspase6, caspase8, caspase9, and caspase10 that play a central role in activation of cell apoptosis [126, 127]. Upon detecting a major change in the normal biochemical processes occurring inside the mitochondria, different signaling pathways are activated, which can trigger the activation of caspase family proteins. One of the last proteins of caspase family to get activated before the cell inadvertently goes into cell-death stage is caspase3 [128]. So, we performed caspase-glo 3/7 assay on CCD18-Co cells exposed to MNPs to check if their presence has activated the caspase signaling pathways leading to apoptosis. On incubating the cells with PEO-MNPs, we did not see any significant change in the levels of caspase3/7 proteins up to 250μg/ml concentrations (Figure 4.10 A). However, cells exposed to 500μg/ml PEO-MNPs showed a substantial increase in activity of caspase3/7 proteins, which suggests that the cells might be undergoing apoptosis. In comparison, cells incubated with GM3-MNPs for 24 hr maintained similar caspase3/7 levels at all concentrations. When the exposure time of MNPs to cells was increased to 48 hr, cells incubated with both 250μg/ml and 500μg/ml concentrations of PEO-MNPs showed a notable rise in caspase3/7 levels (Figure 4.10 B). This proves that even at concentration of 250μg/ml of PEO-MNPs, the cells may be experiencing apoptosis. Surprisingly, when were incubated

with GM3-MNPs for 48 hr, we did not observe a significant change in the caspase levels until the concentration was 500μg/ml. These results suggests that both PEO-MNPs and GM3-MNPs are able to activate caspase signaling events in CCD-18CO cells only when presented with highest concentrations of MNPs. However, it seems that the exposure time does play a critical role in induction of apoptosis as the overall caspase levels were elevated at 48 hr compared to 24 hr. Similar kind of results were obtained in several research findings that showed time-dependent increase in caspase protein levels in presence of MNPs [89]. The results obtained in this experiment are a little different (in terms of concentration-dependent rise in caspase levels) than what has been reported earlier. In one of the study done by Yin et al, the caspase3 levels in rat cerebellum cells showed a dose-dependent increasing trend when exposed to silver nanoparticles [129]. In another study, the size and surface functionalization of polystyrene latex nanoparticles played a significant part in initiating caspase dependent apoptotic pathways in human alveolar epithelial cells [130]. They noticed that cells exposed to 100 nm amine-coated nanoparticles had significantly higher levels of caspase proteins compared to those exposed to 50 nm size nanoparticles and also to carboxyl-coated nanoparticles. Hence, based on our results of caspase3/7 assay, it seems that the surface chemistry and exposure time are important parameters to consider when using MNPs for therapeutic applications. The levels of other apoptotic proteins needs to be determined in order to completely understand the if cellular toxicity mechanism in presence of MNPs is indeed due to activation of apoptosis signaling pathways.
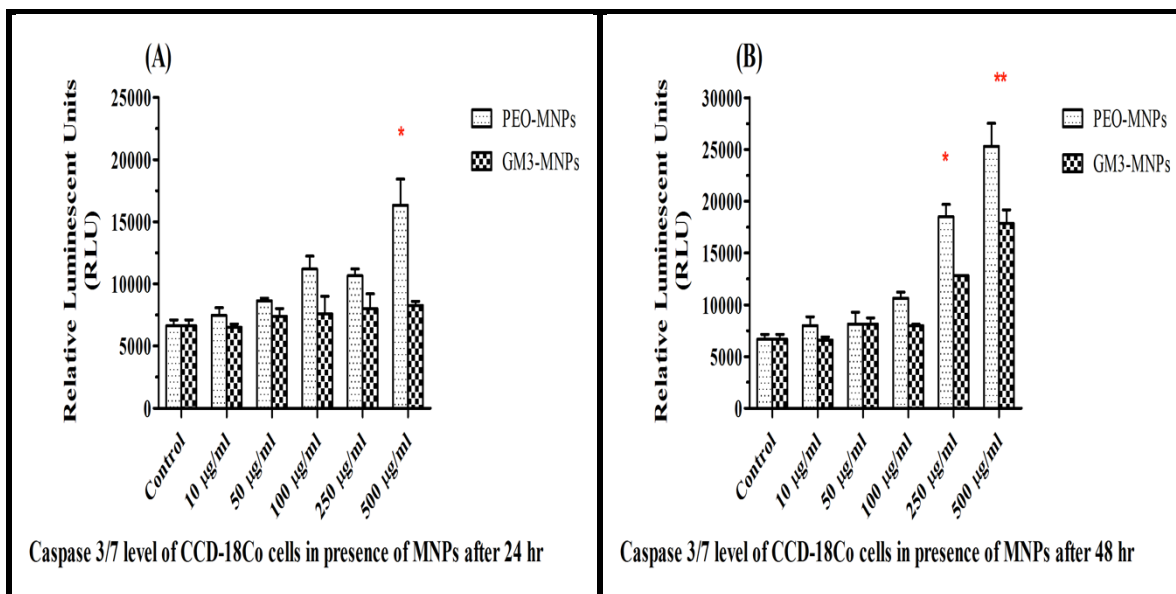
Figure 4.10 Intracellular caspase3/7 activity levels in CCD-18Co cells exposed to MNPs using Caspase-Glo 3/7 assay. A) Caspase3/7 levels of cells exposed to PEO-MNPs at increasing concentrations for 24 hr; B) Caspase3/7 levels of cells exposed to GM3-MNPs at increasing concentrations for 48 hr. Data is expressed as Mean ± SD (n=3); Statistical analysis − Analysis of Variance (ANOVA); * p-value <0.05, ** p-value <0.01, and *** p-value <0.001

Special Discussion: In this study, we have investigated and compared biocompatibility of PEO-MNPs with GM3-MNPs in normal human colon cell-line CCD-18Co. The main difference in terms of chemical functionality between PEO-MNPs and GM3-MNPs was the presence of glycoconjugate molecule GM3 on the surface of GM3-MNPs. As mentioned earlier, the type of surface functional groups present on MNPs plays an important role in regulating overall biocompatibility of the nanoparticle system both in *in vitro* and *in vivo* settings. Other factors that also play their part in imparting nanoparticle biocompatibility include surface charge, size, kind of polymer used, the extent to which it can form protein-corona in cell-culture medium, concentration of

nanoparticles, type of cells interacting with nanoparticles etc. [92, 94]. In order to check if MNPs were able to form protein-corona in protein and salt-rich biological medium, DLS studies were performed and it showed that PEO-MNPs significantly increased their overall size diameter. This increase can be attributed to formation of thick layer of protein-corona on the surface of nanoparticles. More specifically, the free alkyne group present on our heterobifunctional PEO polymer can potentially interact with various thiolated amino acids present in the cell-culture medium DMEM and due to this different protein molecules can bind to the surface of PEO-MNPs forming the corona and thereby increasing the size and possibly even altering the charge of nanoparticles [94, 95]. In contrast, there was only marginal diameter increase (~18 nm) for GM3-MNPs when mixed with DMEM. These results suggest that carbohydrate glycoconjugate coated MNPs can possibly act as drug-delivery agents as they do not significantly interact with the serum proteins, which would help in retaining its original physico-chemical properties. However, further detailed studies involving spectroscopic techniques needs to be done in order to fully identify the proteins interacting with MNPs and understand these mechanisms as the formation of protein-corona can potentially determine the nanoparticle uptake into the cells that would ultimately regulate cellular processes (Figure 4.11).
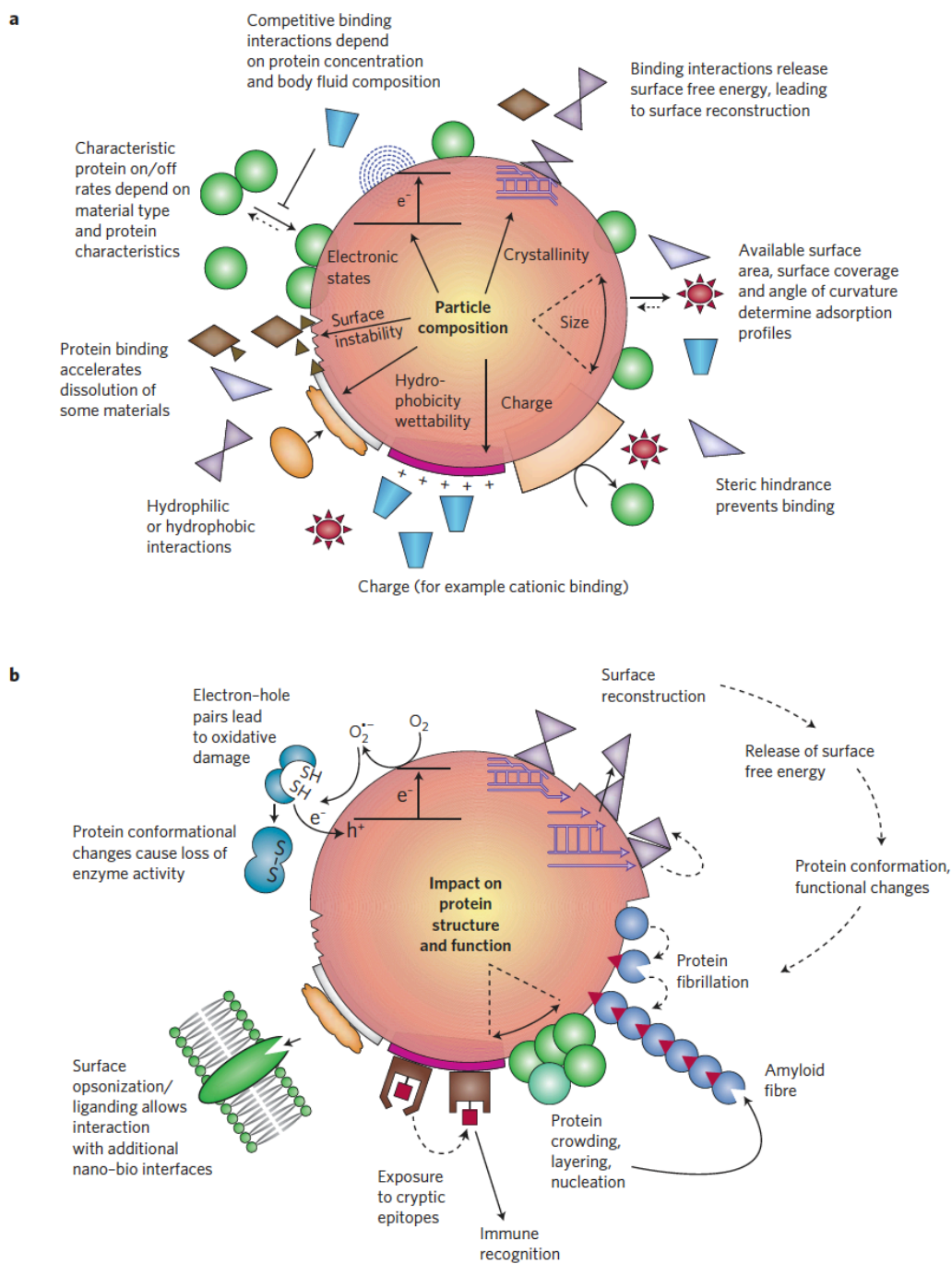
Figure 4.11 Formation of protein-corona on the surface of nanoparticles a) Formation of protein-corona on the nanoparticle surface depending on the physico-chemical properties of the initial material and b) Impact of protein-

corona on structural and functional properties of protein molecules interacting with biological medium. Reprinted from [11] - Reproduced with permission from Nature Publishing Group.

Over the last decade, numerous studies have expressed grave concern regarding the biocompatibility of engineered nanoparticles that are being extensively used for biomedical applications (e.g., gold nanoparticles, silver nanoparticles, magnetic nanoparticles etc.). These nanoparticles have been found to significantly affect the molecular machinery of the cells at different levels. Since nanoparticles have large surface area, even a minute change in their physico-chemical properties can have drastic effect on the way it interacts with cells. Among different factors responsible for these changes, the chemical properties and presence of surface chemical groups tend to outweigh all the other factors. The kind of chemical groups can potentially dictate if the nanoparticles have the ability to alter the electron accepting/donating mechanisms occurring inside the cells. Currently, the best possible explanatory model in determining the toxicological effects of engineered nanoparticles relies heavily on the generation of ROS [114, 120]. Among different type of nanoparticles, MNPs have been known to produce ROS when exposed to mammalian cells [114-116]. It is this very property that has made MNPs to be used for targeted drug delivery for cancer therapy in clinical use. MNPs are able to enter the cells via endocytosis and once inside, they can freely interact with lysosomes or endosomes and in this process they can increase ROS levels via Fenton reaction in the cells putting them under increased oxidative stress environment [114, 122]. In normal metabolic state, the ROS levels are usually found to be low in the cells. To counteract them, different antioxidant enzymes (catalase, superoxide dismutase,

141

etc.) and glutathione are produced by the cells. However, when ROS levels are increased significantly, the GSH levels and antioxidant enzyme levels are reduced and the cell experiences increased oxidative stress. In our experiments too, both PEO-MNPs and GM3-MNPs decreased intracellular GSH levels of CCD-18Co cell indicative of increased oxidative stress. Depending on the amount of oxidative stress, different response elements in the cells are activated. For example, at low level of oxidative stress, transcription factor Nrf-2 gets activated which in turn increases the production of various antioxidant enzymes which would typically restore the redox balance in the cells [120]. However, when the cells are experiencing high level of oxidative stress, numerous cell-signaling pathways related to inflammation and cytotoxicity are activated (e.g., mitogen-activated protein kinase (MAPK), nuclear factor κB (NF-κB), AP-1). Higher ROS levels also interfere with the electron transport system (ETS) of mitochondria that could potentially reduce the activity of ATP synthase pump leading to membrane depolarization and lipid peroxidation, which can induce irreversible damage of plasma membrane. These pathways can also activate pro-apoptosis factors in the cells, which would eventually result in activation of caspase molecules leading to apoptosis (Figure 4.12). Thus, in order to get an overall view of the ROS induced toxicity of our MNPs, elaborate studies on cellular uptake of MNPs, gene expression changes taking place in mitochondria (those involved in ETS chain), and extensive analysis of inflammatory factors involved in these mechanisms are warranted in *in vitro* conditions before these MNPs can be used for toxicity testing in animal models. Moreover, as MNPs are clinical used in magnetically triggered drug delivery through alternate magnetic fields, complete

142

toxicity profile of these MNPs should be evaluated by exposing the cells to magnetic fields.
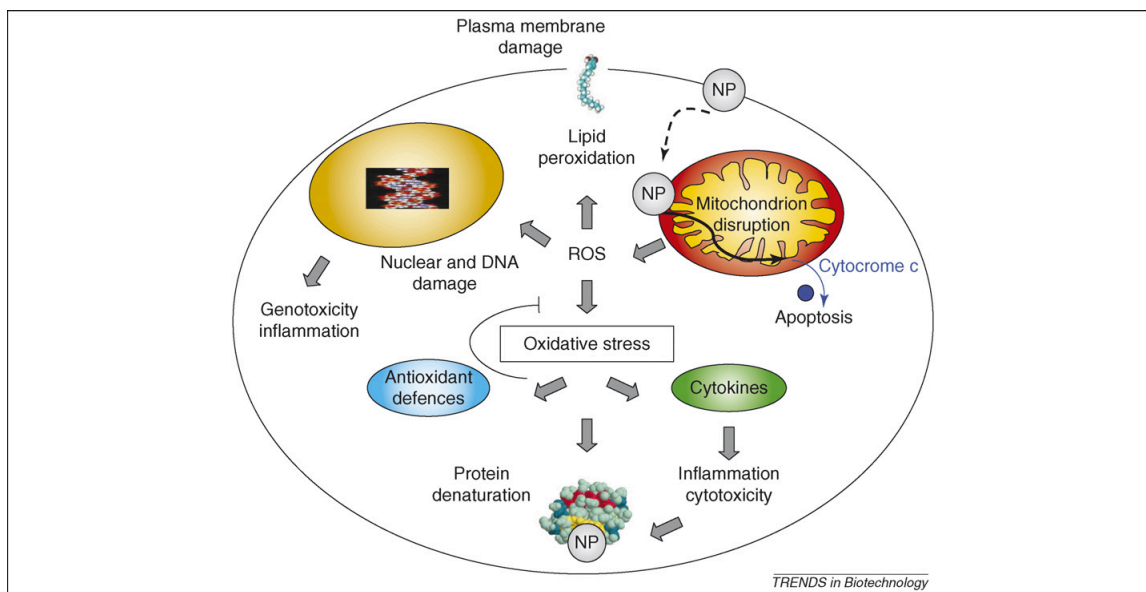
Figure 4.12 Possible mechanisms of nanoparticle toxicity induced by increased ROS levels. Reprinted from [131] - Reproduced with permission from Elsevier Ltd.

4. Conclusion:

We successfully synthesized multi-anchored glycoconjugate functionalized GM3-MNPs based on 'click-chemistry' platform that are stabilized with heterobifunctional PEO-PAA polymer having dopamine molecules as robust anchoring agents to the iron-oxide core. The above-mentioned GM3-MNPs were fully characterized through numerous techniques and their stability in cell-culture medium DMEM was investigated. In the presence of high salt and high protein environment of DMEM, MNPs were able to

form protein-corona layer on their surface within rapid time duration. Size diameter of PEO-MNPs increased significantly compared to GM3-MNPs suggesting formation of thick protein-corona layer. PEO-MNPs are able to cause strong decrease in cell-viability of CCD-18Co cells at concentrations above 100 µg/ml whereas GM3-MNPs did not show any cytotoxic effects on the cells. Also, intracellular ATP levels of CCD-18Co were significantly diminished in presence of PEO-MNPs but not GM3-MNPs indicative of interference in the activity of ATP synthase pump. PEO-MNPs also compromised the membrane integrity of the cells possibly due to apoptosis/necrosis; however, cells exposed to GM3-MNPs showed significantly different cell morphology but no membrane damage which indicates subtle changes in cytoskeleton arrangement of the cells. Also, presence of PEO-MNPs and GM3-MNPs to the cells resulted in substantial decrease in the intracellular GSH levels in a time and concentration-dependent manner that clearly denotes existence of increased oxidative stress via formation of reactive oxygen species. Finally, we also determined if MNPs were able to induce apoptosis in normal colon cells by means of measuring the activity of caspase proteins. The levels of caspase3 and caspase7 proteins were found to be remarkably elevated in the cells in presence of PEO-MNPs at higher concentrations, which was dependent on exposure time. Thus, based on the results that we obtained, it can be appropriate to assume that reduction of GSH due to increase in ROS levels and increased production of caspase3/7 proteins leading to apoptosis are few of the prominent factors responsible for triggering cellular toxicity in CCD-18Co cells in presence of PEO-MNPs. Some of the important nanoparticle synthesis parameters that directly affect toxic potential of MNPs and which warrants

144

further in-depth studies include controlling the amount of PEO-PAA polymer groups that are being grafted onto the surface of MNPs as excessive free groups can interact with protein molecules altering the physico-chemical properties of MNPs, effect of post-synthesis purification steps once the polymer is attached to the core of nanoparticle as chemical residues can also contribute to overall toxicity of MNPs. It is also important to mention here that since presence of glycoconjugate molecules on MNPs renders them relatively biocompatible, efforts should be made to increase the general efficiency of 'click chemistry' reactions so that more glycoconjugate molecules are being attached to PEO-PAA polymer. Furthermore, investigation of immunotoxicity of MNPs is necessary as colon cells can trigger inflammatory response signaling pathways (e.g., nuclear factor κB (NF-κB), mitogen-activated protein kinase (MAPK)) in presence of MNPs, which can also lead to apoptosis. As we observed reduction in GSH levels of colon cells in presence of MNPs implying increased ROS generation, gene expression studies of ROS gene cluster would be valuable to explain the exact underlying mechanisms of increased oxidative stress that could also lead to apoptosis. Also, by attaching proper antioxidant chemicals/drugs to GM3-MNPs, they can be effectively used for targeted drug-delivery to colon cells remotely via magnetothermal drug release mechanisms in presence of alternate magnetic fields for therapeutic applications in treating infections caused during post-IBS.

References:

1. Roco, M.C., *The long view of nanotechnology development: the National Nanotechnology Initiative at 10 years.* Journal of Nanoparticle Research, 2011. **13**(2): p. 427-445.

2.   Gorjiara, T. and C. Baldock, *Nanoscience and nanotechnology research publications: a comparison between Australia and the rest of the world.* Scientometrics, 2014. **100**(1): p. 121-148.

3.   *NNI Budget.* 2017 [cited 2017 5/25/2017]; Available from: https://www.nano.gov/about-nni/what/funding.

4.   Moore, T.L., *et al.*, *Nanoparticle colloidal stability in cell culture media and impact on cellular interactions.* Chemical Society Reviews, 2015. **44**(17): p. 6287-305.

5.   Gupta, A.K. and M. Gupta, *Synthesis and surface engineering of iron oxide nanoparticles for biomedical applications.* Biomaterials, 2005. **26**(18): p. 3995-4021.

6.   Kumar, C.S., *Nanomaterials for cancer therapy.* Vol. 6. 2006: Wiley-VCH Weinheim, Germany.

7.   Kumar, C.S., *Nanomaterials for medical diagnosis and therapy.* Vol. 10. 2007: Wiley-VCH.

8.   Kaittanis, C., S. Santra, and J.M. Perez, *Emerging nanotechnology-based strategies for the identification of microbial pathogenesis.* Advanced Drug Delivery Reviews, 2010. **62**(4-5): p. 408-423.

9.   Dave, S.R. and X. Gao, *Monodisperse magnetic nanoparticles for biodetection, imaging, and drug delivery: a versatile and evolving technology.* Wiley Interdisciplinary Reviews: Nanomedicine and Nanobiotechnology, 2009. **1**(6): p. 583-609.

10.   Min, Y.Z., *et al.*, *Clinical Translation of Nanomedicine.* Chemical Reviews, 2015. **115**(19): p. 11147-11190.

11.   Nel, A.E., *et al.*, *Understanding biophysicochemical interactions at the nano–bio interface.* Nature Materials, 2009. **8**(7): p. 543-557.

12.   Zhu, M., *et al.*, *Physicochemical properties determine nanomaterial cellular uptake, transport, and fate.* Accounts of Chemical Research, 2013. **46**(3): p. 622-31.

13.   Pankhurst, Q.A., *et al.*, *Applications of magnetic nanoparticles in biomedicine.* Journal of physics D: Applied physics, 2003. **36**(13): p. R167.

14.   Jain, T.K., *et al.*, *Magnetic nanoparticles with dual functional properties: drug delivery and magnetic resonance imaging.* Biomaterials, 2008. **29**(29): p. 4012-4021.

15.   Gao, J., H. Gu, and B. Xu, *Multifunctional magnetic nanoparticles: design, synthesis, and biomedical applications.* Accounts of Chemical research, 2009. **42**(8): p. 1097-107.

16.   Khandhar, A.P., *et al.*, *Tailored magnetic nanoparticles for optimizing magnetic fluid hyperthermia.* Journal of Biomedical Materials Research Part A, 2012. **100**(3): p. 728-737.

17.   Stone, R., *et al.*, *Targeted magnetic hyperthermia.* Therapeutic Delivery, 2011. **2**(6): p. 815-838.

18.   Laurent, S., *et al.*, *Magnetic iron oxide nanoparticles: synthesis, stabilization, vectorization, physicochemical characterizations, and biological applications.* Chemical Reviews, 2008. **108**(6): p. 2064-2110.

19.   Kumar, C.S., *Biofunctionalization of nanomaterials*. November 2005, Wiley-VCH.

20.   Amstad, E., M. Textor, and E. Reimhult, *Stabilization and functionalization of iron oxide nanoparticles for biomedical applications.* Nanoscale, 2011. **3**(7): p. 2819-2843.

21.   Aslam, M., *et al.*, *Synthesis of amine-stabilized aqueous colloidal iron oxide nanoparticles.* Crystal Growth & Design, 2007. **7**(3): p. 471-475.

22.   Vadala, M., *et al.*, *Heterobifunctional poly (ethylene oxide) oligomers containing carboxylic acids.* Biomacromolecules, 2008. **9**(3): p. 1035-1043.

23.   Sahoo, Y., *et al.*, *Alkyl phosphonate/phosphate coating on magnetite nanoparticles: a comparison with fatty acids.* Langmuir, 2001. **17**(25): p. 7907-7911.

24.   Griffiths, S.M., *et al.*, *Dextran coated ultrafine superparamagnetic iron oxide nanoparticles: compatibility with common fluorometric and colorimetric dyes.* Analytical Chemistry, 2011. **83**(10): p. 3778-3785.

25.   Wahajuddin and S. Arora, *Superparamagnetic iron oxide nanoparticles: magnetic nanoplatforms as drug carriers.* International Journal of Nanomedicine, 2012. **7**: p. 3445-3471.

26.   Sun, C., *et al.*, *PEG-mediated synthesis of highly dispersive multifunctional superparamagnetic nanoparticles: their physicochemical properties and function in vivo.* ACS Nano, 2010. **4**(4): p. 2402-2410.

27.   Ulbrich, K., *et al.*, *Targeted Drug Delivery with Polymers and Magnetic Nanoparticles: Covalent and Noncovalent Approaches, Release Control, and Clinical Studies.* Chemical Reviews, 2016. **116**(9): p. 5338-5431.

28. Harris, J.M. and R.B. Chess, *Effect of pegylation on pharmaceuticals.* Nature Reviews Drug Discovery, 2003. **2**(3): p. 214-221.

29. Veronese, F.M. and G. Pasut, *PEGylation, successful approach to drug delivery.* Drug Discovery Today, 2005. **10**(21): p. 1451-1458.

30. Amstad, E., *et al.*, *Ultrastable iron oxide nanoparticle colloidal suspensions using dispersants with catechol-derived anchor groups.* Nano Letters, 2009. **9**(12): p. 4042-4048.

31. Na, H.B., *et al.*, *Multidentate catechol-based polyethylene glycol oligomers provide enhanced stability and biocompatibility to iron oxide nanoparticles.* ACS Nano, 2011. **6**(1): p. 389-399.

32. Saville, S.L., *et al.*, *Investigation of the stability of magnetite nanoparticles functionalized with catechol based ligands in biological media.* Journal of Materials Chemistry, 2012. **22**(47): p. 24909-24917.

33. Mondini, S., *et al.*, *Colloidal stability of iron oxide nanocrystals coated with a PEG-based tetra-catechol surfactant.* Nanotechnology, 2013. **24**(10): p. 105702.

34. Stone, R.C., *et al.*, *Highly stable multi-anchored magnetic nanoparticles for optical imaging within biofilms.* J Colloid and Interface Science, 2015. **459**: p. 175-182.

35. Lu, A.H., E.L. Salabas, and F. Schuth, *Magnetic nanoparticles: synthesis, protection, functionalization, and application.* Angewandte Chemie, 2007. **46**(8): p. 1222-1244.

36. Arruebo, M., *et al.*, *Magnetic nanoparticles for drug delivery.* Nano today, 2007. **2**(3): p. 22-32.

37. Laurent, S., *et al.*, *Superparamagnetic iron oxide nanoparticles for delivery of therapeutic agents: opportunities and challenges.* Expert Opinion on Drug Delivery, 2014. **11**(9): p. 1449-1470.

38. Singh, N., *et al.*, *Potential toxicity of superparamagnetic iron oxide nanoparticles (SPION).* Nano Reviews, 2010. **1**.

39. Mahmoudi, M., *et al.*, *Assessing the in vitro and in vivo toxicity of superparamagnetic iron oxide nanoparticles.* Chemical Reviews, 2011. **112**(4): p. 2323-2338.

40. Laurent, S., *et al.*, *Crucial ignored parameters on nanotoxicology: the importance of toxicity assay modifications and "cell vision".* PloS one, 2012. **7**(1): p. e29997.

41. Reddy, L.H., *et al.*, *Magnetic nanoparticles: design and characterization, toxicity and biocompatibility, pharmaceutical and biomedical applications.* Chemical Reviews, 2012. **112**(11): p. 5818-5878.

42. Sengupta, J., *et al.*, *Physiologically important metal nanoparticles and their toxicity.* Journal of Nanoscience and Nanotechnology, 2014. **14**(1): p. 990-1006.

43. Mahmoudi, M., *et al.*, *Toxicity evaluations of superparamagnetic iron oxide nanoparticles: cell "vision" versus physicochemical properties of nanoparticles.* ACS Nano, 2011. **5**(9): p. 7263-7276.

44. Zhang, H., *et al.*, *Use of metal oxide nanoparticle band gap to develop a predictive paradigm for oxidative stress and acute pulmonary inflammation.* ACS Nano, 2012. **6**(5): p. 4349-4368.

45. Feliu, N., *et al.*, *In vivo degeneration and the fate of inorganic nanoparticles.* Chemical Society Reviews, 2016. **45**(9): p. 2440-2457.

46. Joris, F., *et al.*, *Assessing nanoparticle toxicity in cell-based assays: influence of cell culture parameters and optimized models for bridging the in vitro-in vivo gap.* Chemical Society Reviews, 2013. **42**(21): p. 8339-8359.

47. Kozissnik, B., *et al.*, *Magnetic fluid hyperthermia: Advances, challenges, and opportunity.* International Journal of Hyperthermia, 2013. **29**(8): p. 706-714.

48. Hauser, A.K., *et al.*, *Magnetic nanoparticles and nanocomposites for remote controlled therapies.* Journal of Controlled Release, 2015. **219**: p. 76-94.

49. Hauser, A.K., K.W. Anderson, and J.Z. Hilt, *Peptide conjugated magnetic nanoparticles for magnetically mediated energy delivery to lung cancer cells.* Nanomedicine, 2016. **11**(14): p. 1769-1785.

50. Kong, B., *et al.*, *Experimental considerations on the cytotoxicity of nanoparticles.* Nanomedicine (Lond), 2011. **6**(5): p. 929-941.

51. Wang, J., X. Fang, and W. Liang, *Pegylated phospholipid micelles induce endoplasmic reticulum-dependent apoptosis of cancer cells but not normal cells.* ACS Nano, 2012. **6**(6): p. 5018-5030.

52. Chen, X., O. Ramstrom, and M. Yan, *Glyconanomaterials: Emerging applications in biomedical research.* Nano Research, 2014. **7**(10): p. 1381-1403.

53. El-Boubbou, K. and X. Huang, *Glyco-nanomaterials: translating insights from the "sugar-code" to biomedical applications.* Current Medicinal Chemistry, 2011. **18**(14): p. 2060-2078.

54. Sunasee, R., *et al.*, *Therapeutic potential of carbohydrate-based polymeric and nanoparticle systems.* Expert Opinion on Drug Delivery, 2014. **11**(6): p. 867-884.

55. Garcia, I., M. Marradi, and S. Penades, *Glyconanoparticles: multifunctional nanomaterials for biomedical applications.* Nanomedicine, 2010. **5**(5): p. 777-792.

56. Marradi, M., M. Martin-Lomas, and S. Penades, *Glyconanoparticles polyvalent tools to study carbohydrate-based interactions.* Advances in Carbohydrate Chemistry and Biochemistry, 2010. **64**: p. 211-290.

57. Marradi, M., I. Garcia, and S. Penades, *Carbohydrate-based nanoparticles for potential applications in medicine.* Progress in Molecular Biology and Translational Science, 2011. **104**: p. 141-173.

58. Marradi, M., *et al.*, *Glyconanoparticles as multifunctional and multimodal carbohydrate systems.* Chemical Society Reviews, 2013. **42**(11): p. 4728-4745.

59. Raval, Y.S., *et al.*, *Synthesis and application of glycoconjugate-functionalized magnetic nanoparticles as potent anti-adhesion agents for reducing enterotoxigenic Escherichia coli infections.* Nanoscale, 2015. **7**(18): p. 8326-8331.

60. Shukla, R.K. and A. Tiwari, *Carbohydrate polymers: Applications and recent advances in delivering drugs to the colon.* Carbohydrate Polymers, 2012. **88**(2): p. 399-416.

61. Russell-Jones, G.J., H. Veitch, and L. Arthur, *Lectin-mediated transport of nanoparticles across Caco-2 and OK cells.* International Journal of Pharmaceutics, 1999. **190**(2): p. 165-174.

62. Gabor, F., *et al.*, *The lectin-cell interaction and its implications to intestinal lectin-mediated drug delivery.* Advanced Drug Delivery Reviews, 2004. **56**(4): p. 459-480.

63. Hua, S., *et al.*, *Advances in oral nano-delivery systems for colon targeted drug delivery in inflammatory bowel disease: selective targeting to diseased versus healthy tissue.* Nanomedicine, 2015. **11**(5): p. 1117-1132.

64. Lamprecht, A., *et al.*, *Biodegradable nanoparticles for targeted drug delivery in treatment of inflammatory bowel disease.* The Journal of Pharmacology and Experimental Therapeutics, 2001. **299**(2): p. 775-781.

65. Wu, Y., K. Briley, and X. Tao, *Nanoparticle-based imaging of inflammatory bowel disease.* Wiley Interdisciplinary Reviews: Nanomedicine and Nanobiotechnology, 2016. **8**(2): p. 300-315.

66. Laroui, H., *et al.*, *Drug-loaded nanoparticles targeted to the colon with polysaccharide hydrogel reduce colitis in a mouse model.* Gastroenterology, 2010. **138**(3): p. 843-53 e1-2.

67. Zhang, W., *et al.*, *Adsorption of hematite nanoparticles onto Caco-2 cells and the cellular impairments: effect of particle size.* Nanotechnology, 2010. **21**(35): p. 355103.

68. Loh, J.W., M. Saunders, and L.Y. Lim, *Cytotoxicity of monodispersed chitosan nanoparticles against the Caco-2 cells.* Toxicology and Applied Pharmacology, 2012. **262**(3): p. 273-282.

69. Zhang, H.Y., *et al.*, *Mammalian Cells Exhibit a Range of Sensitivities to Silver Nanoparticles that are Partially Explicable by Variations in Antioxidant Defense and Metallothionein Expression.* Small, 2015. **11**(31): p. 3797-3805.

70. Bastos, V., *et al.*, *The influence of Citrate or PEG coating on silver nanoparticle toxicity to a human keratinocyte cell line.* Toxicology Letters, 2016. **249**: p. 29-41.

71. Zhang, X.D., *et al.*, *Size-dependent in vivo toxicity of PEG-coated gold nanoparticles.* Int J Nanomedicine, 2011. **6**: p. 2071-2081.

72. Gu, L., *et al.*, *In vivo clearance and toxicity of monodisperse iron oxide nanocrystals.* ACS Nano, 2012. **6**(6): p. 4947-4954.

73. Cho, W.S., *et al.*, *Acute toxicity and pharmacokinetics of 13 nm-sized PEG-coated gold nanoparticles.* Toxicology and Applied Pharmacology, 2009. **236**(1): p. 16-24.

74. Silva, A.H., *et al.*, *Superparamagnetic iron-oxide nanoparticles mPEG350- and mPEG2000-coated: cell uptake and biocompatibility evaluation.* Nanomedicine, 2016. **12**(4): p. 909-919.

75. Soenen, S.J. and M. De Cuyper, *Assessing iron oxide nanoparticle toxicity in vitro: current status and future prospects.* Nanomedicine (Lond), 2010. **5**(8): p. 1261-1275.

76. Raval, Y.S., *et al.*, *Multianchored Glycoconjugate-Functionalized Magnetic Nanoparticles: A Tool for Selective Killing of Targeted Bacteria via Alternating Magnetic Fields.* Advanced Functional Materials, 2017.

77. Park, J., *et al.*, *Ultra-large-scale syntheses of monodisperse nanocrystals.* Nature Materials, 2004. **3**(12): p. 891-895.

78.   Shen, Y., *et al.*, *Purification of quantum dots by gel permeation chromatography and the effect of excess ligands on shell growth and ligand exchange.* Chemistry of Materials, 2013. **25**(14): p. 2838-2848.

79.   Stone, R., *et al.*, *Highly stable multi-anchored magnetic nanoparticles for optical imaging within biofilms.* Journal of Colloid and Interface Science, 2015. **459**: p. 175-182.

80.   Himo, F., *et al.*, *Copper (I)-catalyzed synthesis of azoles. DFT study predicts unprecedented reactivity and intermediates.* Journal of the American Chemical Society, 2005. **127**(1): p. 210-216.

81.   Hong, V., *et al.*, *Analysis and Optimization of Copper-Catalyzed Azide–Alkyne Cycloaddition for Bioconjugation.* Angewandte Chemie, 2009. **121**(52): p. 10063-10067.

82.   Vreeland, E.C., *et al.*, *Enhanced Nanoparticle Size Control by Extending LaMer's Mechanism.* Chemistry of Materials, 2015. **27**(17): p. 6059-6066.

83.   International, A., *Standard Test Method for Iron in Trace Quantities Using the 1,10-Phenanthroline Method.* 2015, ASTM International.

84.   Bae, J.-E., *et al.*, *The effect of static magnetic fields on the aggregation and cytotoxicity of magnetic nanoparticles.* Biomaterials, 2011. **32**(35): p. 9401-9414.

85.   Chu, M.Q., *et al.*, *Near-infrared laser light mediated cancer therapy by photothermal effect of Fe3O4 magnetic nanoparticles.* Biomaterials, 2013. **34**(16): p. 4078-4088.

86.   Pisanic, T.R., 2nd, *et al.*, *Nanotoxicity of iron oxide nanoparticle internalization in growing neurons.* Biomaterials, 2007. **28**(16): p. 2572-2581.

87.   Prasad, R.Y., *et al.*, *Investigating oxidative stress and inflammatory responses elicited by silver nanoparticles using high-throughput reporter genes in HepG2 cells: Effect of size, surface coating, and intracellular uptake.* Toxicology in Vitro, 2013. **27**(6): p. 2013-2021.

88.   Choi, K.-H., *et al.*, *Size-Dependent Photodynamic Anticancer Activity of Biocompatible Multifunctional Magnetic Submicron Particles in Prostate Cancer Cells.* Molecules, 2016. **21**(9): p. 1187.

89.   Tomitaka, A., T. Yamada, and Y. Takemura, *Magnetic nanoparticle hyperthermia using pluronic-coated Fe3O4 nanoparticles: an in vitro study.* Journal of Nanomaterials, 2012. **2012**: p. 4.

90.   Sun, S., *et al.*, *Monodisperse MFe2O4 (M= Fe, Co, Mn) nanoparticles.* Journal of the American Chemical Society, 2004. **126**(1): p. 273-279.

91.   Amiri, H., *et al.*, *Protein corona affects the relaxivity and MRI contrast efficiency of magnetic nanoparticles.* Nanoscale, 2013. **5**(18): p. 8656-8665.

92.   Sakulkhu, U., *et al.*, *Protein corona composition of superparamagnetic iron oxide nanoparticles with various physico-chemical properties and coatings.* Scientific Reports, 2014. **4**: p. 5020.

93.   Casals, E., *et al.*, *Hardening of the nanoparticle-protein corona in metal (Au, Ag) and oxide (Fe3O4, CoO, and CeO2) nanoparticles.* Small, 2011. **7**(24): p. 3479-3486.

94.   Jedlovszky-Hajdu, A., *et al.*, *Surface coatings shape the protein corona of SPIONs with relevance to their application in vivo.* Langmuir, 2012. **28**(42): p. 14983-14991.

95.   Ekkebus, R., *et al.*, *On terminal alkynes that can react with active-site cysteine nucleophiles in proteases.* Journal of the American Chemical Society, 2013. **135**(8): p. 2867-2870.

96.   Love, S.A., *et al.*, *Assessing nanoparticle toxicity.* The Annual Review of Analytical Chemistry (Palo Alto Calif), 2012. **5**: p. 181-205.

97.   Escamilla-Rivera, V., *et al.*, *Protein corona acts as a protective shield against Fe3O4-PEG inflammation and ROS-induced toxicity in human macrophages.* Toxicology Letters, 2016. **240**(1): p. 172-184.

98.   Couto, D., *et al.*, *Biodistribution of polyacrylic acid-coated iron oxide nanoparticles is associated with proinflammatory activation and liver toxicity.* Journal of Applied Toxicology, 2016. **36**(10): p. 1321-1331.

99.   Iversen, N.K., *et al.*, *Superparamagnetic iron oxide polyacrylic acid coated gamma-Fe2O3 nanoparticles do not affect kidney function but cause acute effect on the cardiovascular function in healthy mice.* Toxicology and Applied Pharmacology, 2013. **266**(2): p. 276-288.

100.   Hafeli, U.O., *et al.*, *Cell uptake and in vitro toxicity of magnetic nanoparticles suitable for drug delivery.* Molecular Pharmaceutics, 2009. **6**(5): p. 1417-1428.

101.   Moros, M., *et al.*, *Monosaccharides versus PEG-functionalized NPs: influence in the cellular uptake.* ACS Nano, 2012. **6**(2): p. 1565-1577.

102.   Patitsa, M., *et al.*, *Magnetic nanoparticles coated with polyarabic acid demonstrate enhanced drug delivery and imaging properties for cancer theranostic applications.* Scientific Reports, 2017. **7**(1): p. 775.

103. JesÚs, M., D. AlcÁntara, and S. PenadÉs, *Cell response to magnetic glyconanoparticles: does the carbohydrate matter?* IEEE Rransactions on Nanobioscience, 2007. **6**(4): p. 275-281.

104. Araujo, F., *et al.*, *The impact of nanoparticles on the mucosal translocation and transport of GLP-1 across the intestinal epithelium.* Biomaterials, 2014. **35**(33): p. 9199-9207.

105. Nazli, C., *et al.*, *RGDS-functionalized polyethylene glycol hydrogel-coated magnetic iron oxide nanoparticles enhance specific intracellular uptake by HeLa cells.* International Journal of Nanomedicine, 2012. **7**: p. 1903-1920.

106. Gornati, R., *et al.*, *Zerovalent Fe, Co and Ni nanoparticle toxicity evaluated on SKOV-3 and U87 cell lines.* Journal of Applied Toxicology, 2016. **36**(3): p. 385-393.

107. Bahring, F., *et al.*, *Suitability of Viability Assays for Testing Biological Effects of Coated Superparamagnetic Nanoparticles.* Ieee Transactions on Magnetics, 2013. **49**(1): p. 383-388.

108. Domey, J., *et al.*, *Long-term prevalence of NIRF-labeled magnetic nanoparticles for the diagnostic and intraoperative imaging of inflammation.* Nanotoxicology, 2016. **10**(1): p. 20-31.

109. Master, A.M., *et al.*, *Remote Actuation of Magnetic Nanoparticles For Cancer Cell Selective Treatment Through Cytoskeletal Disruption.* Scientific Reports, 2016. **6**: p. 33560.

110. Wu, X., *et al.*, *Toxic effects of iron oxide nanoparticles on human umbilical vein endothelial cells.* International Journal of Nanomedicine, 2010. **5**: p. 385-399.

111. Soenen, S.J., *et al.*, *High intracellular iron oxide nanoparticle concentrations affect cellular cytoskeleton and focal adhesion kinase-mediated signaling.* Small, 2010. **6**(7): p. 832-482.

112. Griffith, O.W. and A. Meister, *Origin and Turnover of Mitochondrial Glutathione.* Proceedings of the National Academy of Sciences of the United States of America, 1985. **82**(14): p. 4668-4672.

113. Sies, H., *Glutathione and its role in cellular functions.* Free Radical Biology and Medicine, 1999. **27**(9-10): p. 916-921.

114. Tee, J.K., *et al.*, *Oxidative stress by inorganic nanoparticles.* Wiley Interdisciplinary Reviews-Nanomedicine and Nanobiotechnology, 2016. **8**(3): p. 414-438.

115. Wu, H.H., *et al.*, *Reactive oxygen species-related activities of nano-iron metal and nano-iron oxides.* Journal of Food and Drug Analysis, 2014. **22**(1): p. 86-94.

116. Liu, G., *et al.*, *Applications and Potential Toxicity of Magnetic Iron Oxide Nanoparticles.* Small, 2013. **9**(9-10): p. 1533-1545.

117. Naqvi, S., *et al.*, *Concentration-dependent toxicity of iron oxide nanoparticles mediated by increased oxidative stress.* International Journal of Nanomedicine, 2010. **5**: p. 983-989.

118. Strojan, K., *et al.*, *Glutathione reduces cytotoxicity of polyethyleneimine coated magnetic nanoparticles in CHO cells.* Toxicology In Vitro, 2017. **41**: p. 12-20.

119. Wydra, R.J., *et al.*, *The role of ROS generation from magnetic nanoparticles in an alternating magnetic field on cytotoxicity.* Acta Biomaterialia, 2015. **25**: p. 284-290.

120. Nel, A., *et al.*, *Toxic potential of materials at the nanolevel.* science, 2006. **311**(5761): p. 622-627.

121. Verma, A. and F. Stellacci, *Effect of surface properties on nanoparticle-cell interactions.* Small, 2010. **6**(1): p. 12-21.

122. Wu, H., *et al.*, *Reactive oxygen species-related activities of nano-iron metal and nano-iron oxides.* Journal of Food and Drug Analysis, 2014. **22**(1): p. 86-94.

123. Watanabe, M., *et al.*, *Effects of Fe3O4 magnetic nanoparticles on A549 cells.* International Journal of Molecular Sciences, 2013. **14**(8): p. 15546-15560.

124. Alarifi, S., *et al.*, *Iron oxide nanoparticles induce oxidative stress, DNA damage, and caspase activation in the human breast cancer cell line.* Biological Trace Element Research, 2014. **159**(1-3): p. 416-24.

125. Creixell, M., *et al.*, *EGFR-targeted magnetic nanoparticle heaters kill cancer cells without a perceptible temperature rise.* ACS Nano, 2011. **5**(9): p. 7124-7129.

126. Nicholson, D.W. and N.A. Thornberry, *Caspases: killer proteases.* Trends in Biochemical Sciences, 1997. **22**(8): p. 299-306.

127. Thornberry, N.A. and Y. Lazebnik, *Caspases: Enemies within.* Science, 1998. **281**(5381): p. 1312-1316.

128. Riedl, S.J. and Y.G. Shi, *Molecular mechanisms of caspase regulation during apoptosis.* Nature Reviews Molecular Cell Biology, 2004. **5**(11): p. 897-907.

129. Yin, N.Y., *et al.*, *Silver Nanoparticle Exposure Attenuates the Viability of Rat Cerebellum Granule Cells through Apoptosis Coupled to Oxidative Stress.* Small, 2013. **9**(9-10): p. 1831-1841.

130. Ruenraroengsak, P., *et al.*, *Respiratory epithelial cytotoxicity and membrane damage (holes) caused by amine-modified nanoparticles.* Nanotoxicology, 2012. **6**(1): p. 94-108.

131. Sanvicens, N. and M.P. Marco, *Multifunctional nanoparticles--properties and prospects for their use in human medicine.* Trends in Biotechnology, 2008. **26**(8): p. 425-433.

Chapter 5

Concluding Remarks

Functionalized MNPs are currently one of the most commonly used nanomaterials in biomedical settings. Among different functional groups, MNPs having carbohydrate molecules attached to them have shown excellent biocompatibility in both *in vitro* and *in vivo* conditions. This dissertation work mainly focuses on developing proof-of-concept MNPs functionalized with specific sialic-acid based carbohydrate glycoconjugate molecule (Neu5Ac(α2-3)Gal(β1-4)-Glcβ-sp) (GM3-MNPs) and evaluating their interaction with enterotoxigenic *E. coli* strain *EC* K99. These functionalized MNPs were synthesized by using special heterobifunctional PEO polymer comprising of dopamine molecules on one end and free alkyne groups on other end on which the GM3 molecule is attached via 'click chemistry' linkage. Specific interactions occurred between *EC* K99 and GM3-MNPs, which resulted in formation of aggregates of bacteria-nanoparticle complex as described in chapter 2. These results show that it is possible to create bacteria-specific multifunctional MNPs based on carbohydrate molecules that can find useful applications in rapid detection (ID system) of pathogens in biological samples.

Later, in chapter 3, we evaluated the practicability of using GM3-MNPs developed on multi-anchored PEO-PAA dopamine platform for targeted killing of *EC* K99 in presence

of AMF. High degree of clinically significant specific *in vitro* bacterial killing (in both pure culture and mixed culture environment) was seen in *EC* K99 in presence of AMF possibly due to MagMED phenomenon and destruction of bacterial cell membrane. These results are pivotal since bacterial infections occurring in GI tract has heterogeneous environment i.e. presence of beneficial gut bacteria and using antibiotics for treating such infections would give rise to potential drug-resistant bacteria along with destroying the beneficial micro-flora. Future studies are warranted to test the effectiveness of AMF treatment in multi-drug resistant bacteria e.g., MRSA, carbapenem-resistant enterobacteriaceae group. Several important parameters like core-size of MNPs, polymer length, concentration of MNPs, magnetic field strength and applied frequency of AMF should be fine-tuned to improve the efficacy of treatment regimen in both *in vitro* and *in vivo* conditions. Once these factors are established, MNPs and AMF together would act as novel non-antibiotic agents for treating clinically relevant bacterial infections, thereby, eliminating the need of using antibiotics and diminishing the rise of drug-resistant bacteria.

Different strategies have been employed to impart colloidal stability to MNPs in biological environment. The type of polymer used in stabilizing MNPs plays an important role in this regard. The presence of chemical functional group on surface of MNPs would define how it interacts with serum proteins and mammalian cell in *in vitro* setting, which would then determine its biocompatibility. Thus, finally in chapter 4, biocompatibility studies were undertaken to figure out the toxicity profile of MNPs developed on multi-anchored PEO-PAA dopamine platform. GM3-MNPs were able to

maintain their overall colloidal stability in protein-rich environment as they formed limited 'protein-corona'. They were also found to be fairly biocompatible (other than reducing GSH levels) compared to PEO-MNPs when exposed to normal colon cells CCD-18Co. This shows that presence of carbohydrate groups on MNPs surface can potentially impart biocompatibility. Nonetheless, extensive toxicity studies in animal models are necessitated for these carbohydrates functionalized MNPs. By carefully controlling different parameters of MNPs synthesis like size of MNPs, post-synthesis purification techniques, and efficient ligand-exchange reactions, it is possible to create MNPs functionalized with carbohydrate groups that are fully biocompatible and can be used in therapeutic applications.

The results obtained in this work suggest that carbohydrate glycoconjugate functionalized MNPs have great potential to be effectively used in clinical settings as multifunctional theragnostics agents for e.g., simultaneous detection, isolation & destruction of targeted pathogens, targeted drug-delivery & imaging and as effective vaccine candidates.

Appendix

LIST OF PEER-REVIEWED PUBLICATIONS

1. **Yash Raval**, Benjamin Fellows, Jamie Murbach, Yves Cordeau, O. Thompson Mefford, and Tzuen-Rong Tzeng. "Multi-Anchored Glycoconjugate Functionalized Magnetic Nanoparticles: A Tool for Selective Killing of Targeted Bacteria via Alternate Magnetic Fields". Advanced Functional Materials, (2017); 27, 1701473, DOI: 10.1002/adfm.201701473

2. **Yash Raval**, Roland Stone, Benjamin Fellows, Bin Qi, Guohui Huang, O. Thompson Mefford, and Tzuen-Rong J. Tzeng. "Synthesis and Application of Glycoconjugate-Functionalized Magnetic Nanoparticles as Potent Anti-Adhesion Agents for Reducing Enterotoxigenic *Escherichia coli* Infections". Nanoscale, (2015); 7: 8326-8331, DOI: 10.1039/C5NR00511F

3. Zheng Wang, **Yash Raval**, Tzuen-Rong J. Tzeng, Brian Booth, Briana Flaherty, David Peterson, Julie Moore, Daniel Rosenmann, Ralu Divan, Guofen Yu, Pingshan Wang. "Time Domain Detection and Differentiation of Single Particles and Cells with a Radio Frequency Interferometer". IEEE Topical Conference on Biomedical Wireless Technologies, Networks and Sensing Systems, (2016), DOI: 10.1109/BIOWIRELESS.2016.7445567

4. Fenglin Wang, **Yash Raval**, Tzuen-Rong J. Tzeng, and Jeffrey N. Anker. "X-Ray Excited Luminescence Chemical Imaging of Bacterial Growth on Surfaces Implanted in Tissue". Advanced Healthcare Materials, (2015); 4: 903-910, DOI: 10.1002/adhm.201400685

5. Fenglin Wang, **Yash Raval**, Hongyu Chen, Tzuen-Rong J. Tzeng, John D. DesJardins and Jeffrey N. Anker. "Development of Luminescent pH Sensor Films for Monitoring Bacterial Growth Through Tissue". Advanced Healthcare Materials, (2014); 3: 197-204, DOI: 10.1002/adhm.201300101

6. Unaiza Uzair, Donald Benza, **Yash Raval**, Caleb Behrend, Tzuen-Rong Tzeng, and Jeffrey Anker. "X-Ray Excited Luminescent Chemical Imaging (XELCI) for Non-Invasive Imaging of Implant Infections". SPIE BiOS, (2017); 100810K1-100810K9, DOI: 10.1117/12.2256049

7. Cory Thomas, Xinyu Lu, Andrew Todd, **Yash Raval**, Tzuen-Rong Tzeng, Yongxin Song, Junsheng Wang, Dongqing Li, and Xiangchun Xuan. "Charge-based Separation of Particles and Cells with Similar Size via Wall-Indued Electrical Lift". Electrophoresis, (2017); 38 (2), 320-326, DOI: 10.1002/elps.201600284

8. Lin Zhu, Saurin Patel, Mark Johnson, Akshay Kale, **Yash Raval**, Tzuen-Rong Tzeng, and Xiangchun Xuan. "Enhanced Throughput for Electrokinetic Manipulation of Particles and Cells in a Stacked Microfluidic Device". Micromachines, (2016); 7 (9), 156; DOI: 10.3390/mi7090156

9. Roland Stone, Benjamin Fellows, Bin Qi, David Trebatoski, Brennen Jenkins, **Yash Raval**, Tzuen-Rong Tzeng, Terri Bruce, Tamara Mcnealy, Mariah Austin, Todd Monson, Dale Huber, and O. Thompson Mefford. "Highly Stable Multi-Anchored Magnetic Nanoparticles for Optimal Imaging within Biofilms". Journal of Colloid and Interface Science, (2015); 459: 175-182, DOI: 10.1016/j.jcis.2015.08.012

10. Herbert Harrison, Xinyu Lu, Saurin Patel, Cory Thomas, Andrew Todd, Mark Johnson, **Yash Raval**, Tzuen-Rong J. Tzeng, Yongxin Song, Junsheng Wang, Dongqing Li, and Xiangchun Xuan. "Electrokinetic Preconcentration of Particles and Cells in Microfluidic Reservoirs". Analyst, (2015); 140: 2869-2875, DOI: 10.1039/C5AN00105F

Rights and Permissions

This Agreement between Yash Raval ("You") and Elsevier ("Elsevier") consists of your license details and the terms and conditions provided by Elsevier and Copyright Clearance Center.

License Number	4118900364299
License date	May 30, 2017
Licensed Content Publisher	Elsevier
Licensed Content Publication	Advanced Drug Delivery Reviews
Licensed Content Title	Magnetic nanomaterials for hyperthermia based therapy and controlled drug delivery
Licensed Content Author	Challa S.S.R. Kumar,Faruq Mohammad
Licensed Content Date	Aug 14, 2011
Licensed Content Volume	63
Licensed Content Issue	9
Licensed Content Pages	20
Start Page	789
End Page	808
Type of Use	reuse in a thesis/dissertation
Intended publisher of new work	other
Portion	figures/tables/illustrations
Number of figures/tables/illustrations	3
Format	electronic
Are you the author of this Elsevier article?	No
Will you be translating?	No
Order reference number	
Original figure numbers	figure1, figure2, table 1
Title of your thesis/dissertation	Application of Glycoconjugate functionalized Magnetic Nanoparticles as Anti-adhesion and Antibacterial Agents
Expected completion date	Aug 2017
Estimated size (number of pages)	150
Elsevier VAT number	GB 494 6272 12
Requestor Location	Yash Raval
	143 Life Sciences Facility
	190 Collings St
	CLEMSON, SC 29634
	United States
	Attn: Yash Raval
Publisher Tax ID	980397604
Total	0.00 USD
Terms and Conditions	

INTRODUCTION

GENERAL TERMS

2. Elsevier hereby grants you permission to reproduce the aforementioned material subject to the terms and conditions indicated.

3. Acknowledgement: If any part of the material to be used (for example, figures) has appeared in our publication with credit or acknowledgement to another source, permission must also be sought from that source. If such permission is not obtained then that material may not be included in your publication/copies. Suitable acknowledgement to the source must be made, either as a footnote or in a reference list at the end of your publication, as follows:
"Reprinted from Publication title, Vol /edition number, Author(s), Title of article / title of chapter, Pages No., Copyright (Year), with permission from Elsevier [OR APPLICABLE SOCIETY COPYRIGHT OWNER]." Also Lancet special credit - "Reprinted from The Lancet, Vol. number, Author(s), Title of article, Pages No., Copyright (Year), with permission from Elsevier."

4. Reproduction of this material is confined to the purpose and/or media for which permission is hereby given.

5. Altering/Modifying Material: Not Permitted. However figures and illustrations may be altered/adapted minimally to serve your work. Any other abbreviations, additions, deletions and/or any other alterations shall be made only with prior written authorization of Elsevier Ltd. (Please contact Elsevier at permissions@elsevier.com). No modifications can be made to any Lancet figures/tables and they must be reproduced in full.

6. If the permission fee for the requested use of our material is waived in this instance, please be advised that your future requests for Elsevier materials may attract a fee.

7. Reservation of Rights: Publisher reserves all rights not specifically granted in the combination of (i) the license details provided by you and accepted in the course of this licensing transaction, (ii) these terms and conditions and (iii) CCC's Billing and Payment terms and conditions.

8. License Contingent Upon Payment: While you may exercise the rights licensed immediately upon issuance of the license at the end of the licensing process for the transaction, provided that you have disclosed complete and accurate details of your proposed use, no license is finally effective unless and until full payment is received from you (either by publisher or by CCC) as provided in CCC's Billing and Payment terms and conditions. If full payment is not received on a timely basis, then any license preliminarily granted shall be deemed automatically revoked and shall be void as if never granted. Further, in the event that you breach any of these terms and conditions or any of CCC's Billing and Payment terms and conditions, the license is automatically revoked and shall be void as if never granted. Use of materials as described in a revoked license, as well as any use of the materials beyond the scope of an unrevoked license, may constitute copyright infringement and publisher reserves the right to take any and all action to protect its copyright in the materials.

9. Warranties: Publisher makes no representations or warranties with respect to the licensed material.

10. Indemnity: You hereby indemnify and agree to hold harmless publisher and CCC, and their respective officers, directors, employees and agents, from and against any and all claims arising out of your use of the licensed material other than as specifically authorized pursuant to this license.

11. No Transfer of License: This license is personal to you and may not be sublicensed, assigned, or transferred by you to any other person without publisher's written permission.

12. No Amendment Except in Writing: This license may not be amended except in a writing

signed by both parties (or, in the case of publisher, by CCC on publisher's behalf).
13. Objection to Contrary Terms: Publisher hereby objects to any terms contained in any purchase order, acknowledgment, check endorsement or other writing prepared by you, which terms are inconsistent with these terms and conditions or CCC's Billing and Payment terms and conditions. These terms and conditions, together with CCC's Billing and Payment terms and conditions (which are incorporated herein), comprise the entire agreement between you and publisher (and CCC) concerning this licensing transaction. In the event of any conflict between your obligations established by these terms and conditions and those established by CCC's Billing and Payment terms and conditions, these terms and conditions shall control.
14. Revocation: Elsevier or Copyright Clearance Center may deny the permissions described in this License at their sole discretion, for any reason or no reason, with a full refund payable to you. Notice of such denial will be made using the contact information provided by you. Failure to receive such notice will not alter or invalidate the denial. In no event will Elsevier or Copyright Clearance Center be responsible or liable for any costs, expenses or damage incurred by you as a result of a denial of your permission request, other than a refund of the amount(s) paid by you to Elsevier and/or Copyright Clearance Center for denied permissions.

LIMITED LICENSE
The following terms and conditions apply only to specific license types:
15. **Translation:** This permission is granted for non-exclusive world English rights only unless your license was granted for translation rights. If you licensed translation rights you may only translate this content into the languages you requested. A professional translator must perform all translations and reproduce the content word for word preserving the integrity of the article.
16. **Posting licensed content on any Website:** The following terms and conditions apply as follows: Licensing material from an Elsevier journal: All content posted to the web site must maintain the copyright information line on the bottom of each image; A hyper-text must be included to the Homepage of the journal from which you are licensing at http://www.sciencedirect.com/science/journal/xxxxx or the Elsevier homepage for books at http://www.elsevier.com; Central Storage: This license does not include permission for a scanned version of the material to be stored in a central repository such as that provided by Heron/XanEdu.
Licensing material from an Elsevier book: A hyper-text link must be included to the Elsevier homepage at http://www.elsevier.com . All content posted to the web site must maintain the copyright information line on the bottom of each image.
Posting licensed content on Electronic reserve: In addition to the above the following clauses are applicable: The web site must be password-protected and made available only to bona fide students registered on a relevant course. This permission is granted for 1 year only. You may obtain a new license for future website posting.
17. **For journal authors:** the following clauses are applicable in addition to the above:
Preprints:
A preprint is an author's own write-up of research results and analysis, it has not been peer reviewed, nor has it had any other value added to it by a publisher (such as formatting, copyright, technical enhancement etc.).
Authors can share their preprints anywhere at any time. Preprints should not be added to or enhanced in any way in order to appear more like, or to substitute for, the final versions of articles however authors can update their preprints on arXiv or RePEc with their AcceptedAuthor Manuscript (see below).

If accepted for publication, we encourage authors to link from the preprint to their formal publication via its DOI. Millions of researchers have access to the formal publications on ScienceDirect, and so links will help users to find, access, cite and use the best available version. Please note that Cell Press, The Lancet and some society-owned have different preprint policies. Information on these policies is available on the journal homepage.

Accepted Author Manuscripts: An accepted author manuscript is the manuscript of an article that has been accepted for publication and which typically includes author incorporated changes suggested during submission, peer review and editor-author communications. Authors can share their accepted author manuscript:

- Immediately
  - via their non-commercial person homepage or blog
  - by updating a preprint in arXiv or RePEc with the accepted manuscript via their research institute or institutional repository for internal institutional uses or as part of an invitation-only research collaboration work-group
  - directly by providing copies to their students or to research collaborators for their personal use
  - for private scholarly sharing as part of an invitation-only work group on commercial sites with which Elsevier has an agreement
- After the embargo period
  - via non-commercial hosting platforms such as their institutional repository
  - via commercial sites with which Elsevier has an agreement

In all cases accepted manuscripts should:

- link to the formal publication via its DOI
- bear a CC-BY-NC-ND license - this is easy to do
- if aggregated with other manuscripts, for example in a repository or other site, be shared in alignment with our hosting policy not be added to or enhanced in any way to appear more like, or to substitute for, the published journal article.

Published journal article (JPA): A published journal article (PJA) is the definitive final record of published research that appears or will appear in the journal and embodies all value-adding publishing activities including peer review co-ordination, copy-editing, formatting, (if relevant) pagination and online enrichment.

Policies for sharing publishing journal articles differ for subscription and gold open access articles:

Subscription Articles: If you are an author, please share a link to your article rather than the full-text. Millions of researchers have access to the formal publications on ScienceDirect, and so links will help your users to find, access, cite, and use the best available version.

Theses and dissertations which contain embedded PJAs as part of the formal submission can be posted publicly by the awarding institution with DOI links back to the formal publications on ScienceDirect.

If you are affiliated with a library that subscribes to ScienceDirect you have additional private sharing rights for others' research accessed under that agreement. This includes use for classroom teaching and internal training at the institution (including use in course packs and courseware programs), and inclusion of the article for grant funding purposes.

Gold Open Access Articles: May be shared according to the author-selected end-user license and should contain a CrossMark logo, the end user license, and a DOI link to the

formal publication on ScienceDirect.

Please refer to Elsevier's posting policy for further information.

18. **For book authors** the following clauses are applicable in addition to the above: Authors are permitted to place a brief summary of their work online only. You are not allowed to download and post the published electronic version of your chapter, nor may you scan the printed edition to create an electronic version. Posting to a repository: Authors are permitted to post a summary of their chapter only in their institution's repository.

19. **Thesis/Dissertation:** If your license is for use in a thesis/dissertation your thesis may be submitted to your institution in either print or electronic form. Should your thesis be published commercially, please reapply for permission. These requirements include permission for the Library and Archives of Canada to supply single copies, on demand, of the complete thesis and include permission for Proquest/UMI to supply single copies, on demand, of the complete thesis. Should your thesis be published commercially, please reapply for permission. Theses and dissertations which contain embedded PJAs as part of the formal submission can be posted publicly by the awarding institution with DOI links back to the formal publications on ScienceDirect.

Elsevier Open Access Terms and Conditions

You can publish open access with Elsevier in hundreds of open access journals or in nearly 2000 established subscription journals that support open access publishing. Permitted third party re-use of these open access articles is defined by the author's choice of Creative Commons user license. See our open access license policy for more information.

Terms & Conditions applicable to all Open Access articles published with Elsevier:

Any reuse of the article must not represent the author as endorsing the adaptation of the article nor should the article be modified in such a way as to damage the author's honour or reputation. If any changes have been made, such changes must be clearly indicated.

The author(s) must be appropriately credited and we ask that you include the end user license and a DOI link to the formal publication on ScienceDirect.

If any part of the material to be used (for example, figures) has appeared in our publication with credit or acknowledgement to another source it is the responsibility of the user to ensure their reuse complies with the terms and conditions determined by the rights holder.

Additional Terms & Conditions applicable to each Creative Commons user license:

CC BY: The CC-BY license allows users to copy, to create extracts, abstracts and new works from the Article, to alter and revise the Article and to make commercial use of the Article (including reuse and/or resale of the Article by commercial entities), provided the user gives appropriate credit (with a link to the formal publication through the relevant DOI), provides a link to the license, indicates if changes were made and the licensor is not represented as endorsing the use made of the work. The full details of the license are available at http://creativecommons.org/licenses/by/4.0.

CC BY NC SA: The CC BY-NC-SA license allows users to copy, to create extracts, abstracts and new works from the Article, to alter and revise the Article, provided this is not done for commercial purposes, and that the user gives appropriate credit (with a link to the formal publication through the relevant DOI), provides a link to the license, indicates if changes were made and the licensor is not represented as endorsing the use made of the work. Further, any new works must be made available on the same conditions. The full details of the license are available at http://creativecommons.org/licenses/by-nc-sa/4.0.

CC BY NC ND: The CC BY-NC-ND license allows users to copy and distribute the Article,

provided this is not done for commercial purposes and further does not permit distribution of the Article if it is changed or edited in any way, and provided the user gives appropriate credit (with a link to the formal publication through the relevant DOI), provides a link to the license, and that the licensor is not represented as endorsing the use made of the work. The full details of the license are available at http://creativecommons.org/licenses/by-nc-nd/4.0.

Any commercial reuse of Open Access articles published with a CC BY NC SA or CC BY NC ND license requires permission from Elsevier and will be subject to a fee.

- Commercial reuse includes:
- Associating advertising with the full text of the Article
- Charging fees for document delivery or access
- Article aggregation
- Systematic distribution via e-mail lists or share buttons

Posting or linking by commercial companies for use by customers of those companies.

20. Other Conditions:

v1.9

Questions? customercare@copyright.com or +18552393415(toll free in the US) or +19786462777.

May 30, 2017

This Agreement between Yash Raval ("You") and Nature Publishing Group ("Nature Publishing Group") consists of your license details and the terms and conditions provided by Nature Publishing Group and Copyright Clearance Center.

License Number	4119030222495
License date	May 30, 2017
Licensed Content Publisher	Nature Publishing Group
Licensed Content Publication	Nature Medicine
Licensed Content Title	Antibacterial resistance worldwide: causes, challenges and responses
Licensed Content Author	Stuart B Levy, Bonnie Marshall
Licensed Content Date	Nov 30, 2004
Licensed Content Volume	10
Licensed Content Issue	12s
Type of Use	reuse in a dissertation / thesis
Requestor type	academic/educational
Format	electronic
Portion	figures/tables/illustrations
Number of figures/tables/illustrations	1
Highres required	no
Figures	Box 4
Author of this NPG article	no
Your reference number	
Title of your thesis / dissertation	Application of Glycoconjugate functionalized Magnetic Nanoparticles as Anti-adhesion and Antibacterial Agents
Expected completion date	Aug 2017
Estimated size (number of pages)	150
Requestor Location	Yash Raval 143 Life Sciences Facility 190 Collings St CLEMSON, SC 29634 United States Attn: Yash Raval
Billing Type	Invoice
Billing Address	Yash Raval 143 Life Sciences Facility 190 Collings St CLEMSON, SC 29634 United States Attn: Yash Raval
Total	0.00 USD

Terms and Conditions

Terms and Conditions for Permissions

is essentially equivalent to, or substitutes for, the print version. Where print permission has been granted for a fee, separate permission must

be obtained for any additional, electronic reuse (unless, as in the case of a full paper, this has already been accounted for during your initial request in the calculation of a print run).NB: In all cases, web-based use of full-text articles must be authorized separately through the 'Use on a Web Site' option when requesting permission.

3. Permission granted for a first edition does not apply to second and subsequent editions and for editions in other languages (except for signatories to the STM Permissions Guidelines, or where the first edition permission was granted for free).

4. Nature Publishing Group's permission must be acknowledged next to the figure, table or abstract in print. In electronic form, this acknowledgement must be visible at the same time as the figure/table/abstract, and must be hyperlinked to the journal's homepage.

5. The credit line should read:

Reprinted by permission from Macmillan Publishers Ltd: [JOURNAL NAME] (reference citation), copyright (year of publication)

For AOP papers, the credit line should read:

Reprinted by permission from M   acmillan Publishers Ltd: [JOURNAL NAME], advance online publication, day month year (doi: 10.1038/sj.[JOURNAL ACRONYM].XXXXX)

Note: For republication from the British Journal of Cancer, the following credit lines apply.

Reprinted by permission from Macmillan Publishers Ltd on behalf of Cancer Research UK: [JOURNAL NAME] (reference citation), copyright (year of publication)For AOP papers, the credit line should read:

Reprinted by permission from Macmillan Publishers Ltd on behalf of Cancer Research UK: [JOURNAL NAME], advance online publication, day month year (doi: 10.1038/sj.[JOURNAL ACRONYM].XXXXX)

6. Adaptations of single figures do not require NPG approval. However, the adaptation should be credited as follows:

Adapted by permission from Macmillan Publishers Ltd: [JOURNAL NAME] (reference citation), copyright (year of publication)

Note: For adaptation from the British Journal of Cancer, the following credit line applies.

Adapted by permission from Macmillan Publishers Ltd on behalf of Cancer Research UK: [JOURNAL NAME] (reference citation), copyright (year of publication)

7. Translations of 401 words up to a whole article require NPG approval. Please visit http://www.macmillanmedicalcommunications.com for more information.Translations of up to a 400 words do not require NPG approval. The translation should be credited as follows: Translated by permission from Macmillan Publishers Ltd: [JOURNAL NAME] (reference citation), copyright (year of publication).

Note: For translation from the British Journal of Cancer, the following credit line applies.

Translated by permission from Macmillan Publishers Ltd on behalf of Cancer Research UK: [JOURNAL NAME] (reference citation), copyright (year of publication)

We are certain that all parties will benefit from this agreement and wish you the best in the use of this material. Thank you.

Special Terms:

v1.1

Questions? customercare@copyright.com or +18552393415 (toll free in the US) or +19786462777.

May 30, 2017

This Agreement between Yash Raval ("You") and Elsevier ("Elsevier") consists of your license details and the terms and conditions provided by Elsevier and Copyright Clearance Center.

License Number	4118891404035
License date	May 30, 2017
Licensed Content Publisher	Elsevier
Licensed Content Publication	Biochimica et Biophysica Acta (BBA) General Subjects
Licensed Content Title	Carbohydrates as future anti-adhesion drugs for infectious diseases
Licensed Content Author	Nathan Sharon
Licensed Content Date	Apr 1, 2006
Licensed Content Volume	1760
Licensed Content Issue	4
Licensed Content Pages	11
Start Page	527
End Page	537
Type of Use	reuse in a thesis/dissertation
Portion	figures/tables/illustrations
Number of figures/tables/illustrations	1
Format	electronic
Are you the author of this Elsevier article?	No
Will you be translating?	No
Order reference number	
Original figure numbers	Table 1
Title of your thesis/dissertation	Application of Glycoconjugate functionalized Magnetic Nanoparticles as Anti-adhesion and Anti-bacterial Agents
Expected completion date	Aug 2017
Estimated size (number of pages)	150
Elsevier VAT number	GB 494 6272 12
Requestor Location	Yash Raval 143 Life Sciences Facility 190 Collings St CLEMSON, SC 29634 United States Attn: Yash Raval
Publisher Tax ID	980397604
Total	0.00 USD
Terms and Conditions	

INTRODUCTION

1. The publisher for this copyrighted material is Elsevier. By clicking "accept" in connection with completing this licensing transaction, you agree that the following terms and conditions apply to this transaction (along with the Billing and Payment terms and conditions established by Copyright Clearance Center, Inc. ("CCC"), at the time that you opened your Rightslink account and that are available at any time at http://myaccount.copyright.com).

GENERAL TERMS

2. Elsevier hereby grants you permission to reproduce the aforementioned material subject to the terms and conditions indicated.

3. Acknowledgement: If any part of the material to be used (for example, figures) has appeared in our publication with credit or acknowledgement to another source, permission must also be sought from that source. If such permission is not obtained then that material may not be included in your publication/copies. Suitable acknowledgement to the source must be made, either as a footnote or in a reference list at the end of your publication, as follows: "Reprinted from Publication title, Vol /edition number, Author(s), Title of article / title of chapter, Pages No., Copyright (Year), with permission from Elsevier [OR APPLICABLE SOCIETY COPYRIGHT OWNER]." Also Lancet special credit - "Reprinted from The Lancet, Vol. number, Author(s), Title of article, Pages No., Copyright (Year), with permission from Elsevier."

4. Reproduction of this material is confined to the purpose and/or media for which permission is hereby given.

5. Altering/Modifying Material: Not Permitted. However figures and illustrations may be altered/adapted minimally to serve your work. Any other abbreviations, additions, deletions and/or any other alterations shall be made only with prior written authorization of Elsevier Ltd. (Please contact Elsevier at permissions@elsevier.com). No modifications can be made to any Lancet figures/tables and they must be reproduced in full.

6. If the permission fee for the requested use of our material is waived in this instance, please be advised that your future requests for Elsevier materials may attract a fee.

7. Reservation of Rights: Publisher reserves all rights not specifically granted in the combination of (i) the license details provided by you and accepted in the course of this licensing transaction, (ii) these terms and conditions and (iii) CCC's Billing and Payment terms and conditions.

8. License Contingent Upon Payment: While you may exercise the rights licensed immediately upon issuance of the license at the end of the licensing process for the transaction, provided that you have disclosed complete and accurate details of your proposed use, no license is finally effective unless and until full payment is received from you (either by publisher or by CCC) as provided in CCC's Billing and Payment terms and conditions. If full payment is not received on a timely basis, then any license preliminarily granted shall be deemed automatically revoked and shall be void as if never granted. Further, in the event that you breach any of these terms and conditions or any of CCC's Billing and Payment terms and conditions, the license is automatically revoked and shall be void as if never granted. Use of materials as described in a revoked license, as well as any use of the materials beyond the scope of an unrevoked license, may constitute copyright infringement and publisher reserves the right to take any and all action to protect its copyright in the materials.

9. Warranties: Publisher makes no representations or warranties with respect to the licensed material.

10. Indemnity: You hereby indemnify and agree to hold harmless publisher and CCC, and their respective officers, directors, employees and agents, from and against any and all claims arising out of your use of the licensed material other than as specifically authorized pursuant to this license.

11. No Transfer of License: This license is personal to you and may not be sublicensed, assigned, or transferred by you to any other person without publisher's written permission.

12. No Amendment Except in Writing: This license may not be amended except in a writing signed by both parties (or, in the case of publisher, by CCC on publisher's behalf).

13. Objection to Contrary Terms: Publisher hereby objects to any terms contained in any purchase order, acknowledgment, check endorsement or other writing prepared by you, which terms are inconsistent with these terms and conditions or CCC's Billing and Payment terms

171

and conditions. These terms and conditions, together with CCC's Billing and Payment terms and conditions (which are incorporated herein), comprise the entire agreement between you and publisher (and CCC) concerning this licensing transaction. In the event of any conflict between your obligations established by these terms and conditions and those established by CCC's Billing and Payment terms and conditions, these terms and conditions shall control.

14. Revocation: Elsevier or Copyright Clearance Center may deny the permissions described in this License at their sole discretion, for any reason or no reason, with a full refund payable to you. Notice of such denial will be made using the contact information provided by you. Failure to receive such notice will not alter or invalidate the denial. In no event will Elsevier or Copyright Clearance Center be responsible or liable for any costs, expenses or damage incurred by you as a result of a denial of your permission request, other than a refund of the amount(s) paid by you to Elsevier and/or Copyright Clearance Center for denied permissions.

LIMITED LICENSE

The following terms and conditions apply only to specific license types:

15. **Translation:** This permission is granted for non-exclusive world English rights only unless your license was granted for translation rights. If you licensed translation rights you may only translate this content into the languages you requested. A professional translator must perform all translations and reproduce the content word for word preserving the integrity of the article.

16. **Posting licensed content on any Website:** The following terms and conditions apply as follows: Licensing material from an Elsevier journal: All content posted to the web site must maintain the copyright information line on the bottom of each image; A hyper-text must be included to the Homepage of the journal from which you are licensing at http://www.sciencedirect.com/science/journal/xxxxx or the Elsevier homepage for books at http://www.elsevier.com; Central Storage: This license does not include permission for a scanned version of the material to be stored in a central repository such as that provided by Heron/XanEdu.

Licensing material from an Elsevier book: A hyper-text link must be included to the Elsevier homepage at http://www.elsevier.com . All content posted to the web site must maintain the copyright information line on the bottom of each image.

Posting licensed content on Electronic reserve: In addition to the above the following clauses are applicable: The web site must be password-protected and made available only to bona fide students registered on a relevant course. This permission is granted for 1 year only. You may obtain a new license for future website posting.

17. **For journal authors:** the following clauses are applicable in addition to the above:
Preprints:
A preprint is an author's own write-up of research results and analysis, it has not been peer reviewed, nor has it had any other value added to it by a publisher (such as formatting, copyright, technical enhancement etc.).

Authors can share their preprints anywhere at any time. Preprints should not be added to or enhanced in any way in order to appear more like, or to substitute for, the final versions of articles however authors can update their preprints on arXiv or RePEc with their AcceptedAuthor Manuscript (see below).

If accepted for publication, we encourage authors to link from the preprint to their formal publication via its DOI. Millions of researchers have access to the formal publications on ScienceDirect, and so links will help users to find, access, cite and use the best available version. Please note that Cell Press, The Lancet and some society-owned have different preprint policies. Information on these policies is available on the journal homepage.

Accepted Author Manuscripts: An accepted author manuscript is the manuscript of an article that has been accepted for publication and which typically includes author incorporated changes suggested during submission, peer review and editor-author communications.
Authors can share their accepted author manuscript:

- Immediately
  - via their non-commercial person homepage or blog
  - by updating a preprint in arXiv or RePEc with the accepted manuscript via their research institute or institutional repository for internal institutional uses or as part of an invitation-only research collaboration work-group
  - directly by providing copies to their students or to research collaborators for their personal use
  - for private scholarly sharing as part of an invitation-only work group on commercial sites with which Elsevier has an agreement
- After the embargo period
  - via non-commercial hosting platforms such as their institutional repository
  - via commercial sites with which Elsevier has an agreement

In all cases accepted manuscripts should:

- link to the formal publication via its DOI
- bear a CC-BY-NC-ND license - this is easy to do
- if aggregated with other manuscripts, for example in a repository or other site, be shared in alignment with our hosting policy not be added to or enhanced in any way to appear more like, or to substitute for, the published journal article.

Published journal article (JPA): A published journal article (PJA) is the definitive final record of published research that appears or will appear in the journal and embodies all value-adding publishing activities including peer review co-ordination, copy-editing, formatting, (if relevant) pagination and online enrichment.
Policies for sharing publishing journal articles differ for subscription and gold open access articles:
Subscription Articles: If you are an author, please share a link to your article rather than the full-text. Millions of researchers have access to the formal publications on ScienceDirect, and so links will help your users to find, access, cite, and use the best available version.
Theses and dissertations which contain embedded PJAs as part of the formal submission can be posted publicly by the awarding institution with DOI links back to the formal publications on ScienceDirect.
If you are affiliated with a library that subscribes to ScienceDirect you have additional private sharing rights for others' research accessed under that agreement. This includes use for classroom teaching and internal training at the institution (including use in course packs and courseware programs), and inclusion of the article for grant funding purposes.
Gold Open Access Articles: May be shared according to the author-selected end-user license and should contain a CrossMark logo, the end user license, and a DOI link to the formal publication on ScienceDirect.
Please refer to Elsevier's posting policy for further information.
18. **For book authors** the following clauses are applicable in addition to the above:
Authors are permitted to place a brief summary of their work online only. You are not allowed to download and post the published electronic version of your chapter, nor may you scan the printed edition to create an electronic version. Posting to a repository: Authors are permitted to post a summary of their chapter only in their institution's repository.

19. **Thesis/Dissertation:** If your license is for use in a thesis/dissertation your thesis may be submitted to your institution in either print or electronic form. Should your thesis be published commercially, please reapply for permission. These requirements include permission for the Library and Archives of Canada to supply single copies, on demand, of the complete thesis and include permission for Proquest/UMI to supply single copies, on demand, of the complete thesis. Should your thesis be published commercially, please reapply for permission. Theses and dissertations which contain embedded PJAs as part of the formal submission can be posted publicly by the awarding institution with DOI links back to the formal publications on ScienceDirect.

Elsevier Open Access Terms and Conditions

You can publish open access with Elsevier in hundreds of open access journals or in nearly 2000 established subscription journals that support open access publishing. Permitted third party re-use of these open access articles is defined by the author's choice of Creative Commons user license. See our open access license policy for more information.

Terms & Conditions applicable to all Open Access articles published with Elsevier:

Any reuse of the article must not represent the author as endorsing the adaptation of the article nor should the article be modified in such a way as to damage the author's honour or reputation. If any changes have been made, such changes must be clearly indicated.

The author(s) must be appropriately credited and we ask that you include the end user license and a DOI link to the formal publication on ScienceDirect.

If any part of the material to be used (for example, figures) has appeared in our publication with credit or acknowledgement to another source it is the responsibility of the user to ensure their reuse complies with the terms and conditions determined by the rights holder.

Additional Terms & Conditions applicable to each Creative Commons user license:

CC BY: The CC-BY license allows users to copy, to create extracts, abstracts and new works from the Article, to alter and revise the Article and to make commercial use of the Article (including reuse and/or resale of the Article by commercial entities), provided the user gives appropriate credit (with a link to the formal publication through the relevant DOI), provides a link to the license, indicates if changes were made and the licensor is not represented as endorsing the use made of the work. The full details of the license are available at http://creativecommons.org/licenses/by/4.0.

CC BY NC SA: The CC BY-NC-SA license allows users to copy, to create extracts, abstracts and new works from the Article, to alter and revise the Article, provided this is not done for commercial purposes, and that the user gives appropriate credit (with a link to the formal publication through the relevant DOI), provides a link to the license, indicates if changes were made and the licensor is not represented as endorsing the use made of the work. Further, any new works must be made available on the same conditions. The full details of the license are available at http://creativecommons.org/licenses/by-nc-sa/4.0.

CC BY NC ND: The CC BY-NC-ND license allows users to copy and distribute the Article, provided this is not done for commercial purposes and further does not permit distribution of the Article if it is changed or edited in any way, and provided the user gives appropriate credit (with a link to the formal publication through the relevant DOI), provides a link to the license, and that the licensor is not represented as endorsing the use made of the work. The full details of the license are available at http://creativecommons.org/licenses/by-nc-nd/4.0.

Any commercial reuse of Open Access articles published with a CC BY NC SA or CC BY NC ND license requires permission from Elsevier and will be subject to a fee.

- Commercial reuse includes:
- Associating advertising with the full text of the Article

- Charging fees for document delivery or access
- Article aggregation
- Systematic distribution via e-mail lists or share buttons

Posting or linking by commercial companies for use by customers of those companies.

20. Other Conditions:

v1.9

Dear Yash,

The Royal Society of Chemistry (RSC) hereby grants permission for the use of your paper(s) specified below in the printed and microfilm version of your thesis. You may also make available the PDF version of your paper(s) that the RSC sent to the corresponding author(s) of your paper(s) upon publication of the paper(s) in the following ways: in your thesis via any website that your university may have for the deposition of theses, via your university's Intranet or via your own personal website. We are however unable to grant you permission to include the PDF version of the paper(s) on its own in your institutional repository. The Royal Society of Chemistry is a signatory to the STM Guidelines on Permissions (available on request).

Please note that if the material specified below or any part of it appears with credit or acknowledgement to a third party then you must also secure permission from that third party before reproducing that material.

Please ensure that the thesis states the following:

Reproduced by permission of The Royal Society of Chemistry

and include a link to the paper on the Royal Society of Chemistry's website.

Please ensure that your co-authors are aware that you are including the paper in your thesis.

Regards,
Antonella

From: Yash Raval [mailto:yraval@g.clemson.edu]
Sent: 30 May 2017 19:03
To: CONTRACTS-COPYRIGHT (shared) <Contracts-Copyright@rsc.org>
Subject: Permission to Reuse Article for Dissertation

Dear Sir/Madam,

I am original author for the following article, which was published in Nanoscale journal.

http://pubs.rsc.org/en/Content/ArticleLanding/2015/NR/C5NR00511F#!divAbstract

I would like your permission to reuse the entire article as part of my dissertation work.

Regards,
Yash.

May 30, 2017

This Agreement between Yash Raval ("You") and John Wiley and Sons ("John Wiley and Sons") consists of your license details and the terms and conditions provided by John Wiley and Sons and Copyright Clearance Center.

License Number	4118900980179
License date	May 30, 2017
Licensed Content Publisher	John Wiley and Sons
Licensed Content Publication	Advanced Functional Materials
Licensed Content Title	Multianchored Glycoconjugate-Functionalized Magnetic Nanoparticles: A Tool for Selective Killing of Targeted Bacteria via Alternating Magnetic Fields
Licensed Content Author	Yash S. Raval, Benjamin D. Fellows, Jamie Murbach, Yves Cordeau, Olin Thompson Mefford, Tzuen-Rong J. Tzeng
Licensed Content Date	May 15, 2017
Licensed Content Pages	1
Type of use	Dissertation/Thesis
Requestor type	Author of this Wiley article
Format	Electronic
Portion	Full article
Will you be translating?	No
Title of your thesis / Dissertation	Application of Glycoconjugate functionalized Magnetic Nanoparticles as Anti-adhesion and Anti-bacterial Agents
Expected completion date	Aug 2017
Expected size (number of pages)	150
Requestor Location	Yash Raval 143 Life Sciences Facility 190 Collings St CLEMSON, SC 29634 United States Attn: Yash Raval
Publisher Tax ID	EU826007151
Billing Type	Invoice
Billing Address	Yash Raval 143 Life Sciences Facility 190 Collings St CLEMSON, SC 29634 United States Attn: Yash Raval
Total	0.00 USD
Terms and Conditions	

TERMS AND CONDITIONS

This copyrighted material is owned by or exclusively licensed to John Wiley & Sons, Inc. or one of its group companies (each a"Wiley Company") or handled on behalf of a society with which a Wiley Company has exclusive publishing rights in relation to a particular work (collectively "WILEY"). By clicking "accept" in connection with completing this licensing transaction, you agree that the following terms and conditions apply to this transaction (along with the billing and payment terms and conditions established by the Copyright Clearance Center Inc., ("CCC's Billing and Payment terms and conditions"), at the time that you opened your RightsLink account (these are

available at any time at).

Terms and Conditions

- The materials you have requested permission to reproduce or reuse (the "Wiley Materials") are protected by copyright.
- You are hereby granted a personal, non-exclusive, non-sub licensable (on a standalone basis), non-transferable, worldwide, limited license to reproduce the Wiley Materials for the purpose specified in the licensing process. This license, and any CONTENT (PDF or image file) purchased as part of your order, is for a one-time use only and limited to any maximum distribution number specified in the license. The first instance of republication or reuse granted by this license must be completed within two years of the date of the grant of this license (although copies prepared before the end date may be distributed thereafter). The Wiley Materials shall not be used in any other manner or for any other purpose, beyond what is granted in the license. Permission is granted subject to an appropriate acknowledgement given to the author, title of the material/book/journal and the publisher. You shall also duplicate the copyright notice that appears in the Wiley publication in your use of the Wiley Material. Permission is also granted on the understanding that nowhere in the text is a previously published source acknowledged for all or part of this Wiley Material. Any third party content is expressly excluded from this permission.
- With respect to the Wiley Materials, all rights are reserved. Except as expressly granted by the terms of the license, no part of the Wiley Materials may be copied, modified, adapted (except for minor reformatting required by the new Publication), translated, reproduced, transferred or distributed, in any form or by any means, and no derivative works may be made based on the Wiley Materials without the prior permission of the respective copyright owner.For STM Signatory Publishers clearing permission under the terms of the STM Permissions Guidelines only, the terms of the license are extended to include subsequent editions and for editionsvin other languages, provided such editions are for the work as a whole in situ and does not involve the separate exploitation of the permitted figures or extracts, You may not alter, remove or suppress in any manner any copyright, trademark or other notices displayed by the Wiley Materials. You may not license, rent, sell, loan, lease, pledge, offer as security, transfer or assign the Wiley Materials on a stand-alone basis, or any of the rights granted to you hereunder to any other person.
- The Wiley Materials and all of the intellectual property rights therein shall at all times remain the exclusive property of John Wiley & Sons Inc, the Wiley Companies, or their respective licensors, and your interest therein is only that of having possession of and the right to reproduce the Wiley Materials pursuant to Section 2 herein during the continuance of this Agreement. You agree that you own no right, title or interest in or to the Wiley Materials or any of the intellectual property rights therein. You shall have no rights hereunder other than the license as provided for above in Section 2. No right, license or interest to any trademark,

trade name, service mark or other branding ("Marks") of WILEY or its licensors is granted hereunder, and you agree that you shall not assert any such right, license or interest with respect thereto

- NEITHER WILEY NOR ITS LICENSORS MAKES ANY WARRANTY OR REPRESENTATION OF ANY KIND TO YOU OR ANY THIRD PARTY, EXPRESS, IMPLIED OR STATUTORY, WITH RESPECT TO THE MATERIALS OR THE ACCURACY OF ANY INFORMATION CONTAINED IN THE MATERIALS, INCLUDING, WITHOUT LIMITATION, ANY IMPLIED WARRANTY OF MERCHANTABILITY, ACCURACY, SATISFACTORY QUALITY, FITNESS FOR A PARTICULAR PURPOSE, USABILITY, INTEGRATION OR NON-INFRINGEMENT AND ALL SUCH WARRANTIES ARE HEREBY EXCLUDED BY WILEY AND ITS LICENSORS AND WAIVED BY YOU.
- WILEY shall have the right to terminate this Agreement immediately upon breach of this Agreement by you.
- You shall indemnify, defend and hold harmless WILEY, its Licensors and their respective directors, officers, agents and employees, from and against any actual or threatened claims, demands, causes of action or proceedings arising from any breach of this Agreement by you.
- IN NO EVENT SHALL WILEY OR ITS LICENSORS BE LIABLE TO YOU OR ANY OTHER PARTY OR ANY OTHER PERSON OR ENTITY FOR ANY SPECIAL, CONSEQUENTIAL, INCIDENTAL, INDIRECT, EXEMPLARY OR PUNITIVE DAMAGES, HOWEVER CAUSED, ARISING OUT OF OR IN CONNECTION WITH THE DOWNLOADING, PROVISIONING, VIEWING OR USE OF THE MATERIALS REGARDLESS OF THE FORM OF ACTION, WHETHER FOR BREACH OF CONTRACT, BREACH OF WARRANTY, TORT, NEGLIGENCE, INFRINGEMENT OR OTHERWISE (INCLUDING, WITHOUT LIMITATION, DAMAGES BASED ON LOSS OF PROFITS, DATA, FILES, USE, BUSINESS OPPORTUNITY OR CLAIMS OF THIRD PARTIES), AND WHETHER OR NOT THE PARTY HAS BEEN ADVISED OF THE POSSIBILITY OF SUCH DAMAGES. THIS LIMITATION SHALL APPLY NOTWITHSTANDING ANY FAILURE OF ESSENTIAL PURPOSE OF ANY LIMITED REMEDY PROVIDED HEREIN.
- Should any provision of this Agreement be held by a court of competent jurisdiction to be illegal, invalid, or unenforceable, that provision shall be deemed amended to achieve as nearly as possible the same economic effect as the original provision, and the legality, validity and enforceability of the remaining provisions of this Agreement shall not be affected or impaired thereby.
- The failure of either party to enforce any term or condition of this Agreement shall not constitute a waiver of either party's right to enforce each and every term and condition of this Agreement. No breach under this agreement shall be deemed waived or excused by either party unless such waiver or consent is in writing signed by the party granting such waiver or consent. The waiver by or consent of

a party to a breach of any provision of this Agreement shall not operate or be construed as a waiver of or consent to any other or subsequent breach by such other party.

- This Agreement may not be assigned (including by operation of law or otherwise) by you without WILEY's prior written consent.
- Any fee required for this permission shall be non-refundable after thirty (30) days from receipt by the CCC.
- These terms and conditions together with CCC's Billing and Payment terms and conditions (which are incorporated herein) form the entire agreement between you and WILEY concerning this licensing transaction and (in the absence of fraud) supersedes all prior agreements and representations of the parties, oral or written. This Agreement may not be amended except in writing signed by both parties. This Agreement shall be binding upon and inure to the benefit of the parties' successors, legal representatives, and authorized assigns.
- In the event of any conflict between your obligations established by these terms and conditions and those established by CCC's Billing and Payment terms and conditions, these terms and conditions shall prevail.
- WILEY expressly reserves all rights not specifically granted in the combination of (i) the license details provided by you and accepted in the course of this licensing transaction, (ii) these terms and conditions and (iii) CCC's Billing and Payment terms and conditions.
- This Agreement will be void if the Type of Use, Format, Circulation, or Requestor Type was misrepresented during the licensing process.
- This Agreement shall be governed by and construed in accordance with the laws of the State of New York, USA, without regards to such state's conflict of law rules. Any legal action, suit or proceeding arising out of or relating to these Terms and Conditions or the breach thereof shall be instituted in a court of competent jurisdiction in New York County in the State of New York in the United States of America and each party hereby consents and submits to the personal jurisdiction of such court, waives any objection to venue in such court and consents to service of process by registered or certified mail, return receipt requested, at the last known address of such party.

WILEY OPEN ACCESS TERMS AND CONDITIONS

Wiley Publishes Open Access Articles in fully Open Access Journals and in Subscription journals offering Online Open. Although most of the fully Open Access journals publish open access articles under the terms of the Creative Commons Attribution (CC BY) License only, the subscription journals and a few of the Open Access Journals offer a choice of Creative Commons Licenses. The license type is clearly identified on the article.
The Creative Commons Attribution License
The Creative Commons Attribution License (CC-BY) allows users to copy, distribute and

Jul 23, 2017

This Agreement between Yash Raval ("You") and Nature Publishing Group ("Nature Publishing Group") consists of your license details and the terms and conditions provided by Nature Publishing Group and Copyright Clearance Center.

License Number	4154950428132
License date	Jul 23, 2017
Licensed Content Publisher	Nature Publishing Group
Licensed Content Publication	Nature Materials
Licensed Content Title	Understanding biophysicochemical interactions at the nano–bio interface
Licensed Content Author	Andre E. Nel, Lutz Madler, Darrell Velegol, Tian Xia, Eric M. V. Hoek *et al.*
Licensed Content Date	Jun 14, 2009
Licensed Content Volume	8
Licensed Content Issue	7
Type of Use	reuse in a dissertation / thesis
Requestor type	academic/educational
Format	electronic
Portion	figures/tables/illustrations
Number of figures/tables/illustrations	1
Highres required	no
Figures	Figure 3
Author of this NPG article	no
Your reference number	
Title of your thesis / Dissertation	Application of Glycoconjugate functionalized Magnetic Nanoparticles as Anti-adhesion and Anti-bacterial Agents
Expected completion date	Aug 2017
Estimated size (number of pages)	150
Requestor Location	Yash Raval 143 Life Sciences Facility 190 Collings St CLEMSON, SC 29634 United States Attn: Yash Raval
Billing Type	Invoice
Billing Address	Yash Raval 143 Life Sciences Facility 190 Collings St CLEMSON, SC 29634 United States Attn: Yash Raval
Total	0.00 USD

Terms and Conditions

Terms and Conditions for Permissions

Nature Publishing Group hereby grants you a non-exclusive license to reproduce this material for this purpose, and for no other use, subject to the conditions below:

1. NPG warrants that it has, to the best of its knowledge, the rights to license reuse of this material. However, you should ensure that the material you are requesting is original to Nature Publishing Group and does not carry the copyright of another entity (as credited in the published version). If the credit line on any part of the material you have requested indicates that it was reprinted or adapted by NPG with permission

from another source, then you should also seek permission from that source to reuse the material.

2. Permission granted free of charge for material in print is also usually granted for any electronic version of that work, provided that the material is incidental to the work as a whole and that the electronic version is essentially equivalent to, or substitutes for, the print version. Where print permission has been granted for a fee, separate permission must

be obtained for any additional, electronic reuse (unless, as in the case of a full paper, this has already been accounted for during your initial request in the calculation of a print run).NB: In all cases, web-based use of full-text articles must be authorized separately through the 'Use on a Web Site' option when requesting permission.

3. Permission granted for a first edition does not apply to second and subsequent editions and for editions in other languages (except for signatories to the STM Permissions Guidelines, or where the first edition permission was granted for free).

4. Nature Publishing Group's permission must be acknowledged next to the figure, table or abstract in print. In electronic form, this acknowledgement must be visible at the same time as the figure/table/abstract, and must be hyperlinked to the journal's homepage.

5. The credit line should read:

Reprinted by permission from Macmillan Publishers Ltd: [JOURNAL NAME] (reference citation), copyright (year of publication)

For AOP papers, the credit line should read:

Reprinted by permission from M   acmillan Publishers Ltd: [JOURNAL NAME], advance online publication, day month year (doi: 10.1038/sj.[JOURNAL ACRONYM].XXXXX)

Note: For republication from the British Journal of Cancer, the following credit lines apply.

Reprinted by permission from Macmillan Publishers Ltd on behalf of Cancer Research UK: [JOURNAL NAME] (reference citation), copyright (year of publication)For AOP papers, the credit line should read:

Reprinted by permission from Macmillan Publishers Ltd on behalf of Cancer Research UK: [JOURNAL NAME], advance online publication, day month year (doi: 10.1038/sj.[JOURNAL ACRONYM].XXXXX)

6. Adaptations of single figures do not require NPG approval. However, the adaptation should be credited as follows:

Adapted by permission from Macmillan Publishers Ltd: [JOURNAL NAME] (reference citation), copyright (year of publication)

Note: For adaptation from the British Journal of Cancer, the following credit line applies.

Adapted by permission from Macmillan Publishers Ltd on behalf of Cancer Research UK: [JOURNAL NAME] (reference citation), copyright (year of publication)

7. Translations of 401 words up to a whole article require NPG approval. Please visit http://www.macmillanmedicalcommunications.com for more information.Translations of up to a 400 words do not require NPG approval. The translation should be credited as follows:

Translated by permission from Macmillan Publishers Ltd: [JOURNAL NAME] (reference citation), copyright (year of publication).

Note: For translation from the British Journal of Cancer, the following credit line applies.

Translated by permission from Macmillan Publishers Ltd on behalf of Cancer Research UK: [JOURNAL NAME] (reference citation), copyright (year of publication)

We are certain that all parties will benefit from this agreement and wish you the best in the use of this material. Thank you.

Special Terms:

v1.1

Questions? customercare@copyright.com or +18552393415 (toll free in the US) or +19786462777.

Jul 23, 2017

This Agreement between Yash Raval ("You") and Elsevier ("Elsevier") consists of your license details and the terms and conditions provided by Elsevier and Copyright Clearance Center.

License Number	4154941415868
License date	Jul 23, 2017
Licensed Content Publisher	Elsevier
Licensed Content Publication	Trends in Biotechnology
Licensed Content Title	Multifunctional nanoparticles – properties and prospects for their use in human medicine
Licensed Content Author	Nuria Sanvicens,M. Pilar Marco
Licensed Content Date	Aug 1, 2008
Licensed Content Volume	26
Licensed Content Issue	8
Licensed Content Pages	9
Start Page	425
End Page	433
Type of Use	reuse in a thesis/dissertation
Intended publisher of new work	other
Portion	figures/tables/illustrations
Number of figures/tables/illustrations	1
Format	electronic
Are you the author of this Elsevier article?	No
Will you be translating?	No
Original figure numbers	Figure 3
Title of your thesis/dissertation	Application of Glycoconjugate functionalized Magnetic Nanoparticles as Anti-adhesion and Anti-bacterial Agents
Expected completion date	Aug 2017
Estimated size (number of pages)	150
Requestor Location	Yash Raval 143 Life Sciences Facility 190 Collings St CLEMSON, SC 29634 United States Attn: Yash Raval
Publisher Tax ID	980397604
Total	0.00 USD
Terms and Conditions	

INTRODUCTION

1. The publisher for this copyrighted material is Elsevier. By clicking "accept" in connection with completing this licensing transaction, you agree that the following terms and conditions apply to this transaction (along with the Billing and Payment terms and conditions established by Copyright Clearance Center, Inc. ("CCC"), at the time that you opened your Rightslink account and that are available at any time at http://myaccount.copyright.com).

GENERAL TERMS

2. Elsevier hereby grants you permission to reproduce the aforementioned material subject to the terms and conditions indicated.

3. Acknowledgement: If any part of the material to be used (for example, figures) has appeared in our publication with credit or acknowledgement to another source, permission must also be sought from that source. If such permission is not obtained then that material may not be included in your publication/copies. Suitable acknowledgement to the source must be made, either as a footnote or in a reference list at the end of your publication, as follows: "Reprinted from Publication title, Vol /edition number, Author(s), Title of article / title of chapter, Pages No., Copyright (Year), with permission from Elsevier [OR APPLICABLE SOCIETY COPYRIGHT OWNER]." Also Lancet special credit - "Reprinted from The Lancet, Vol. number, Author(s), Title of article, Pages No., Copyright (Year), with permission from Elsevier."

4. Reproduction of this material is confined to the purpose and/or media for which permission is hereby given.

5. Altering/Modifying Material: Not Permitted. However figures and illustrations may be altered/adapted minimally to serve your work. Any other abbreviations, additions, deletions and/or any other alterations shall be made only with prior written authorization of Elsevier Ltd. (Please contact Elsevier at permissions@elsevier.com). No modifications can be made to any Lancet figures/tables and they must be reproduced in full.

6. If the permission fee for the requested use of our material is waived in this instance, please be advised that your future requests for Elsevier materials may attract a fee.

7. Reservation of Rights: Publisher reserves all rights not specifically granted in the combination of (i) the license details provided by you and accepted in the course of this licensing transaction, (ii) these terms and conditions and (iii) CCC's Billing and Payment terms and conditions.

8. License Contingent Upon Payment: While you may exercise the rights licensed immediately upon issuance of the license at the end of the licensing process for the transaction, provided that you have disclosed complete and accurate details of your proposed use, no license is finally effective unless and until full payment is received from you (either by publisher or by CCC) as provided in CCC's Billing and Payment terms and conditions. If full payment is not received on a timely basis, then any license preliminarily granted shall be deemed automatically revoked and shall be void as if never granted. Further, in the event that you breach any of these terms and conditions or any of CCC's Billing and Payment terms and conditions, the license is automatically revoked and shall be void as if never granted. Use of materials as described in a revoked license, as well as any use of the materials beyond the scope of an unrevoked license, may constitute copyright infringement and publisher reserves the right to take any and all action to protect its copyright in the materials.

9. Warranties: Publisher makes no representations or warranties with respect to the licensed material.

10. Indemnity: You hereby indemnify and agree to hold harmless publisher and CCC, and their respective officers, directors, employees and agents, from and against any and all claims arising out of your use of the licensed material other than as specifically authorized pursuant to this license.

11. No Transfer of License: This license is personal to you and may not be sublicensed, assigned, or transferred by you to any other person without publisher's written permission.

12. No Amendment Except in Writing: This license may not be amended except in a writing signed by both parties (or, in the case of publisher, by CCC on publisher's behalf).

13. Objection to Contrary Terms: Publisher hereby objects to any terms contained in any

purchase order, acknowledgment, check endorsement or other writing prepared by you, which terms are inconsistent with these terms and conditions or CCC's Billing and Payment terms and conditions. These terms and conditions, together with CCC's Billing and Payment terms and conditions (which are incorporated herein), comprise the entire agreement between you and publisher (and CCC) concerning this licensing transaction. In the event of any conflict between your obligations established by these terms and conditions and those established by CCC's Billing and Payment terms and conditions, these terms and conditions shall control.

14. Revocation: Elsevier or Copyright Clearance Center may deny the permissions described in this License at their sole discretion, for any reason or no reason, with a full refund payable to you. Notice of such denial will be made using the contact information provided by you. Failure to receive such notice will not alter or invalidate the denial. In no event will Elsevier or Copyright Clearance Center be responsible or liable for any costs, expenses or damage incurred by you as a result of a denial of your permission request, other than a refund of the amount(s) paid by you to Elsevier and/or Copyright Clearance Center for denied permissions.

LIMITED LICENSE

The following terms and conditions apply only to specific license types:

15. **Translation:** This permission is granted for non-exclusive world English rights only unless your license was granted for translation rights. If you licensed translation rights you may only translate this content into the languages you requested. A professional translator must perform all translations and reproduce the content word for word preserving the integrity of the article.

16. **Posting licensed content on any Website:** The following terms and conditions apply as follows: Licensing material from an Elsevier journal: All content posted to the web site must maintain the copyright information line on the bottom of each image; A hyper-text must be included to the Homepage of the journal from which you are licensing at http://www.sciencedirect.com/science/journal/xxxxx or the Elsevier homepage for books at http://www.elsevier.com; Central Storage: This license does not include permission for a scanned version of the material to be stored in a central repository such as that provided by Heron/XanEdu.

Licensing material from an Elsevier book: A hyper-text link must be included to the Elsevier homepage at http://www.elsevier.com . All content posted to the web site must maintain the copyright information line on the bottom of each image.

Posting licensed content on Electronic reserve: In addition to the above the following clauses are applicable: The web site must be password-protected and made available only to bona fide students registered on a relevant course. This permission is granted for 1 year only. You may obtain a new license for future website posting.

17. **For journal authors:** the following clauses are applicable in addition to the above:
Preprints:
A preprint is an author's own write-up of research results and analysis, it has not been peer reviewed, nor has it had any other value added to it by a publisher (such as formatting, copyright, technical enhancement etc.).

Authors can share their preprints anywhere at any time. Preprints should not be added to or enhanced in any way in order to appear more like, or to substitute for, the final versions of articles however authors can update their preprints on arXiv or RePEc with their AcceptedAuthor Manuscript (see below).

If accepted for publication, we encourage authors to link from the preprint to their formal publication via its DOI. Millions of researchers have access to the formal publications on ScienceDirect, and so links will help users to find, access, cite and use the best available

version. Please note that Cell Press, The Lancet and some society-owned have different preprint policies. Information on these policies is available on the journal homepage.

Accepted Author Manuscripts: An accepted author manuscript is the manuscript of an article that has been accepted for publication and which typically includes author incorporated changes suggested during submission, peer review and editor-author communications.

Authors can share their accepted author manuscript:

- Immediately
  - via their non-commercial person homepage or blog
  - by updating a preprint in arXiv or RePEc with the accepted manuscript via their research institute or institutional repository for internal institutional uses or as part of an invitation-only research collaboration work-group
  - directly by providing copies to their students or to research collaborators for their personal use
  - for private scholarly sharing as part of an invitation-only work group on commercial sites with which Elsevier has an agreement
- After the embargo period
  - via non-commercial hosting platforms such as their institutional repository
  - via commercial sites with which Elsevier has an agreement

In all cases accepted manuscripts should:

- link to the formal publication via its DOI
- bear a CC-BY-NC-ND license - this is easy to do
- if aggregated with other manuscripts, for example in a repository or other site, be shared in alignment with our hosting policy not be added to or enhanced in any way to appear more like, or to substitute for, the published journal article.

Published journal article (JPA): A published journal article (PJA) is the definitive final record of published research that appears or will appear in the journal and embodies all value-adding publishing activities including peer review co-ordination, copy-editing, formatting, (if relevant) pagination and online enrichment.

Policies for sharing publishing journal articles differ for subscription and gold open access articles:

Subscription Articles: If you are an author, please share a link to your article rather than the full-text. Millions of researchers have access to the formal publications on ScienceDirect, and so links will help your users to find, access, cite, and use the best available version.

Theses and dissertations which contain embedded PJAs as part of the formal submission can be posted publicly by the awarding institution with DOI links back to the formal publications on ScienceDirect.

If you are affiliated with a library that subscribes to ScienceDirect you have additional private sharing rights for others' research accessed under that agreement. This includes use for classroom teaching and internal training at the institution (including use in course packs and courseware programs), and inclusion of the article for grant funding purposes.

Gold Open Access Articles: May be shared according to the author-selected end-user license and should contain a CrossMark logo, the end user license, and a DOI link to the formal publication on ScienceDirect.

Please refer to Elsevier's posting policy for further information.

18. **For book authors** the following clauses are applicable in addition to the above:

Authors are permitted to place a brief summary of their work online only. You are not allowed to download and post the published electronic version of your chapter, nor may you scan

the printed edition to create an electronic version. Posting to a repository: Authors are permitted to post a summary of their chapter only in their institution's repository.

19. **Thesis/Dissertation:** If your license is for use in a thesis/dissertation your thesis may be submitted to your institution in either print or electronic form. Should your thesis be published commercially, please reapply for permission. These requirements include permission for the Library and Archives of Canada to supply single copies, on demand, of the complete thesis and include permission for Proquest/UMI to supply single copies, on demand, of the complete thesis. Should your thesis be published commercially, please reapply for permission. Theses and dissertations which contain embedded PJAs as part of the formal submission can be posted publicly by the awarding institution with DOI links back to the formal publications on ScienceDirect.

Elsevier Open Access Terms and Conditions

You can publish open access with Elsevier in hundreds of open access journals or in nearly 2000 established subscription journals that support open access publishing. Permitted third party re-use of these open access articles is defined by the author's choice of Creative Commons user license. See our open access license policy for more information.

Terms & Conditions applicable to all Open Access articles published with Elsevier:

Any reuse of the article must not represent the author as endorsing the adaptation of the article nor should the article be modified in such a way as to damage the author's honour or reputation. If any changes have been made, such changes must be clearly indicated.

The author(s) must be appropriately credited and we ask that you include the end user license and a DOI link to the formal publication on ScienceDirect.

If any part of the material to be used (for example, figures) has appeared in our publication with credit or acknowledgement to another source it is the responsibility of the user to ensure their reuse complies with the terms and conditions determined by the rights holder.

Additional Terms & Conditions applicable to each Creative Commons user license:

CC BY: The CC-BY license allows users to copy, to create extracts, abstracts and new works from the Article, to alter and revise the Article and to make commercial use of the Article (including reuse and/or resale of the Article by commercial entities), provided the user gives appropriate credit (with a link to the formal publication through the relevant DOI), provides a link to the license, indicates if changes were made and the licensor is not represented as endorsing the use made of the work. The full details of the license are available at http://creativecommons.org/licenses/by/4.0.

CC BY NC SA: The CC BY-NC-SA license allows users to copy, to create extracts, abstracts and new works from the Article, to alter and revise the Article, provided this is not done for commercial purposes, and that the user gives appropriate credit (with a link to the formal publication through the relevant DOI), provides a link to the license, indicates if changes were made and the licensor is not represented as endorsing the use made of the work. Further, any new works must be made available on the same conditions. The full details of the license are available at http://creativecommons.org/licenses/by-nc-sa/4.0.

CC BY NC ND: The CC BY-NC-ND license allows users to copy and distribute the Article, provided this is not done for commercial purposes and further does not permit distribution of the Article if it is changed or edited in any way, and provided the user gives appropriate credit (with a link to the formal publication through the relevant DOI), provides a link to the license, and that the licensor is not represented as endorsing the use made of the work. The full details of the license are available at http://creativecommons.org/licenses/by-nc-nd/4.0.

Any commercial reuse of Open Access articles published with a CC BY NC SA or CC BY NC ND license requires permission from Elsevier and will be subject to a fee.

- Commercial reuse includes:
- Associating advertising with the full text of the Article
- Charging fees for document delivery or access
- Article aggregation
- Systematic distribution via e-mail lists or share buttons

Posting or linking by commercial companies for use by customers of those companies.

20. Other Conditions:

v1.9